A STUDY OF AIR FILTER FLOW BY COMPUTATIONAL FLUID DYNAMICS

By

QIAN CAI

Bachelor of Science

Zhejiang University

Hangzhou, China

1989

Submitted to the Faculty of the
Graduate College of the
Oklahoma State University
in partial fulfillment of
the requirements for
the Degree of
MASTER OF SCIENCE
July, 1993

OKLAHOMA STATE UNIVERSITY

A STUDY OF AIR FILTER FLOW BY

COMPUTATIONAL FLUID DYNAMICS

Thesis Approved:

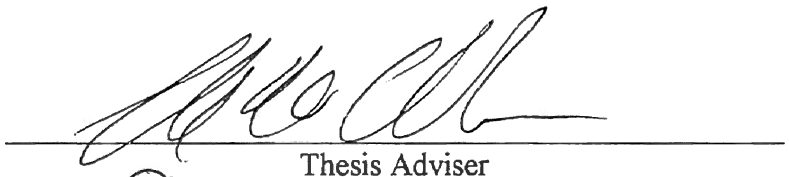

Thesis Adviser

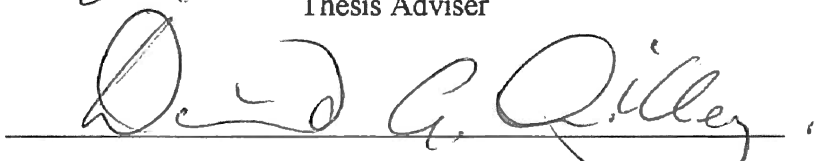

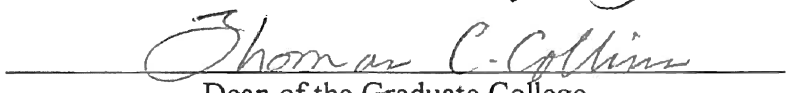

Dean of the Graduate College

ACKNOWLEDGMENTS

I am very grateful to my advisor, Dr. Frank W. Chambers, who gives me much more knowledge that I can not learn from the book. His nice attitude and patience toward the student will be in my mind forever.

I also would like to thank my other committee members, Dr. R. L. Dougherty, Dr. D. G. Lilley for their helpful suggestions and patient instructions. Extra thanks is due to Dr. Lilley for his help with the computer program and program inspection. I like to express my thanks to Dr. Gary Ferrell, the engineer and project monitor from Purolator Products, Inc.*, who helped me with very useful practical suggestions.

The successful cooperation between my colleague Rajendra Sabnis and me was a very important factor in accomplishing the filter experiment project. As well as him, I will also remember Faqiu Liang and Manoj Haldhani, who also were all involved in the filtration experiment.

Finally, I would like to thank my parents who always give me the encouragement to surmount numerous difficulties. I will also give special thanks to my wife, Xia Chen, whose love and understanding make me feel how beautiful this world is.

* This air filter filtration project is supported by Purolator Products Inc. and Oklahoma Center for the Advancement of Science and Technology (OCAST).

TABLE OF CONTENTS

Chapter Page

LIST OF TABLES

LIST OF FIGURES

Figure Page

NOMENCLATURE

The following list of nomenclature and symbols are used throughout this thesis.

b	inertial factor	m^{-1}
C	distance between two fiber center	m
$C_\mu, C_D, C_{1\varepsilon}, C_{2\varepsilon}$	constants of k-ε model	
d	pleat distance in derivation of uniform normal velocity	m
D	fiber diameter	m
D	mass divergence of continuity equation	
g	gravity acceleration	m^2 / s
h	distance of the flow point from centerline	m
J	unit vector in extended Darcy's law	
k	turbulent kinetic energy	m^2/s^2
$k_{i,j}$	k at the cell (i, j)	m^2/s^2
K	permeability coefficient	m^2
l	Prandtl's mixing length	m
L	turbulent length scale in one equation model	
p	pressure	Pa
$p_{i,j}$	p at the cell (i, j)	Pa
Δp	pressure change or correction	Pa
$\langle P \rangle^f$	pressure read off a pressure gauge	Pa

t	time	s
t_p	paper thickness of pleat filter	m
t_x	horizontal paper thickness of pleat	m
u_i, u_j	velocity vector form	m/s
x_i, x_j	flow position in vector form	m
u'	u fluctuation velocity	m/s
$u_{i,j}$, $U_{i,j}$	u velocity at the cell (i,j)	m/s
Uin	inlet velocity	m/s
v'	v fluctuation velocity	m/s
$v_{i,j}$, $V_{i,j}$	v velocity at the cell (i,j)	m/s
$\overline{u}, \overline{v}, \overline{w}$	mean velocity components	m/s
u,v,w	velocity components in x, y, and z directions	m/s
V	velocity vector	m/s
V	volume bounded by a closed surface in local volume average process	m^3
W	width of flow domain	m
v_f	portion of V containing the fluid in local volume process	m^3
y	width of flow domain	m
x, y, z	cell space	m
α	donor cell coefficient	
β	packing density	kg/m^3
δ	porosity of the porous medium	
$\delta_{i,j}$	unit vector in turbulent kinetic energy equation	
ε	turbulent energy dissipation rate	m /s
$\varepsilon_{i,j}$	ε at the cell (i, j)	m^2 / s^3
ϕ	parameter	

γ	pleat angle	degree
μ	fluid dynamic viscosity	kg/m·s
μ_f	fluid dynamic viscosity	kg/m·s
θ	arrow head angle	degree
ρ	density	kg/m^3
$\sigma_k, \sigma_\varepsilon$	constants for the k-ε model	
τ, τ_t	turbulent stress	
ν_t	eddy viscosity	
ω	relaxation factor	
ξ	a coefficient constant	
$< >$	local volume average of a quantity	

Superscript

n	denotes the value at current time step t
n+1	denotes the value at advanced time step $t+\Delta t$

Subscript

x	horizontal component value
y	vertical component value

CHAPTER I

INTRODUCTION

1.1 Background

Air filters are widely used in the intake system of internal combustion engines to prevent wear-producing dust or corrosive particles from entering the engine. The efficiency and capacity of the filter are very important in establishing the quality of the filter. The engineers always struggle to improve these two parameters. Better understanding of the filtration mechanism can help to determine which part of the filtration system is critical to improving filter efficiency and capacity.

There are several types of filters, including centrifugal filters, oil bath filters, and fiber filters. This thesis considers the pleated paper air filter.

Since there is a much larger surface area for pleated paper than for flat paper, the pleated paper filter is widely used in vehicle or other ventilation systems. The knowledge of how air enters the filter cartridge and how it goes through the pleated filter will help improve the filter design. However, it is difficult to use experimental methods to determine how flow is approaching and crossing the filter. Mathematical methods which employ computational fluid dynamics may allow engineers to obtain this information from the computational results.

1.2 Porous Media and Air Filter

The air filters are usually made from wet-laid non-woven paper. One of the approaches that has been taken for numerical calculations is to consider the filter as a

porous medium[13]. This enables the calculations to be performed using the porous media equations.

1.3 Application of Computational Fluid Dynamics (CFD) to Air Filter Calculations

Mathematical models to calculate the air filtration performance of non-woven media can be divided into two groups. The first is based on the microstructural model of the material. The second considers the filter media in the flow field as an integral part and computes the overall pressure drop and velocity distributions.

1.3.1 Microstructural Model

There are four main approaches to model non-woven fibrous materials: single fiber or single-cylinder model, the parallel-cylinder array model, the pore theory approach, and offset screen theory[18]. The single-fiber theory is the simplest model for particle capture mechanisms such as impaction-impingement and diffusion.

In using parallel-cylinder models, the interfiber influences are considered and in turn improve the model, making it more realistic than that of the single cylinder model. Based on this method, numerical computer simulations are available for calculating the particle capture efficiency and pressure drop.

The pore theory, which is considered to provide a more realistic representation of microstructural geometry of the air filter, varies the pore size created by the random orientation and intersection of fibers in planes transverse to the mean flow[18].

The offset screen theory is a new method to describe the filtration performance of non-woven fiber structures. It is based on anisotropy of fiber orientation, inhomogeneity of fiber dispersion, and the three-dimensional nature of fiber structures.

1.3.2 Macrostructural Model

The mechanics of flow through porous media is an old topic from the nineteenth century. The early work is mostly based on Darcy's law, which neglects the effects of a solid boundary or inertial forces on fluid flow. In Darcy's law, the pressure gradient is represented as:

$$\text{Darcy's Law} \qquad \nabla P = -\frac{\mu_f}{K} V \tag{1-1}$$

The inertial effect becomes more significant near the boundaries, and in high-porosity media that may cause the simple Darcy's law to be invalid. Vafai and Tien [20] applied the local volume-averaging techniques to develop a governing equation, the extended Darcy's law, that includes the inertial term and viscous terms for general use. This extended equation bridges the gap between the simple Darcy's law and Navier-Stokes Equation which will be discussed later.

Extended Darcy's law:

$$\nabla\langle P\rangle = \mu\nabla^2\langle V\rangle - \frac{\mu}{K}\langle V\rangle + b(\langle V\rangle\cdot\langle V\rangle)J \tag{1-2}$$

In his doctoral thesis, Cheng[4] uses the PHOENICS code to simulate the steady, three-dimensional, incompressible turbulent flow in a clean heavy-duty air filter. The porous media flow submodel is based on the extended Darcy's law. Some characteristic parameters of the flow through the filter cartridge were obtained by experimental techniques. The calculation results include overall pressure drops and wall static pressures. The contribution of the filter-housing geometry to the overall pressure drop at

the higher flow rate is much more than that of the filter cartridge. A simple correlation method is established to estimate the pressure drop of the heavy-duty filter system.

Gurumoorthy[7], extending Cheng's work, also used the PHOENICS code to analyze an automotive Air Induction System (AIS). The model is in three-dimensional Cartesian coordinates with k-ε turbulent model. The extended Darcy's law is solved in his thesis. The flow distribution through the filter panel is also investigated by calculating the flow through different areas of the filter. From the velocity vector plot and contour plot, he demonstrated that flow distribution was very non-uniform and would cause the filter to be used in an ineffective manner.

1.4 SOLA - A Numerical Solution Algorithm Method

In 1965, Harlow and Welch [8] presented a new technique, the Marker-and-Cell method, for the numerical solution of problems in the dynamics of an incompressible fluid with a free surface. They used the finite difference method to solve the full unsteady Navier-Stokes equations. The velocity and pressure are considered as primary dependent variables.

Full Navier-Stokes Equation:

$$\frac{\partial \overline{u}_i}{\partial t} + \overline{u}_j \frac{\partial \overline{u}_i}{\partial x_j} = -\frac{1}{\rho}\frac{\partial p}{\partial x_i} + g + \nu \frac{\partial^2 \overline{u}_i}{\partial x_j^2} \qquad (1\text{-}3)$$

In 1975, Hirt [10] el. al. described the SOLA (SOLution Algorithm) methods in detail in their SOLA report and presented the numerical equation setup in the FORTRAN code. They also stressed that with some modifications, the basic equations of the SOLA solution algorithm may be adapted to saturated or unsaturated flow in porous media, to three-dimensional shallow water motions, to a drift flux approximation for two-phase

flow, and to almost any three-dimensional flow of air or water over variable terrain for pollution dispersal models.

Lilley[12] extended the SOLA method to include the computation of an axisymmetric swirling flow in cyclone chambers. With a little modification of the equation for vector variables, the scalar variable swirl velocity is solved. This work extended SOLA to solve the scalar variables. In his thesis, Weathers[21] used the basic SOLA algorithm to simulate the flow within a 15x9x9 ft room through implementation of the turbulent k-ε model. The work demonstrated SOLA can be successfully applied to turbulent flow.

In previous works, the macro method for filter computation usually considered the filter as an integrated part which causes the extra pressure drop. But how the flow goes through the pleated filter has not been investigated in detail.

1.5 Justification to Use CFD Method

There are different ways to find the flow domain information: experimental methods, analytical methods and CFD methods. Experimental methods are limited for this filter study because the interesting flow area deep inside the filter pleats can not be reached by the experimental techniques. It is not possible to use analytical methods to solve the partial differential equations like full Navier-Stokes Equations. However, if the problem is setup properly, the computational solution provides the results of interest, and is cheaper and quicker than other possible means. Computational solutions are especially valuable if other methods cannot be used.

1.6 Background of Thesis

Practically, the vehicle air filter designs are based on the uniform surface or face velocity for a flat sheet. The real filter is pleated but not flat as that assumed for design.

It is interesting to know how pleats change the filter performance and why it is different from design. One factor could be variations in velocity into the pleat surface.

The Laser Doppler Anemometer (LDA) has been used to investigate the flow field upstream of the filter. It is difficult for the LDA to probe the flow area inside the very narrow filter pleats. Thus, the flow distribution deep inside the filter pleats is still unknown.

Computational fluid dynamics is strongly suggested for use to carry out the acquisition of the difficult to obtain information on flow distribution deep inside the pleats.

This thesis is part of research conducted for Purolator Products, Inc. and OCAST. It is hoped that this study can help engineers to design the efficient air filters.

1.7 Objective

Since the flow inside the non-woven paper or between the fibers is not the research interest, the micro fabric flow inside the filter is not considered in this thesis. The interest here is to know how the macro flow will go through the pleated air filter and how this flow is affected by the filter and flow field geometry, filter properties and outside conditions. The main purpose is to use computational fluid dynamics to predict the flow distribution of air very close to the filter or the flow pattern crossing the filter surface.

CHAPTER II

NUMERICAL METHOD

2.1 The Governing Equations

Practically, the uniform inlet flow separates before it enters the filter in the test housing, such as the housing specified in SAE J726 standard. The irregular geometry of the actual car filter plenums will also cause nonuniform flow and flow separation. Thus, the flow upstream and downstream of the filter in the test housing and car plenums is turbulent.

The laminar flow happens inside the filter media because the Reynolds number between the fibers is very small. This means that one has to use two classes of governing equations to represent the flow field. Since the filter can be modeled as a porous medium, the Darcy's law can be applied in that region. The turbulent model is employed in the turbulent flow calculation in the domain without filter. The extended Darcy's law is used in the filter domain.

Figure 2.4 shows the calculation domain which will be discussed later.

2.1.1 Turbulence Modeling

The time-averaging treatments of the turbulent flow is most common application to predict the turbulent flow. The instantaneous term can be decomposed into time-averages or ensemble-averages and fluctuating components[5]:

$$\phi = \overline{\phi} + \phi' \tag{2.1}$$

Applying this technique, we can find the tensor mean flow continuity and momentum equations for incompressible fluid.

Continuity equation:

$$\frac{\partial \overline{u}_i}{\partial x_i} = 0 \tag{2.2}$$

Momentum equations or Reynolds equation:

$$\frac{\partial \overline{u}_i}{\partial t} + \overline{u}_j \frac{\partial \overline{u}_i}{\partial x_j} = -\frac{1}{\rho}\frac{\partial p}{\partial x_i} + \nu \frac{\partial^2 \overline{u}_i}{\partial x_j^2} - \frac{\partial \overline{u_i' u_j'}}{\partial x_j} \tag{2.3}$$

These equations present the turbulence closure problem, because predictions of the mean velocities require knowledge of the Reynolds Stress term $\overline{u_i' u_j'}$, which themselves are unknown. Thus, approximate modeling is necessary for the Reynolds Stress terms. With the modeling, the approximate relationship between the Reynolds Stress terms $\overline{u_i' u_j'}$, the mean velocity and other parameters can be established. If we use the following Boussinesq hypothesis,

$$\tau_t \equiv -\rho \overline{u_i' u_j'} = \rho \nu_t \left(\frac{\partial \overline{u}_i}{\partial x_j} + \frac{\partial \overline{u}_j}{\partial x_i}\right) - \frac{2}{3} k \delta_{ij} \tag{2.4}$$

we can derive three types of turbulent models: zero-equation, one-equation and two-equation models, each providing a way to compute the eddy viscosity, ν_t.

For the zero-equation model, only an algebraic equation is added to solve the problem. One may find the relation between the eddy viscosity and turbulent stress with Prandtl's mixing length hypothesis, for example

$$\nu_t = l^2 \left| \frac{\partial \overline{u}}{\partial y} \right| \tag{2.5}$$

$$\tau_t = \rho \nu_t \frac{\partial \overline{u}}{\partial y} \tag{2.6}$$

Here the mixing length also needs to be estimated but it is more physically meaningful than the eddy viscosity[16].

For the one-equation model, one turbulent kinetic energy partial differential equation is added to be solved.

$$\frac{\partial k}{\partial t} + \frac{\partial(\overline{u}_i k)}{\partial x_i} = \frac{\partial}{\partial x_j}[(\nu + \frac{\nu_t}{\sigma_k})\frac{\partial k}{\partial x_j}] + \nu_t \frac{\partial \overline{u}_i}{\partial x_j}(\frac{\partial \overline{u}_i}{\partial x_j} + \frac{\partial \overline{u}_j}{\partial x_i}) - \varepsilon \tag{2.7}$$

Here the viscous dissipation ε is modeled as follows:

$$\varepsilon = C_D \frac{k^{3/2}}{L} \tag{2.8}$$

For this formulation, the new turbulent length scale L has to be supplied. There are lots of choices in determining L. The complexity of determining L leads to the addition of a new differential equation and yields the two equation k-ε model.

The two-equation model adds a transport equation of viscous dissipation ε, which is coupled with the previous kinetic energy equation and solved. This forms the most popular two-equation model, k-ε model.

$$\frac{\partial \varepsilon}{\partial t}+\frac{\partial(\overline{u}_i \varepsilon)}{\partial x_i}=\frac{\partial}{\partial x_j}[(\nu+\frac{\nu_t}{\sigma_\varepsilon})\frac{\partial \varepsilon}{\partial x_j}]+C_{1\varepsilon}\frac{\varepsilon}{k}\nu_t\frac{\partial \overline{u}_i}{\partial x_j}(\frac{\partial \overline{u}_i}{\partial x_j}+\frac{\partial \overline{u}_j}{\partial x_i})-C_{2\varepsilon}\frac{\varepsilon^2}{k} \qquad (2.9)$$

$$\nu_t = C_\mu \frac{k^2}{\varepsilon} \qquad (2.10)$$

Rodi[16] suggested the empirical constants below for the k-ε model for standard modeling which is applied for high Reynolds number turbulent flow. Different flows must use different empirical constants.

TABLE 2.1

VALUES OF CONSTANTS IN STANDARD k-ε MODEL

C_μ	$C_{1\varepsilon}$	$C_{2\varepsilon}$	σ_k	σ_ε
0.09	1.44	1.92	1.0	1.3

2.1.2 Justification for Using Turbulent Modeling

Practically, the flow in the non-filter regions is turbulent flow. If the inlet is very uniform and it is assumed that wall boundaries are free slip boundary, the turbulent effect may not be strong. To make the program be used generally and make the simulation realistic, the turbulent model is necessary to use. It will be shown in the results of this

work that there is little difference in the calculation time with the turbulent model or without the turbulent model.

2.2 Flow Inside the Filter Media Region

The filter is a kind of porous medium in the flow field. Darcy's law can be applied for this region.

$$\nabla P = -\frac{\mu_f}{K} V \tag{2.10}$$

K is permeability of the porous structure. If a solid wall is present in the flow field or the porous media has high permeability, inertial effects must be considered. The viscous effect in the filter is usually smaller than the Darcian and inertial effect, but for general use, the viscous term should also be added into Darcy's law, forming the extended Darcy's law [20]

$$\nabla P = -\frac{\mu}{K} V - b \cdot (V \cdot V) J + \mu \nabla^2 V \tag{2.11}$$

b is inertial effect constant that can be determined from experiment.

Although the transport equations in the porous media are still valid, the complex structure prevents obtaining the general solutions of detailed velocities. Thus, the volume averaging technique is used which introduces the 'macroscopic' balance equation [14]. The definition of the volume averaging can be expressed as below:

$$\langle \Psi \rangle \equiv \frac{1}{V} \int_{v_f} \Psi \, dV \tag{2.12}$$

One must note the local volume averaged quantities are different from the actual value of that point. Due to the volume-averaging process, some information is lost. Thus empirical

relations are needed for setting up the 'macroscopic' governing equations. Based on the above definition, Vafai and Tien[20] presented the general transport equation that can be used in the porous media.

Continuity Equation: $$\nabla \cdot \langle V \rangle = 0 \tag{2.13}$$

Momentum Equation: $$\rho \frac{D\langle V \rangle}{Dt} = -\nabla \langle P \rangle^f + g + \mu \nabla^2 \langle V \rangle - \frac{\mu}{K} \langle V \rangle + b(\langle V \rangle \cdot \langle V \rangle) \cdot J \tag{2.14}$$

Here J is the unit vector and can be defined as:

$$J = \frac{\langle V \rangle}{|\langle V \rangle|} \tag{2.15}$$

The equations, discussed previously, which describe the flow field are all partial differential equations (PDEs). Usually one cannot find the analytical solutions of these partial differential equations. However, the power of the computer allows us to solve these equations numerically.

2.3 Numerical Approximation Method

Basically, there are three major methods that can be used to make numerical approximations of the flow equation [5].

The Spectral Method expands each flow variable as a set of basis functions. These must satisfy the appropriate boundary conditions. By substituting the resulting expressions into the governing differential equations, a set of algebraic equations can be derived, whose unknowns are the coefficients of the expansion or, equivalently, the values of the variables at appropriate nodal locations[5]. This method is not widely used because of its limitation to simple flow geometry.

The Finite-Element Method (FEM) divides the computational domain into a number of non-overlapping subdomains (elements), and on each approximates the generic flow variable by standard 'shape functions', depending on a limited number of coefficients per element. The big advantage of this method is that it can apply to complex geometry with a highly non uniform grid[5].

The Finite Volume/Finite Difference Methods (FV/FD), divide the flow domain into a set of mesh or control volumes. This method is most widely used in the CFD calculations. In this thesis, the finite difference method is employed with the Marker-and-Cell method.

2.4 Marker-and-Cell

Harlow and Welch[8] gave the detail description of this method in 1965. The basic cell representation is show in Figure 2.1. The vector quantities, like all the velocities, are represented at the edge of the cell and the scalar quantities, like the pressure, kinetic energy and viscous dissipation, are represented at the center of the cell.

2.5 Finite Difference Approximation to the Equations

The finite difference is used in SOLA to discretize the transport equation, continuity and momentum equations. As we mentioned before, the flow in filter region is laminar flow with extended Darcy's law and turbulent inside the non-filter field. Since the flow differs in the two regions, we must discretize the governing equation accordingly. The assumptions of the flow equation are 2-dimensional, incompressible and unsteady.

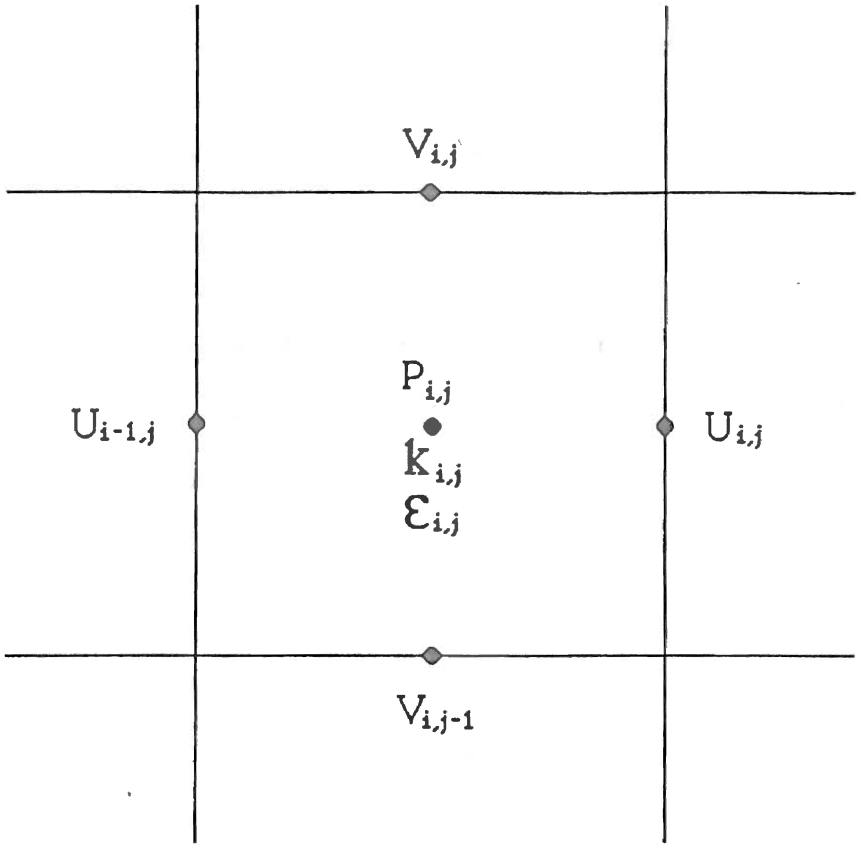

Figure 2.1 Arrangement of Finite Difference Variables in a Typical Cell

2.5.1 Discretized Continuity in Non-Filter Region

Applying the time-averaging technique, one can obtain the discretized continuity equation. One must note that the velocities are mean velocities in the equation. The term with superscript (n+1) denotes the advanced value at t=t+Δt and superscript n denotes the value at one time earlier in the unsteady calculation.

$$\frac{u_{i,j}^{n+1} - u_{i-1,j}^{n+1}}{\Delta x} + \frac{v_{i,j}^{n+1} - v_{i,j-1}^{n+1}}{\Delta y} = 0 \qquad (2.16)$$

2.5.2 Discretized Momentum Equations in Non-Filter Region

The horizontal and vertical component, x component and y component, equations are given below, where fux, fuy, fvx, fvy are flux terms and visx, visy are viscous terms.

x-component

$$u_{i,j}^{n+1} = u_{i,j}^{n} + \Delta t[\frac{1}{\Delta x}(p_{i,j}^{n} - p_{i+1,j}^{n}) + g_x - fux - fuy + visx + \tau_x] \qquad (2.17)$$

y-component

$$v_{i,j}^{n+1} = v_{i,j}^{n} + \Delta t[\frac{1}{\Delta y}(p_{i,j}^{n} - p_{i,j+1}^{n}) + g_y - fvx - fvy + visy + \tau_y] \qquad (2.18)$$

The discretized form of the convection flux terms, and the viscous terms are presented as follows with finite difference method:

$$fux = \frac{\partial u^2}{\partial x}$$

$$= \frac{1}{4\Delta x}\left[(u_{i,j}+u_{i+1,j})^2+\alpha\left|u_{i,j}+u_{i+1,j}\right|(u_{i,j}-u_{i+1,j})-(u_{i-1,j}+u_{i,j})^2-\alpha\left|u_{i-1,j}+u_{i,j}\right|(u_{i-1,j}-u_{i,j})\right]$$

(2.19)

$$f\,u\,y = \frac{\partial(u\,v)}{\partial y}$$

$$= \frac{1}{4\Delta y}\left[(v_{i,j}+v_{i+1,j})(u_{i,j}+u_{i,j+1})+\alpha\left|v_{i,j}+v_{i+1,j}\right|\cdot(u_{i,j}-u_{i,j+1})-(v_{i,j-1}+v_{i+1,j-1})(u_{i,j}+u_{i,j+1})\right.$$

$$\left.-\alpha\left|v_{i,j-1}+v_{i+1,j-1}\right|(u_{i,j-1}-u_{i,j})\right] \qquad (2.20)$$

$$f\,v\,x = \frac{\partial(u\,v)}{\partial x}$$

$$= \frac{1}{4\Delta y}\left[(u_{i,j}+u_{i,j+1})(v_{i,j}+v_{i+1,j})+\alpha\left|(u_{i,j}+u_{i,j+1})\right|\cdot(v_{i,j}-v_{i+1,j})-(u_{i-1,j}+u_{i-1,j+1})(v_{i-1,j}+v_{i,j})\right.$$

$$\left.-\alpha\left|u_{i-1,j}+u_{i+1,j+1}\right|(v_{i-1,j}-v_{i,j})\right] \qquad (2.21)$$

$$f\,v\,y = \frac{\partial v^2}{\partial y}$$

$$= \frac{1}{4\Delta y}\left[(v_{i,j}+v_{i,j+1})^2+\alpha\left|v_{i,j}+v_{i,j+1}\right|(v_{i,j}-v_{i,j+1})-(v_{i,j-1}+v_{i,j})^2-\alpha\left|v_{i,j-1}+v_{i,j}\right|(v_{i,j-1}-v_{i,j})\right]$$

(2.22)

The viscous terms are:

$$visx = \nu\left(\frac{\partial^2 u}{\partial x^2} + \frac{\partial^2 u}{\partial y^2}\right)$$

$$= \nu\left[\frac{1}{\Delta x^2}(u_{i+1,j} - 2u_{i,j} + u_{i-1,j}) + \frac{1}{\Delta y^2}(u_{i,j+1} - 2u_{i,j} + u_{i,j-1})\right] \tag{2.23}$$

$$visy = \nu\left(\frac{\partial^2 v}{\partial x^2} + \frac{\partial^2 v}{\partial y^2}\right)$$

$$= \nu\left[\frac{1}{\Delta x^2}(v_{i+1,j} - 2v_{i,j} + v_{i-1,j}) + \frac{1}{\Delta y^2}(v_{i,j+1} - 2v_{i,j} + v_{i,j-1})\right] \tag{2.24}$$

The Reynolds Stresses are:

$$\tau_x = -\left[\frac{\partial \overline{u'u'}}{\partial x} + \frac{\partial \overline{u'v'}}{\partial y}\right]$$

$$= \frac{\partial}{\partial x}\left[\nu_t\left(\frac{\partial u}{\partial x} + \frac{\partial u}{\partial x}\right) - \frac{2}{3}k\delta_{11}\right] + \frac{\partial}{\partial y}\left[\nu_t\left(\frac{\partial u}{\partial y} + \frac{\partial v}{\partial x}\right) - \frac{2}{3}k\delta_{12}\right]$$

$$= -\frac{2}{3}\frac{\partial k}{\partial x} + \nu_t\left[2\frac{\partial^2 u}{\partial x^2} + \frac{\partial^2 u}{\partial x^2} + \frac{\partial^2 u}{\partial x \partial y}\right] + 2\frac{\partial u}{\partial x}\frac{\partial \nu_t}{\partial x} + \left(\frac{\partial u}{\partial y} + \frac{\partial v}{\partial x}\right)\frac{\partial \nu_t}{\partial y} \tag{2.25}$$

$$\tau_y = -\left[\frac{\partial \overline{u'v'}}{\partial x} + \frac{\partial \overline{v'v'}}{\partial y}\right]$$

$$= \frac{\partial}{\partial y}\left[\nu_t\left(\frac{\partial v}{\partial x} + \frac{\partial u}{\partial y}\right) - \frac{2}{3}k\delta_{12}\right] + \frac{\partial}{\partial x}\left[\nu_t\left(\frac{\partial v}{\partial y} + \frac{\partial v}{\partial y}\right) - \frac{2}{3}k\delta_{11}\right]$$

$$= -\frac{2}{3}\frac{\partial k}{\partial y} + \nu_t\left[2\frac{\partial^2 v}{\partial x^2} + \frac{\partial^2 v}{\partial y^2} + \frac{\partial^2 u}{\partial x \partial y}\right] + 2\frac{\partial v}{\partial y}\frac{\partial \nu_t}{\partial y} + \left(\frac{\partial v}{\partial x} + \frac{\partial u}{\partial y}\right)\frac{\partial \nu_t}{\partial x} \tag{2.26}$$

2.5.3 Kinetic Energy Equations in Non-Filter Region

Since the kinetic energy k and turbulent energy dissipation ε are scalar variables, the method of discretizing the convection terms in the momentum equation are different from such vector variables as velocities. The major consideration is how to use the donor cell coefficient, α. The derivation of these equations presented here follows reference[1].

$$k_{i,j}^{n+1} = k_{i,j}^{n} + \Delta t[-fuk - fvk + Diffusion + Production - \varepsilon] \tag{2.27}$$

$$fuk = \frac{\partial uk}{\partial x}$$

$$= \frac{1}{2\Delta x}\left[u_{i,j}(k_{i,j} + k_{i+1,j}) + \alpha\left|u_{i,j}\right|(k_{i,j} - k_{i+1,j}) - u_{i-1,j}(k_{i-1,j} + k_{i,j}) - \alpha\left|u_{i-1,j}\right|(k_{i-1,j} - k_{i,j})\right] \tag{2.28}$$

$$fvk = \frac{\partial vk}{\partial x}$$

$$= \frac{1}{2\Delta y}\left[v_{i,j}(k_{i,j} + k_{i,j+1}) + \alpha\left|v_{i,j}\right|(k_{i,j} - k_{i,j+1}) - v_{i-1,j}(k_{i,j-1} + k_{i,j}) - \alpha\left|v_{i,j-1}\right|(k_{i,j-1} - k_{i,j})\right] \tag{2.29}$$

$$Diffusion = \frac{\partial}{\partial x_i}[(\nu + \nu_t)\frac{\partial k}{\partial x_i}]$$

$$= (\nu + \frac{\nu_t}{\sigma_k})(\frac{\partial^2 k}{\partial x^2} + \frac{\partial^2 k}{\partial y^2}) + \frac{1}{\sigma_k}[\frac{\partial \nu_t}{\partial x}\frac{\partial k}{\partial x} + \frac{\partial \nu_t}{\partial y}\frac{\partial k}{\partial y}] \tag{2.30}$$

$$\text{Production} = \nu_t \frac{\partial \bar{u}_i}{\partial x_j}\left(\frac{\partial \bar{u}_i}{\partial x_j} + \frac{\partial \bar{u}_j}{\partial x_i}\right) - \frac{2}{3}\delta_{ij} k \frac{\partial \bar{u}_i}{\partial x_j}$$

$$= \nu_t\left[2\left(\frac{\partial u}{\partial x}\right)^2 + 2\left(\frac{\partial v}{\partial y}\right)^2 + \left(\frac{\partial u}{\partial y}\right)^2 + \left(\frac{\partial v}{\partial x}\right)^2 + 2\frac{\partial u}{\partial y}\frac{\partial v}{\partial x}\right] \tag{2.31}$$

2.5.4 Viscous Dissipation Equation in Non-Filter Region

$$\varepsilon_{i,j}^{n+1} = \varepsilon_{i,j}^{n} + \Delta t[-f_u\varepsilon - f_v\varepsilon + \text{Diffusion} + \text{Generation} + \text{Destruction}] \tag{2.32}$$

$$f_u\varepsilon = \frac{\partial(u\varepsilon)}{\partial x}$$

$$= \frac{1}{2\Delta x}\left[u_{i,j}(\varepsilon_{i,j} + \varepsilon_{i+1,j}) + \alpha\left|u_{i,j}\right|(\varepsilon_{i,j} - \varepsilon_{i+1,j}) - u_{i-1,j}(\varepsilon_{i-1,j} + \varepsilon_{i,j}) - \alpha\left|u_{i-1,j}\right|(\varepsilon_{i-1,j} - \varepsilon_{i,j})\right] \tag{2.33}$$

$$f_v\varepsilon = \frac{\partial(v\varepsilon)}{\partial x}$$

$$= \frac{1}{2\Delta y}\left[v_{i,j}(\varepsilon_{i,j} + \varepsilon_{i,j+1}) + \alpha\left|v_{i,j}\right|(\varepsilon_{i,j} - \varepsilon_{i,j+1}) - v_{i-1,j}(\varepsilon_{i,j-1} + \varepsilon_{i,j}) - \alpha\left|v_{i,j-1}\right|(\varepsilon_{i,j-1} - \varepsilon_{i,j})\right] \tag{2.34}$$

$$\text{Diffusion} = \frac{\partial}{\partial x_i}\left[\left(\nu + \frac{\nu_t}{\sigma_\varepsilon}\right)\frac{\partial \varepsilon}{\partial x_i}\right]$$

$$= \left(\nu + \frac{\nu_t}{\sigma_\varepsilon}\right)\left(\frac{\partial^2 \varepsilon}{\partial x^2} + \frac{\partial^2 \varepsilon}{\partial y^2}\right) + \frac{1}{\sigma_\varepsilon}\left[\frac{\partial \nu_t}{\partial x}\frac{\partial \varepsilon}{\partial x} + \frac{\partial \nu_t}{\partial y}\frac{\partial \varepsilon}{\partial y}\right] \tag{2.35}$$

$$\text{Generation+Destruction}=C_{1\varepsilon}\frac{\varepsilon}{k}(\text{Production})-C_{2\varepsilon}\frac{\varepsilon^2}{k} \tag{2.36}$$

2.5.5 Continuity Equation Inside Filter

The continuity equation in filter region is same as that in the non-filter region.

$$\frac{u_{i,j}^{n+1}-u_{i-1,j}^{n+1}}{\Delta x}+\frac{v_{i,j}^{n+1}-v_{i,j-1}^{n+1}}{\Delta y}=0 \tag{2.37}$$

2.5.6 Momentum Equation Inside Filter Region

Once again the extended Darcy's law is presented here:

$$\rho\frac{D\langle V\rangle}{Dt}=-\nabla\langle P\rangle^f+g+\mu\nabla^2\langle V\rangle-\frac{\mu}{K}\langle V\rangle+b(\langle V\rangle\cdot\langle V\rangle)J \tag{2.38}$$

This can be written into two component equations:

$$u_{i,j}^{n+1}=u_{i,j}^{n}+\Delta t[\frac{\delta}{\Delta x}(p_{i,j}^{n}-p_{i+1,j}^{n})+g_x-fux-fuy+visx-Darcy_x-Inertial_x] \tag{2.39}$$

$$v_{i,j}^{n+1}=v_{i,j}^{n}+\Delta t[\frac{\delta}{\Delta y}(p_{i,j}^{n}-p_{i,j+1}^{n})+g_y-fvx-fvy+visy-Darcy_y-Inertial_y] \tag{2.40}$$

The components fux, fuy, fvx, fvy, visx and visy are all the same as the form in the turbulent equation. The newly added terms $Darcy_x$, $Darcy_y$, $Inertial_x$ and $Inertial_y$ are presented as follows:

Horizontal component

$$Darcy_x=-\frac{\nu}{K}u_{i,j} \tag{2.41}$$

$$\text{Inertial}_x = -\frac{1}{2} b \cdot u_{i,j} \cdot \sqrt{u_{i,j}^2 + v_{i,j}^2} \tag{2.42}$$

Vertical component

$$\text{Darcy}_y = -\frac{\nu}{K} v_{i,j} \tag{2.43}$$

$$\text{Inertial}_y = -\frac{1}{2} b \cdot v_{i,j} \cdot \sqrt{u_{i,j}^2 + v_{i,j}^2} \tag{2.44}$$

2.6 Numerical Stability Considerations

It is important to choose correct mesh increments Δx and Δy, the time increment Δt, and upstream difference parameter α [10]. The mesh increments must be small enough for all dependent variables in order to yield reasonable results.

Once the mesh space is determined, there are three conditions that need to be considered to select a reasonable time increment. First, material cannot move more than one cell size for the given time step. This leads to the inequality

$$\Delta t_1 < \min\{\frac{\Delta x}{|u|}, \frac{\Delta y}{|v|}\} \tag{2.45}$$

Second, the non zero value of kinematic viscosity requires that the momentum diffusion cannot be over one cell size in the given time step. Then the following condition must be satisfied

$$\nu \cdot \Delta t_1 < \frac{1}{2} \frac{\Delta x^2 \Delta y^2}{\Delta x^2 + \Delta y^2} \tag{2.46}$$

The Δt is chosen as the minimum value of those two criteria

$$\Delta t = \min\{\Delta t_1, \Delta t_2\}$$

The upstream difference coefficient α employed in the flux terms of the momentum equation also has to satisfy certain conditions to provide stability. Usually, the following equation can be applied.

$$1 \geq \alpha \geq \max\left\{\left|\frac{u\Delta t}{\Delta x}\right|, \left|\frac{v\Delta t}{\Delta y}\right|\right\} \tag{2.47}$$

The value of α should be in the range 0 to 1. The case of α equals to 0 is equivalent to the central difference and 1 refers to the fully upwind or donor cell difference.

2.6.1 Special Consideration in This Thesis

The criteria discussed above are for general cases. In this particular filter calculation, there are some special problems. First is the grid size is very small in order to have a few nodes set inside the filter. This forces the time increment size to be very small. Under this circumstance, the donor cell coefficient α may be too small to satisfy the donor cell difference. Thus the forced donor cell difference coefficient α might be supplied in the source code like 0.7 or 0.8. Otherwise, the calculation will be divergent with very small α value.

2.7 Pressure Iteration

The velocities calculated from momentum equations Eq.2.17 and 2.18 in the laminar case or Eq.2.39 and 2.40 in the turbulent case will not satisfy the continuity equation, Eq.2.16 or Eq.2.37. The "adjusting the cell pressure method" is used in the SOLA algorithm to obtain better estimated velocity values. The basic theory of this

technique is the varying pressure will change the mass flow either entering or exiting the cell. If the divergence value D in Eq.2.48 is negative, the net mass flow is into the cell and increasing pressure is needed to eliminate the inflow. On the other hand, when D is positive, the net mass outlet flow is compensated by decreasing pressure. The one pressure variable in each cell allows the divergence "D" be driven to zero. Since the adjustment of the cell will affect its neighbor cell's values, the iteration of pressure adjustment must be performed throughout the whole flow domain. The divergence D is calculated by using the most recently updated velocity values.

$$D = \frac{u_{i,j}^{n+1} - u_{i-1,j}^{n+1}}{\Delta x} + \frac{v_{i,j}^{n+1} - v_{i,j-1}^{n+1}}{\Delta y} \tag{2.48}$$

When a cell pressure changes from p to p+Δp, the velocity components on the four faces of that cell change as:

$$u_{i,j}^{n+1} = u_{i,j}^{n} + \frac{\Delta t \cdot \Delta p}{\Delta x} \tag{2.49}$$

$$u_{i-1,j}^{n+1} = u_{i-1,j}^{n} - \frac{\Delta t \cdot \Delta p}{\Delta x} \tag{2.50}$$

$$v_{i,j}^{n+1} = v_{i,j}^{n} + \frac{\Delta t \cdot \Delta p}{\Delta y} \tag{2.51}$$

$$v_{i,j-1}^{n+1} = v_{i,j-1}^{n} - \frac{\Delta t \cdot \Delta p}{\Delta y} \tag{2.52}$$

Substituting these equations into the continuity equation will yield the required difference pressure form:

$$\Delta p = -D \Big/ [2\Delta t(\frac{1}{\Delta x^2} + \frac{1}{\Delta y^2})] \tag{2.53}$$

The over-relaxation factor ω usually is used to accelerate the iteration convergence. The value of ω is usually chosen as 1.7. Then, the form of Δp is revised as:

$$\Delta p = -(\omega \cdot D) \Big/ [2\Delta t(\frac{1}{\Delta x^2} + \frac{1}{\Delta y^2})] \tag{2.54}$$

2.8 Grid System in Calculation Domain

Figure 2.2 presents the grid arrangement in the flow field domain. The fictitious points are used to help to specify the boundary. In the figure, the fictitious boundary cells are shaded. The fictitious boundary helps to set the boundary conditions.

2.8.1 Grids Inside the Pleated Filter

The major task of this thesis is to use CFD to predict how flow is crossing the pleated filter. The important work is how to set the grids inside the filter media.

Since the cell geometry is rectangular, it is hard to match the triangular pleated filter geometry exactly. Patankar suggested the regular grid in Cartesian grid still can be improved to handle an irregular shaped calculation domain. The method is to render inactive, or "block off" some of the control volumes of the regular grids so that the remaining active control volumes form the desired domain. Figure 2.3 shows the examples in Patankar's book[15]. Based on the "blocked off" idea, the triangular shaped pleated filter is in Figure 2.4. If the cell size is small enough, we can think the stair geometry, in Figure 2.4 setup is a reasonable approximation.

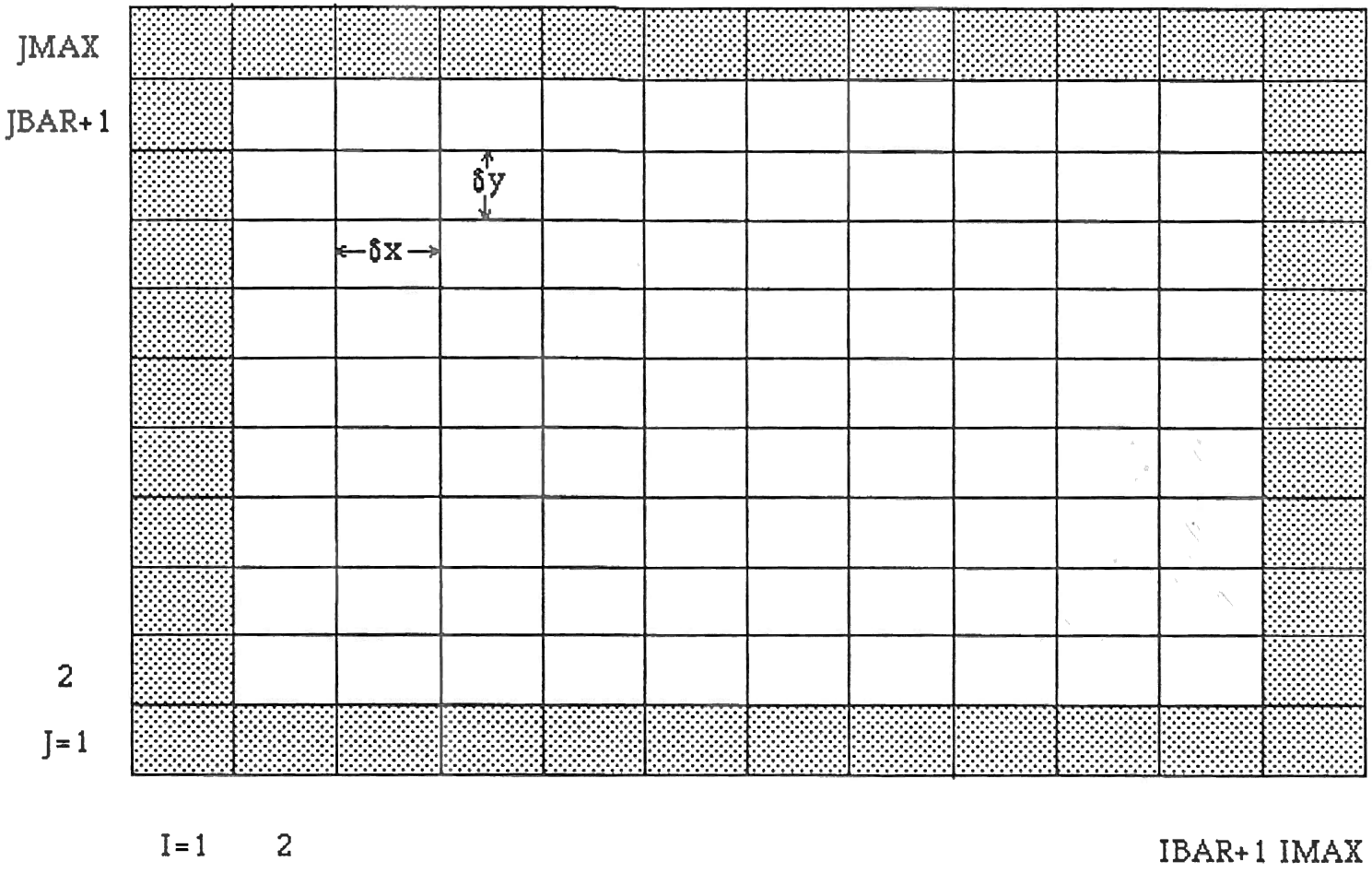

Figure 2.2 General Mesh Arrangement in SOLA Calculation

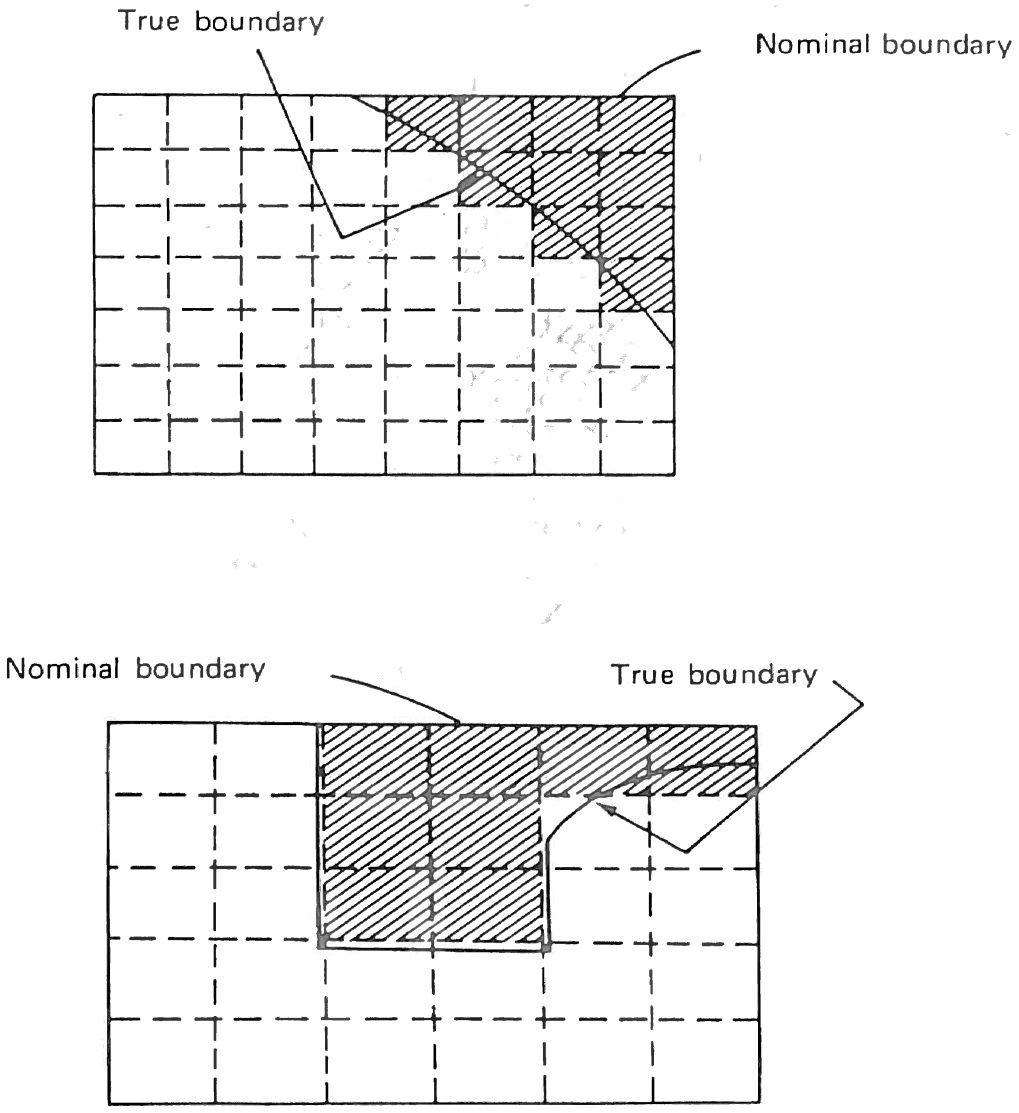

Figure 2.3 Block-off Method in Flow Domain

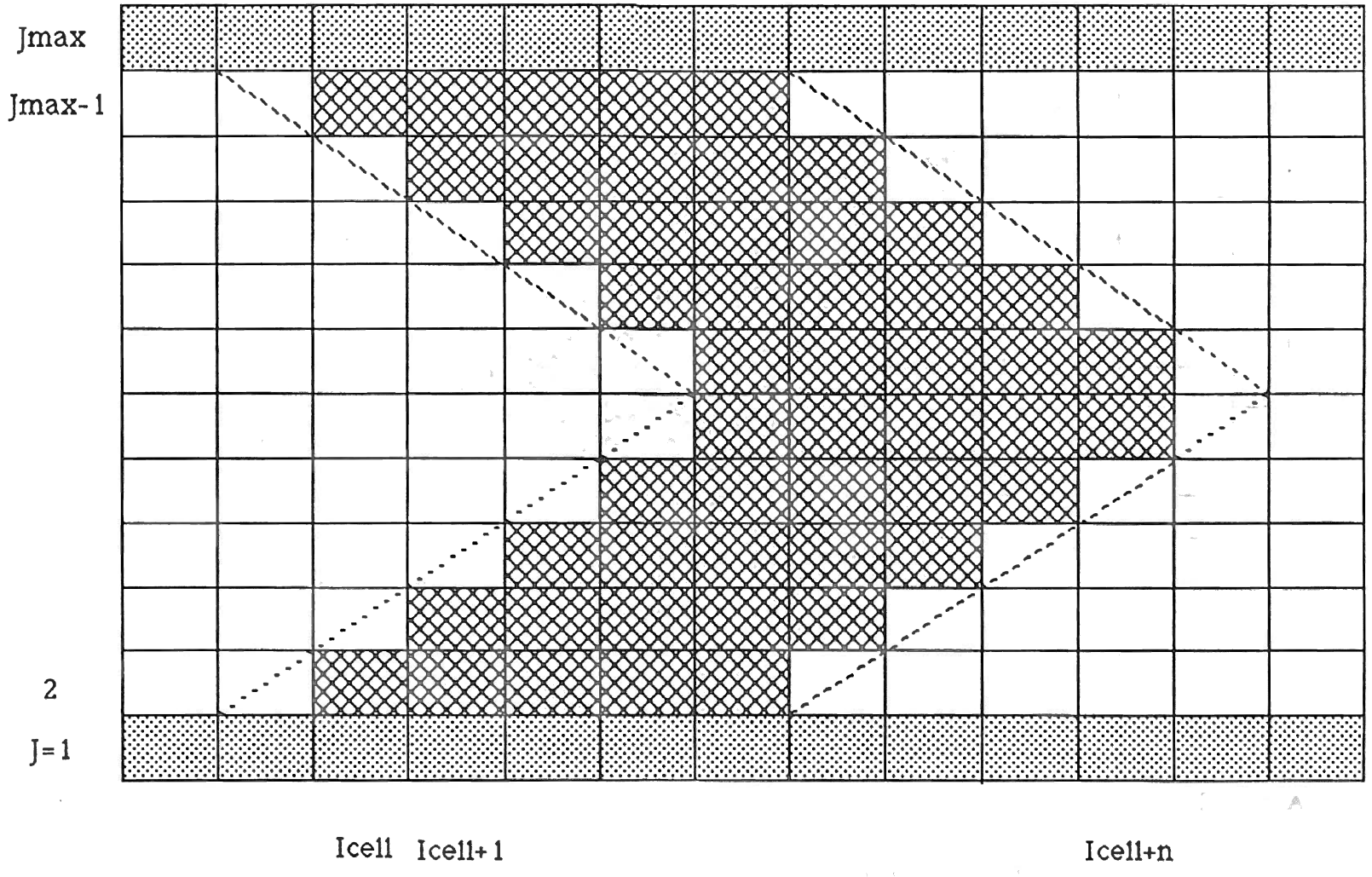

Figure 2.4 Triangular Filter Pleat in Calculations

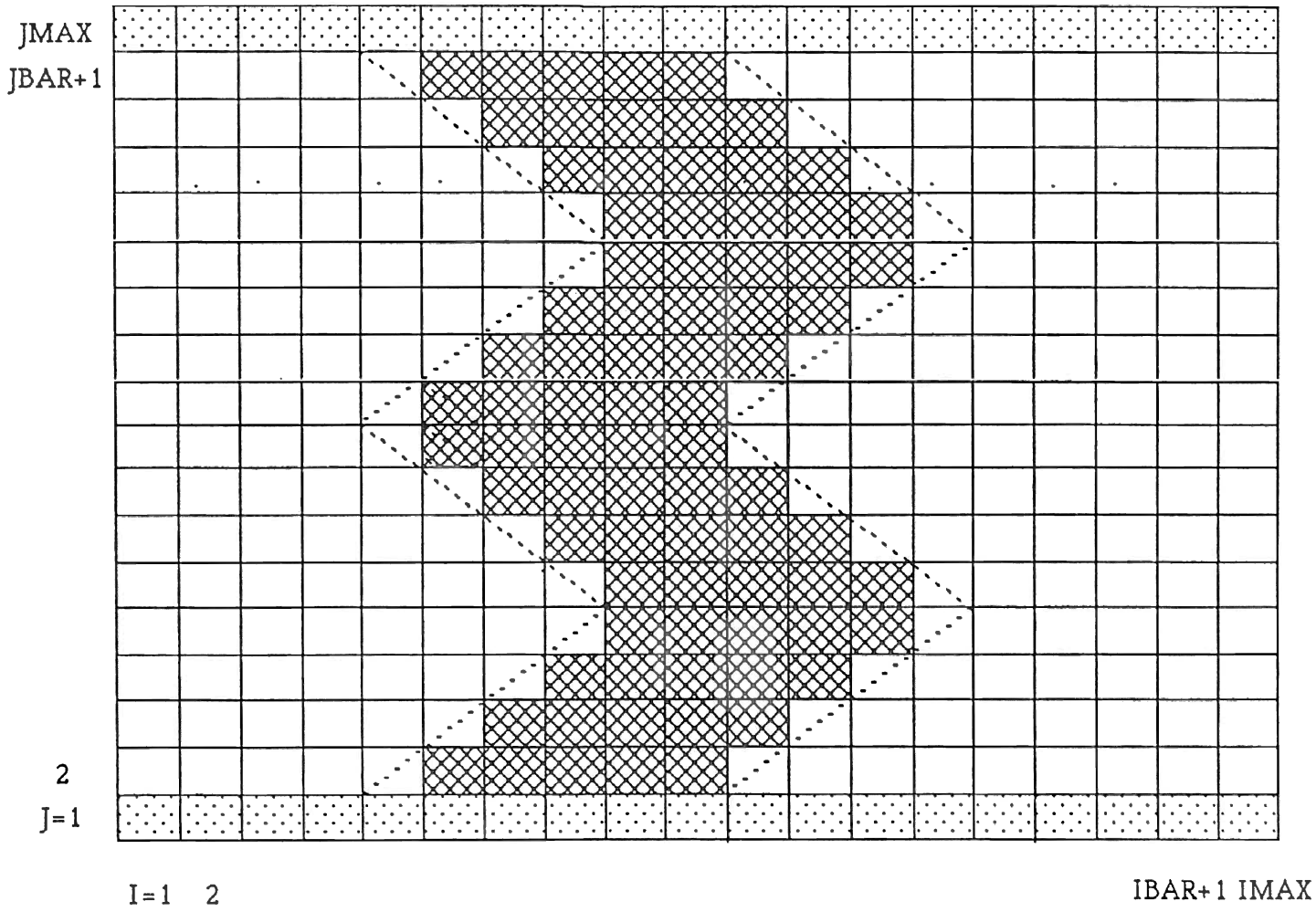

Figure 2.5 Two Triangular Filter Pleats in Calculations

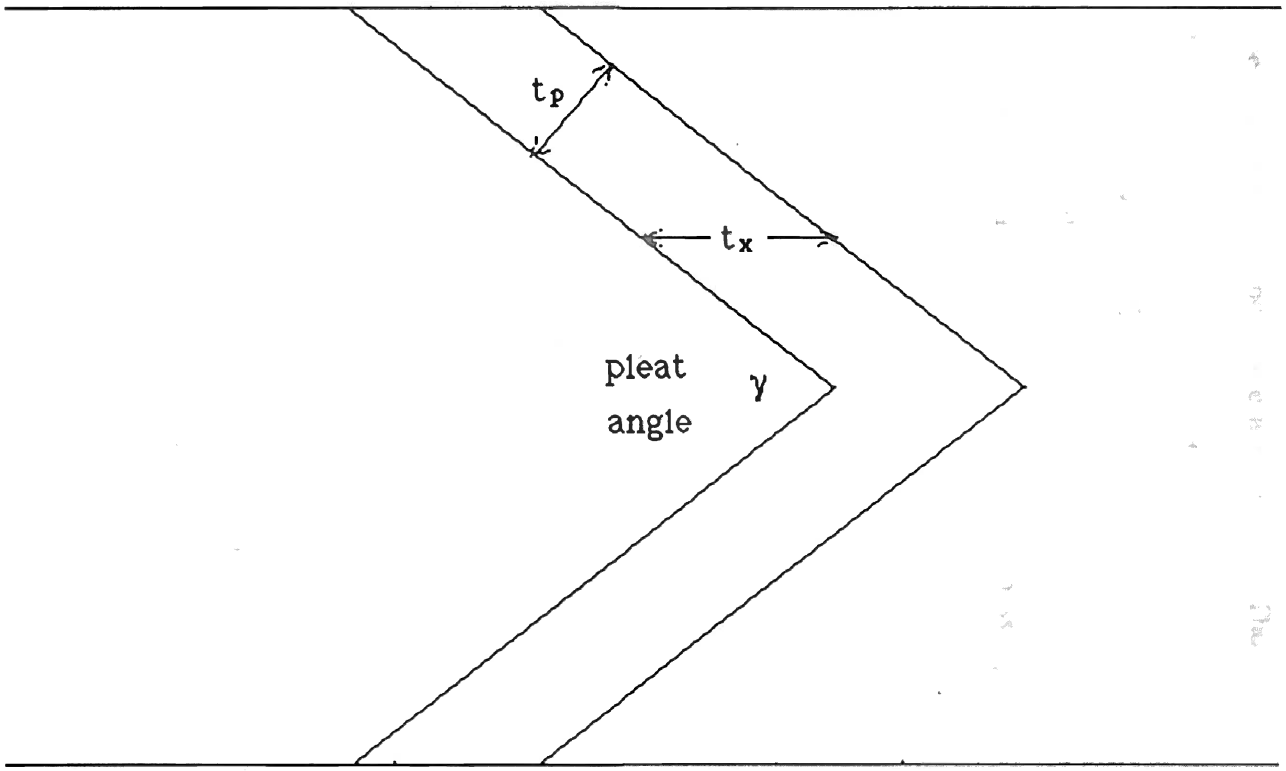

Figure 2.6 Filter Paper Thickness Definition

In Figure 2.5, one more filter pleat is added into the flow domain. The purpose of this setup is to investigate how the neighboring pleats will affect each other in this particular problem.

It is understood that the flow would like to cross the filter by passing through the grid corner, because the resistance there is minimum. Thus, there must be a reasonable number of cells set up inside the filter. In the source code, there are eight nodes set inside the filter. Figure 2.4 only shows five nodes.

Figure 2.6 shows the two different thicknesses caused by the small pleat angle γ. The paper thickness t_p and horizontal paper thickness t_x can be calculated by the following equation:

$$t_x = t_p / \sin(\frac{\gamma}{2}) \tag{2.55}$$

One must notice when the pleat angle γ is very small, t_p and t_x will be much different. For example, if paper thickness is 2mm and pleat angle is 15°, the horizontal paper thickness is 15.3mm. The pleat angle of real filter is usually smaller than 15°, hence this difference has to be considered.

2.9 Boundary Conditions

As described previously, it is assumed that the flow is uniform before the filter and a free slip boundary wall is used. For a free slip wall, the normal at the wall velocity there must be zero and tangential velocity should have no normal gradient. Interior normal velocity calculations take the zero normal wall values at the top and bottom side walls. The interior normal velocity at the inlet side wall takes given normal inlet velocity. All the external tangential velocities at the four side walls are set equal to their immediate interior values. Specification of normal velocities at an outflow boundary will influence the

upstream values. The method to determine the values is to impose the zero-normal gradient condition and set these values equal to their immediately upstream values[12].

For the SOLA algorithm, the free-slip boundary condition is usually considered more appropriate than the no-slip boundary condition [8] [10] [12], especially for coarse grid size. The boundary conditions at the four boundaries are specified in detail as follows:

Top Wall (free slip):

$$v_{i,jmax-1} = 0$$
$$u_{i,jmax} = u_{i,jmax-1}$$
$$k_{i,jmax} = k_{i,jmax-1}$$
$$\varepsilon_{i,jmax} = \varepsilon_{i,jmax-1}$$

Bottom Wall (free slip):

$$v_{i,1} = 0$$
$$u_{i,1} = u_{i,2}$$
$$k_{i,1} = k_{i,2}$$
$$\varepsilon_{i,1} = \varepsilon_{i,2}$$

Inlet Wall:

$$v_{1,j} = v_{2,j}$$
$$u_{1,j} = u_{2,j}$$
$$k_{1,j} = \frac{3}{2}(0.01V_{in})^2$$
$$\varepsilon_{1,j} = \frac{C_\mu k_{1,j}^{3/2}}{0.03D_{in}}$$

where V_{in} is inlet velocity, D_{in} is inlet diameter

Outlet Wall:

$$v_{imax,j} = v_{imax-1,j}$$
$$u_{imax,j} = u_{imax-1,j}$$
$$k_{imax,j} = k_{imax-1,j}$$
$$\varepsilon_{imax,j} = \varepsilon_{imax-1,j}$$

The notation of imax, jmax, imax-1 and jmax-1 correspond to Figure 2.2.

2.10 Flow Diagram of Source Code

Figure 2.7 displays the flow diagram of the FORTRAN code.

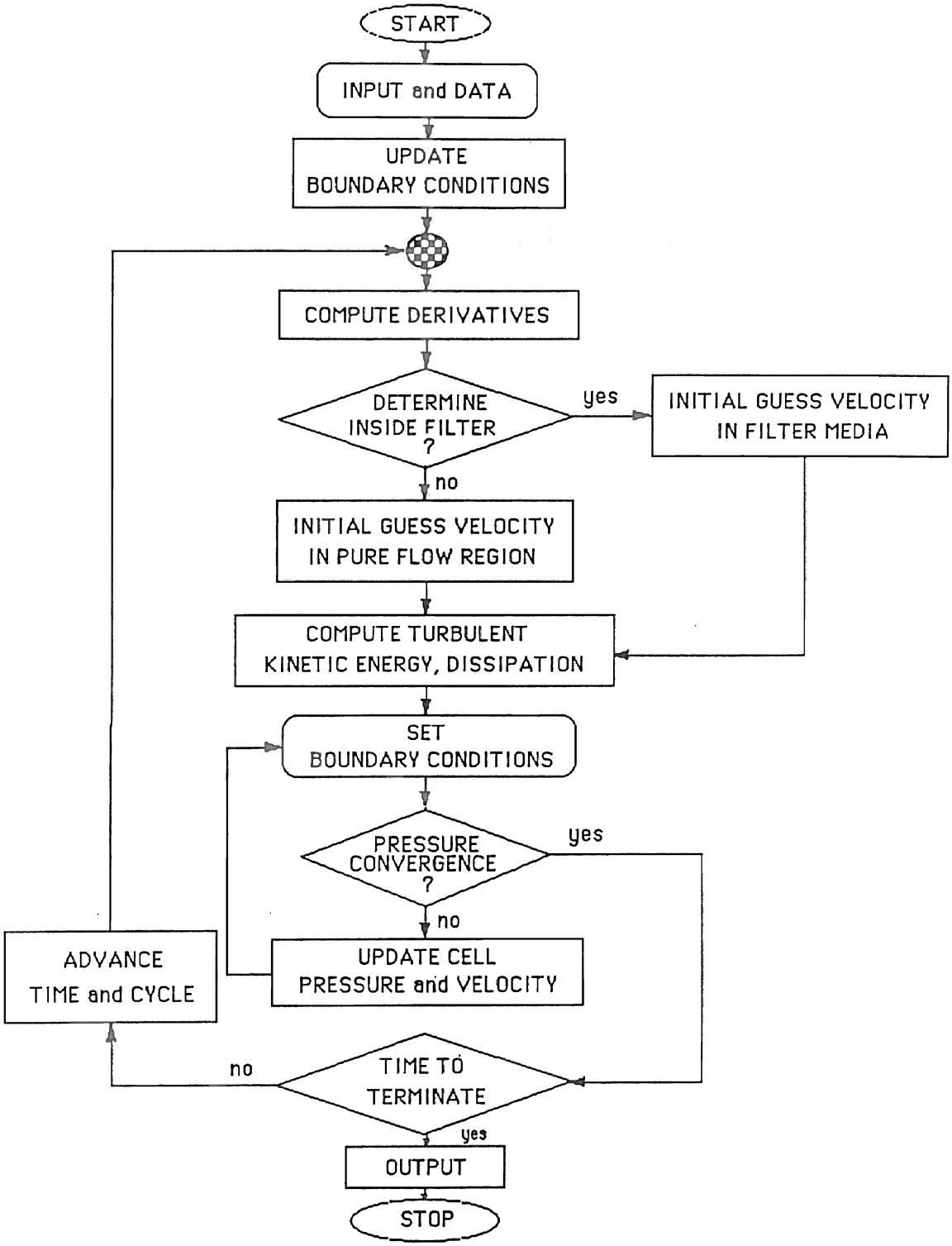

Figure 2.7 Flow Diagram of FORTRAN Code

CHAPTER III

INVESTIGATION OF PARAMETERS

Simple Calculations with Rectangular Shape Filter

In the filter flow calculation, the parameters that greatly affect the calculation must be investigated. These are the permeability coefficient, K, the inertial effect factor, b, the filter thickness, and the flow inlet velocity, Uin. Since there are not many references that can be used for choosing the proper parameters, we may try some of the options for test. This test also gives the ideas for setting the parameters of later calculations.

Three values of the permeability coefficient K are chosen for comparison. The value of $K=10^{-6}$ m^2 is considered as high permeability porous media [20]. The magnitude of $K=10^{-8}$ m^2 as lower permeability porous media is proposed by the experiment in reference [7].

The grid system for the simple calculations in this chapter is show in Figure 3.1. It is considered that there must be at least five layers of grid in the porous media. Since the filter paper is very thin compared with the flow field, a very small step size has to be chosen in order to make enough nodes in the porous media.

The simplest case for calculation is only to set one node inside filter. One can obtain some ideas from the following result figures about the porous media in this very simple calculation.

References[4, 7, 20] suggest using the extended Darcy's law with the extra inertial term in the filter calculation. However, one may still like to know what is the real

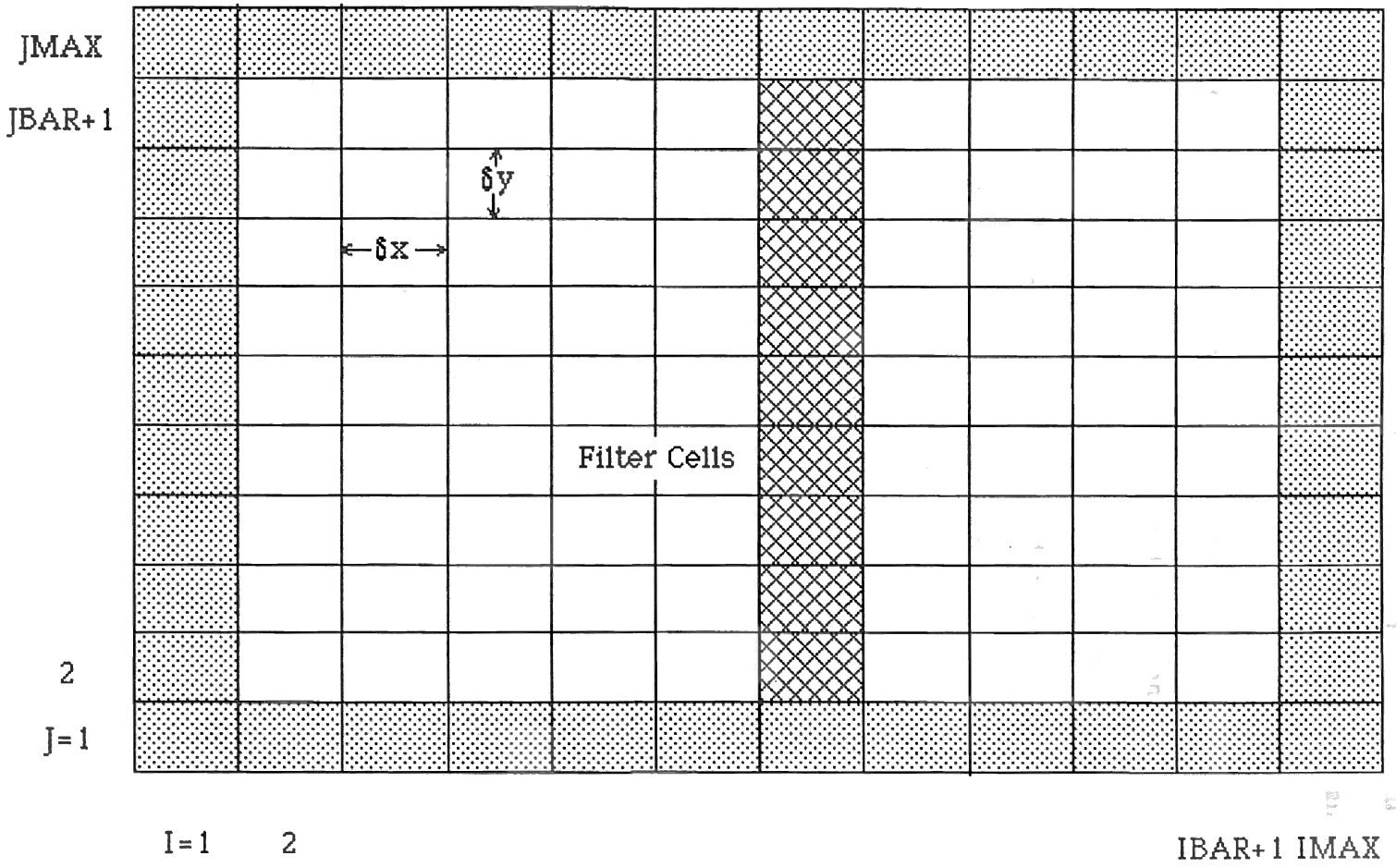

Figure 3.1 Rectangular Shape Filter in Simple Calculations

significance of the inertial effect. Two values of inertial factor were chosen for the calculation, 0 for non-inertial effect and 1147 m^{-1} with the inertial effect. The experimental value 1147 m^{-1} is used by Gurumoorthy [7] in his thesis on air intake system calculation.

The inlet velocity is also a very important parameter to affect the result of the calculation and the filter performance. The values of 1m/s and 5m/s are used in two cases of calculations for comparison. The comparison shows the effect of inlet velocity.

Table 3.1 lists all the parameters that are used in the FORTRAN code. IBAR and JBAR will determine the length of the flow field in the calculation. The value of cell size is chosen to determine reasonable thickness of porous media in the flow field. Since the filter media step size is very small, the time increment is also very small.

TABLE 3.1

PARAMETERS IN RECTANGULAR FILTER CALCULATION

number of cells in x direction	IBAR	42
number of cells in y direction	JBAR	10
width of cell in x direction	DELX	0.001m
width of cell in y direction	DELY	0.001m
time increment step size	DELT	5×10^{-5} sec
kinematics viscosity	NU	1.5×10^{-5} m^2/sec
pressure iteration criterion	EPSI	5×10^{-3}
scaling factor for convergence	D0	1.0
inlet velocity in x direction	Uin	1.0 or 5.0 m/s
computing time to be terminated	TWFIN	10^{-2} sec
over relaxation factor	OMG	1.7
donor cell fluxing coefficient	ALPHA	0.70

TABLE 3.1 (Continued)

porous media permeability in x	Kx	$10^{-6}, 10^{-7}$ or 10^{-8} m^2
porous media permeability in y	Ky	$10^{-6}, 10^{-7}$ or 10^{-8} m^2
inertial term factor in x	bx	1147.0 or 0 m^{-1}
inertial term factor in y	by	1147.0 or 0 m^{-1}
boundary conditions	Free Slip	

The parameters are tested by comparing the pressure change along the flow domain. The reference pressure is at outlet which is 0 Pa. In Figures 3.2 to 3.7, the third node is set as filter node. The filter thickness is equal to the increment step size.

For all cases, the pressure drop with $K=10^{-8}\,m^2$ is much greater than with the other two K values. Since the permeability of the filter is usually of the order of 10^{-8} m^2 [7], one must pay attention to the different result of pressure drop caused by this parameter.

The first three Figures 3.2, 3.3, and 3.4 give comparisons of the pressure drop in one node layer filter by changing the size of the nodes. Increasing the node size is equivalent to increasing the filter thickness, thus making greater pressure drop. The increase of pressure drop is linear with the change in node size.

The flow position in figures is counted from inlet, 0 m. If the increment step size is 0.001 and there are ten nodes in the flow domain. the outlet flow position is 0.011 m.

The only difference in parameters between Figure 3.5 and 3.2 is the inertial factor is set to 0 m^{-1}. By the comparison of figures, it is observed that the inertial factor cannot be neglected. Since the inertial effect really significantly affects the flow pressure field, it has to be included in the later calculations.

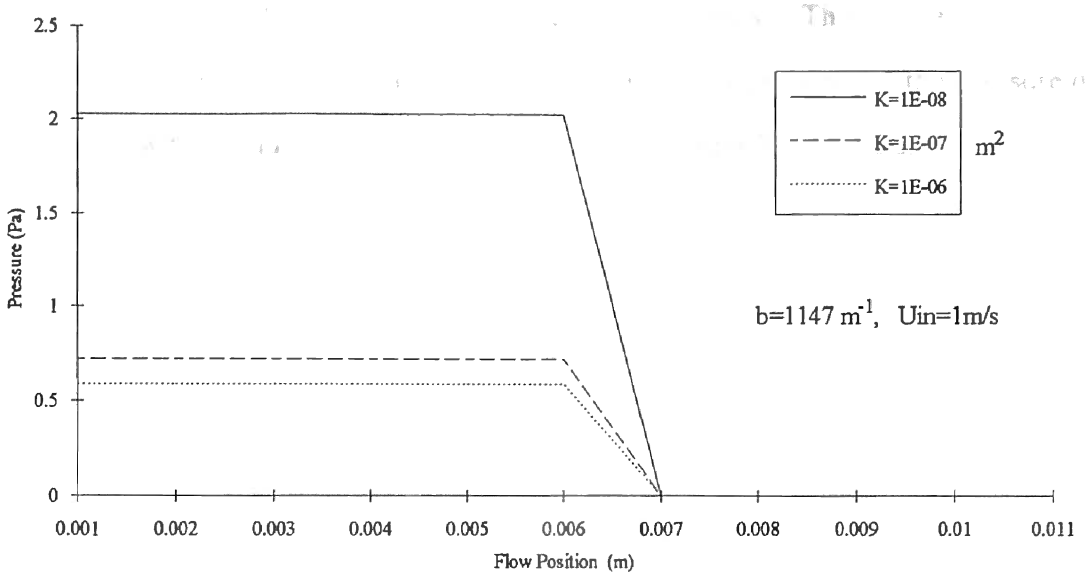

Figure 3.2 Pressure Profile Across the Filter with Node Size 0.001 m, $b=1147\,m^{-1}$, Uin=1m/s

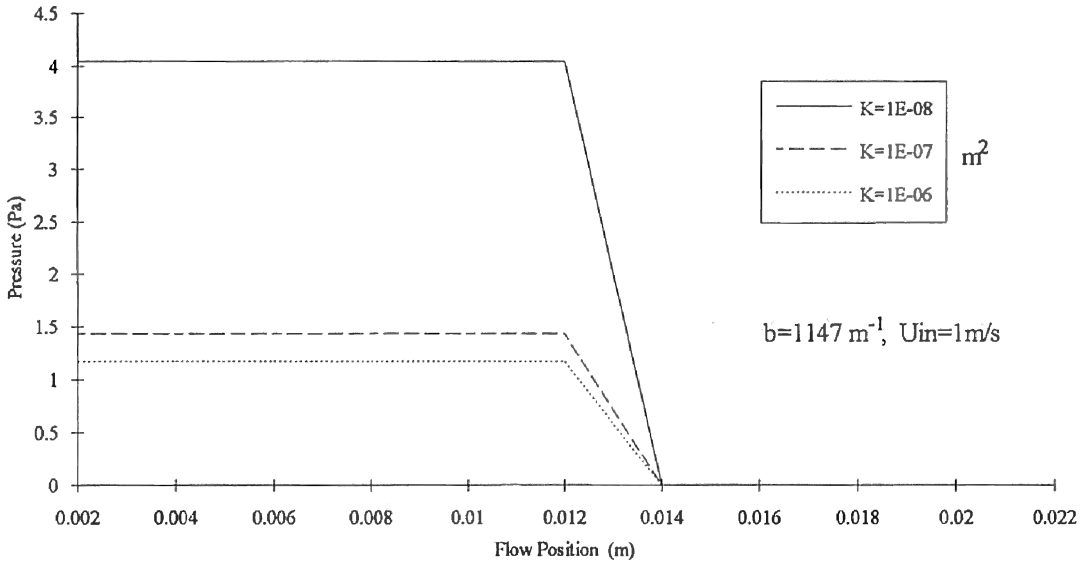

Figure 3.3 Pressure Profile Across the Filter with Node Size 0.002 m, $b=1147\,m^{-1}$, Uin=1m/s

In Figure 3.6, the inlet velocity is increased to 5m/s. This causes much larger pressure drop than the inlet velocity of 1m/s in Figure 3.2. For example, the pressure drop in Figure 3.2 with K equal to $10^{-7}\,m^2$ is 0.7 Pa, but in Figure 3.6 is 15 Pa.

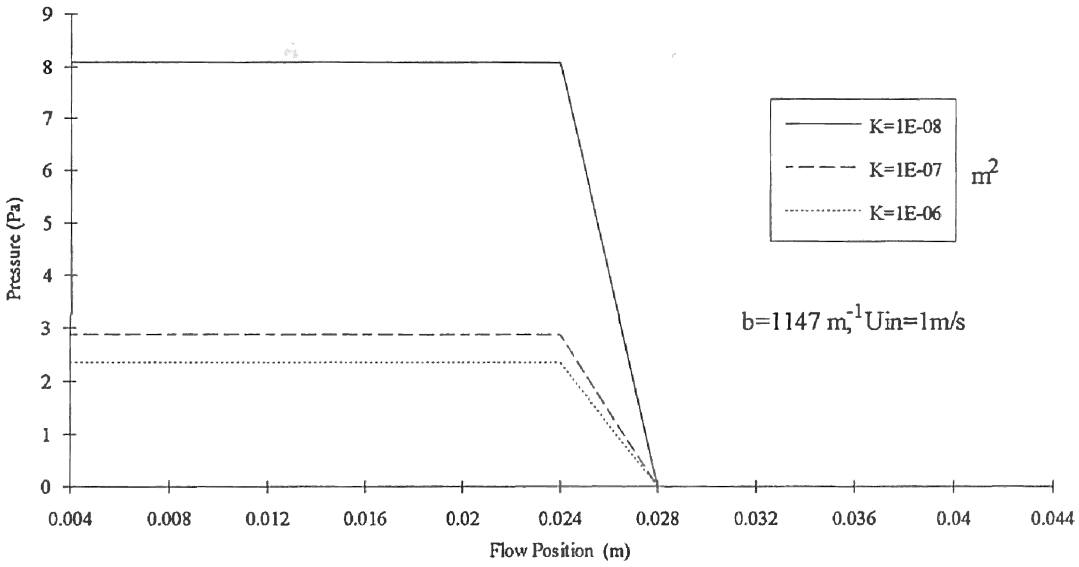

Figure 3.4 Pressure Profile Across the Filter with Node Size 0.004 m, $b=1147\,m^{-1}$, Uin=1m/s

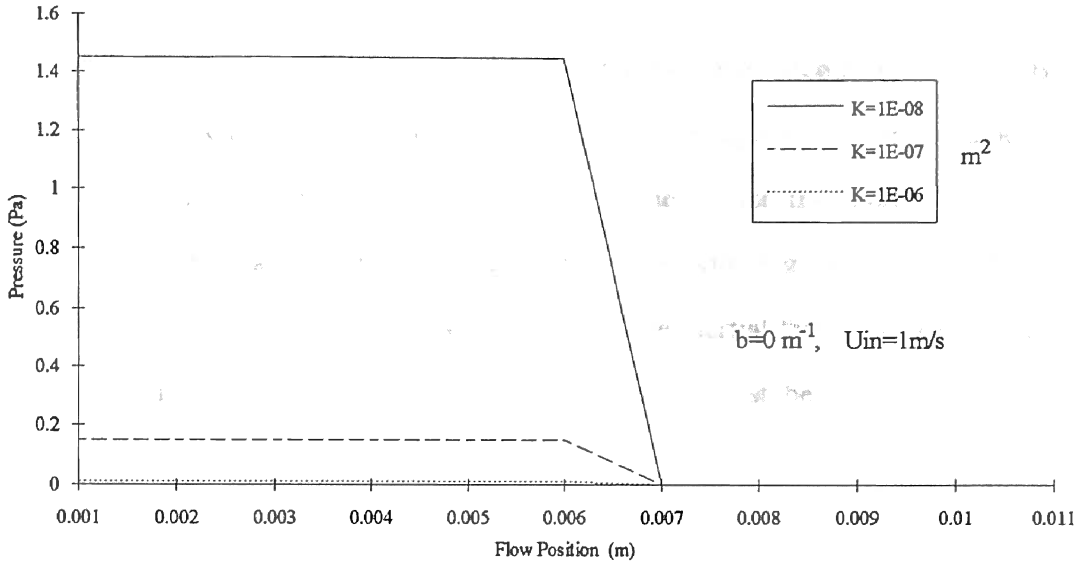

Figure 3.5 Pressure Profile Across the Filter with Node Size 0.001 m, $b=0\,m^{-1}$, Uin=1m/s

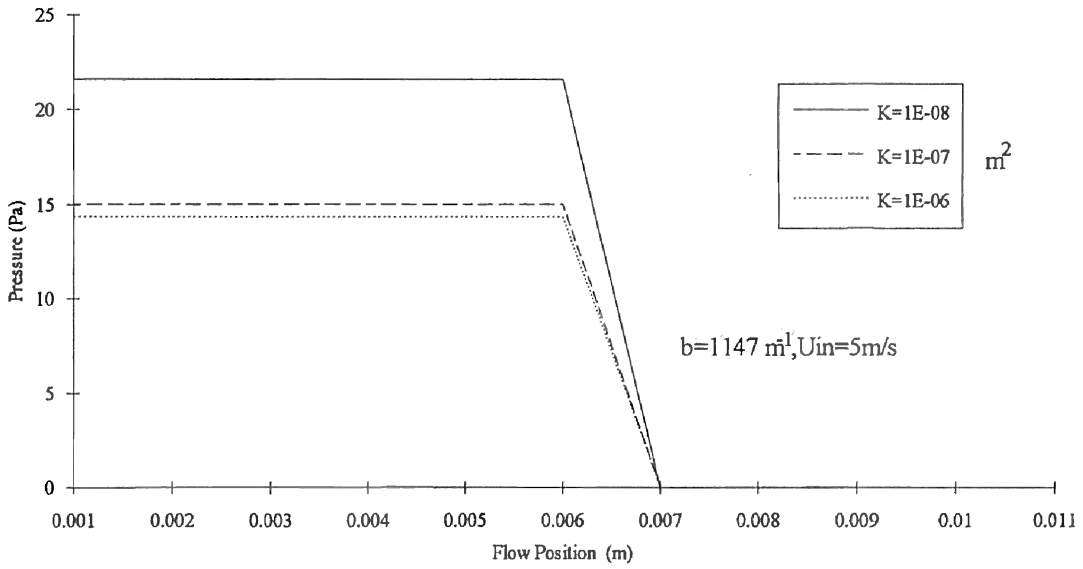

Figure 3.6 Pressure Profile Across the Filter with Node Size 0.001 m, $b=1147\,m^{-1}$, Uin=5m/s

In Figure 3.7, the significance of the inertial factor is once again tested. But this time, the inlet velocity is 5m/s. There is a big pressure change at the higher velocity. This makes sense, since the higher the flow velocity, the higher the inertial energy that it contains. Then the larger kinetic energy it will lose with higher pressure drop. This comparison provides two conclusions. One is that the inertial factor has to be considered especially at high velocity and another is that velocity must be chosen properly in the calculation.

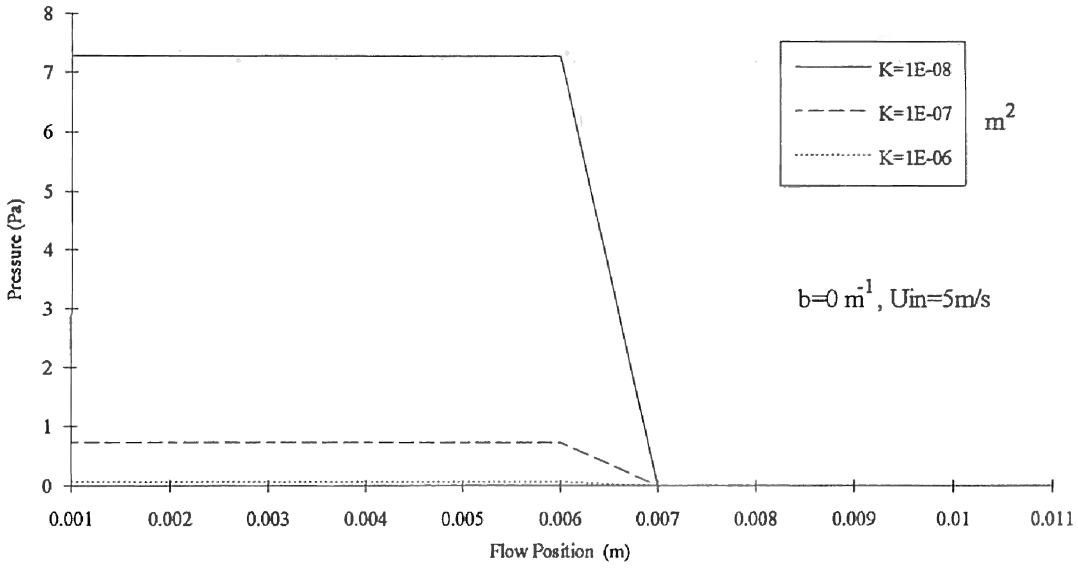

Figure 3.7 Pressure Profile Across the Filter with Node Size 0.001 m, b=0 m^{-1}, Uin=5m/s

From Figure 3.8 to Figure 3.10, there are five nodes of porous media put in the flow calculation field. The common conclusion in these figures is the pressure drop is linear. The more nodes in the flow field, the more pressure drop in the flow.

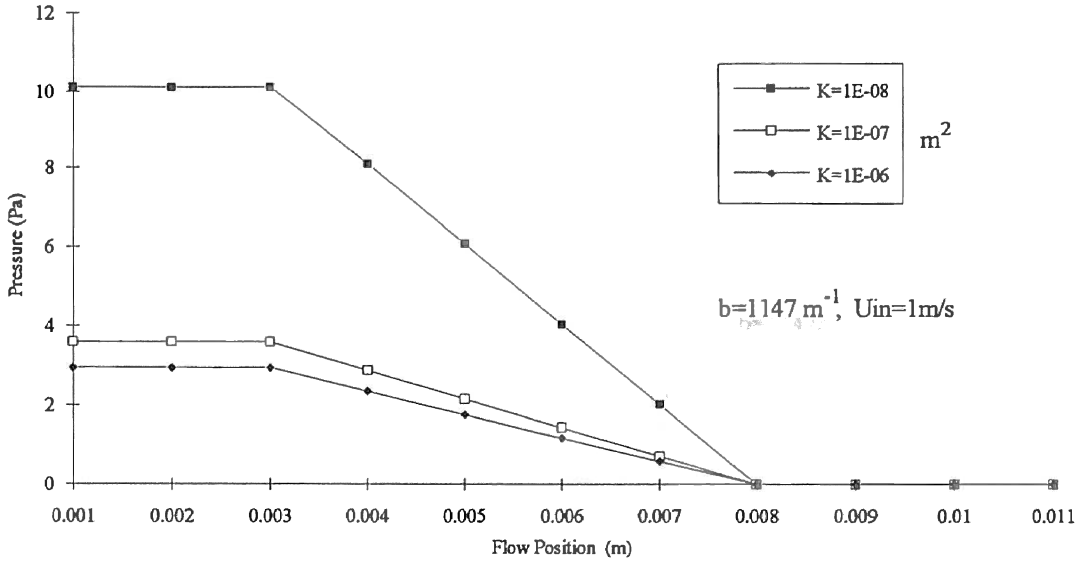

Figure 3.8 Pressure Profile Across the Filter with Node Size 0.001 m, b=1147 m^{-1}, Uin=1m/s, Five Nodes inside Filter

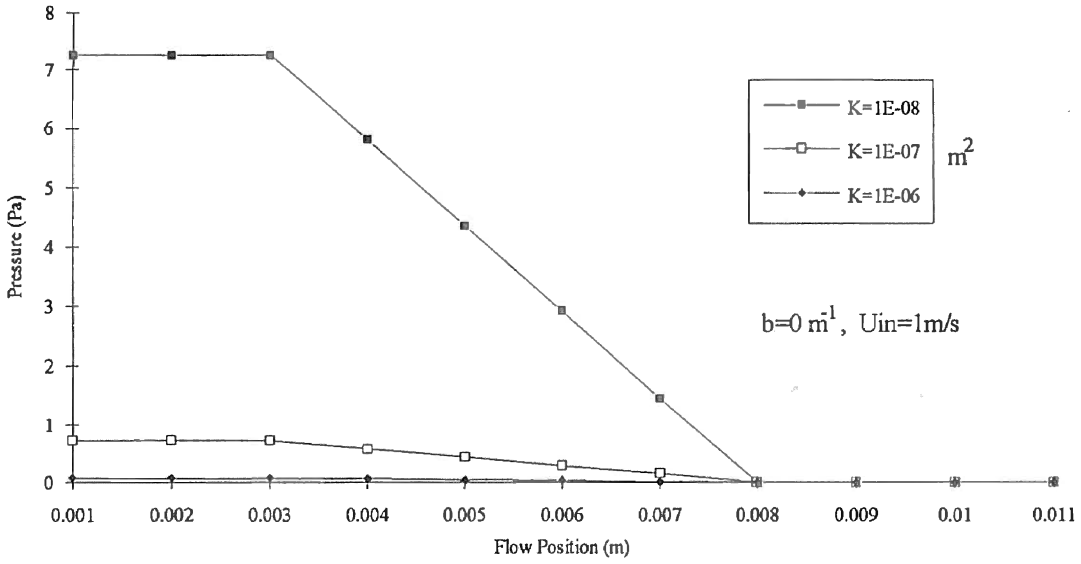

Figure 3.9 Pressure Profile Across the Filter with Node Size 0.001 m, b=0 m^{-1}, Uin=1m/s, Five Nodes inside Filter

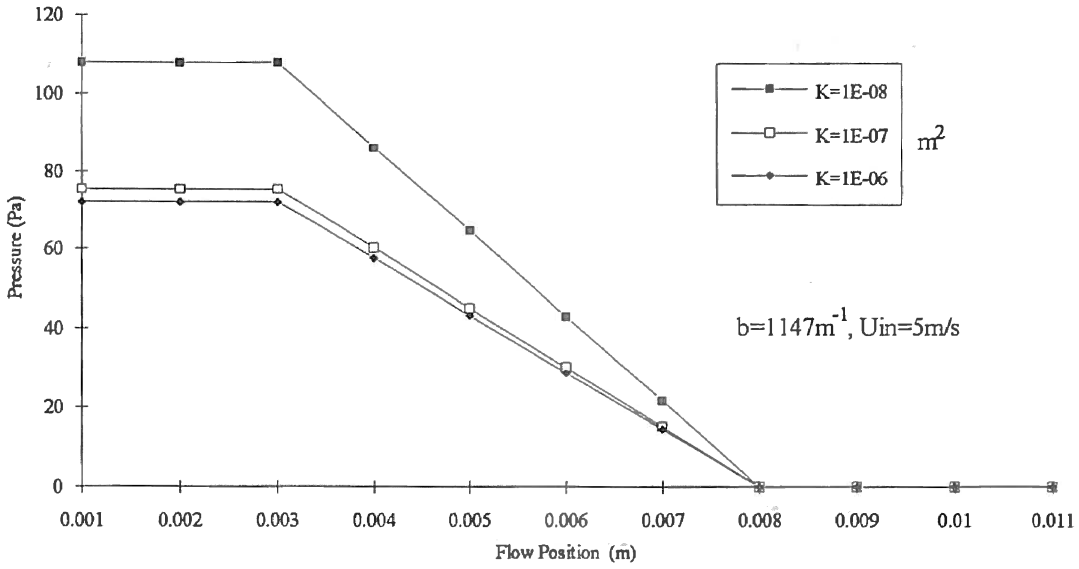

Figure 3.10 Pressure Profile Across the Filter with Node Size 0.001m, $b=1147m^{-1}$, Uin=5m/s, Five Nodes inside Filter

The next figure, Figure 3.11, is obtained from calculations using the assumption that the whole flow field is porous media, without any pure flow region ($K=\infty$). We still find the pressure drop is linear in the porous media.

Figure 3.12 and Figure 3.13 present the pressure change with the inlet velocity. This is equivalent to changing the flow rate in an experiment. The pressure change is slightly nonlinear in Figure 3.12. This is caused by the inertial term with velocity squared. The effect of computation without the inertial term is also presented for comparison. It is straight forward that the relationship is linear. Once again, the permeability coefficient K with value 10^{-8} m^2 showed a stronger effect in the calculation.

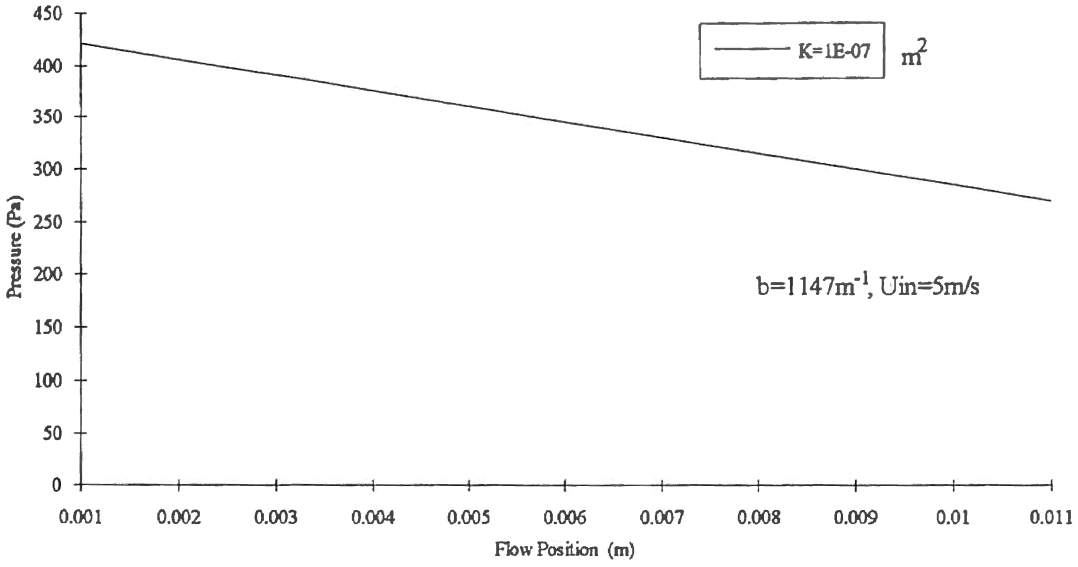

Figure 3.11 Pressure Profile Inside Filter with node size 0.001m, b=1147m^{-1}, Uin=5m/s

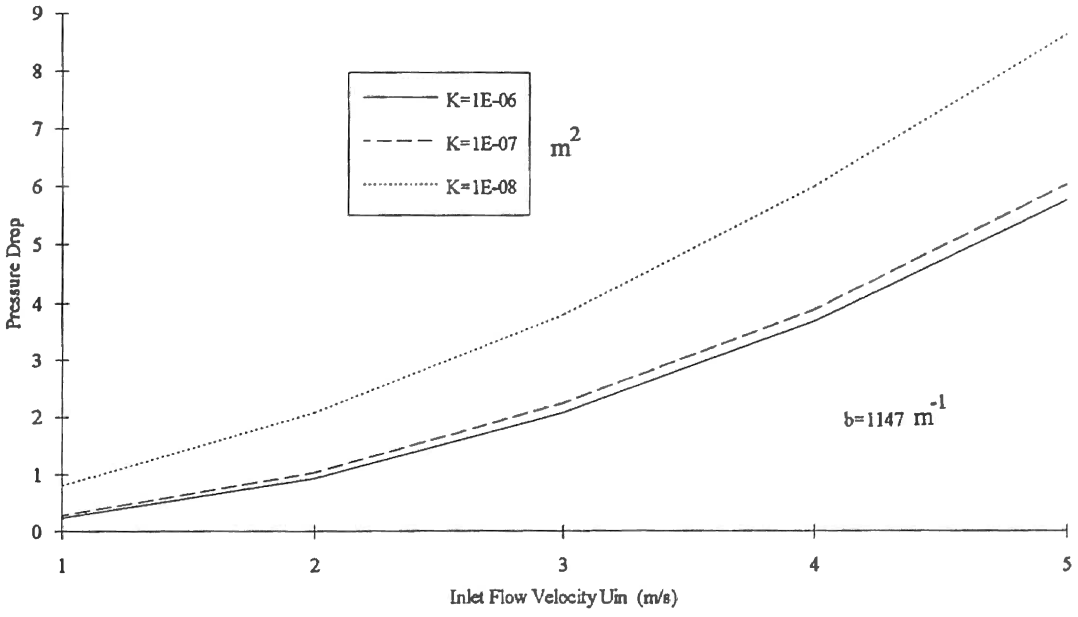

Figure 3.12 Pressure Profile for Changing Flow Velocity with b=1147m^{-1}

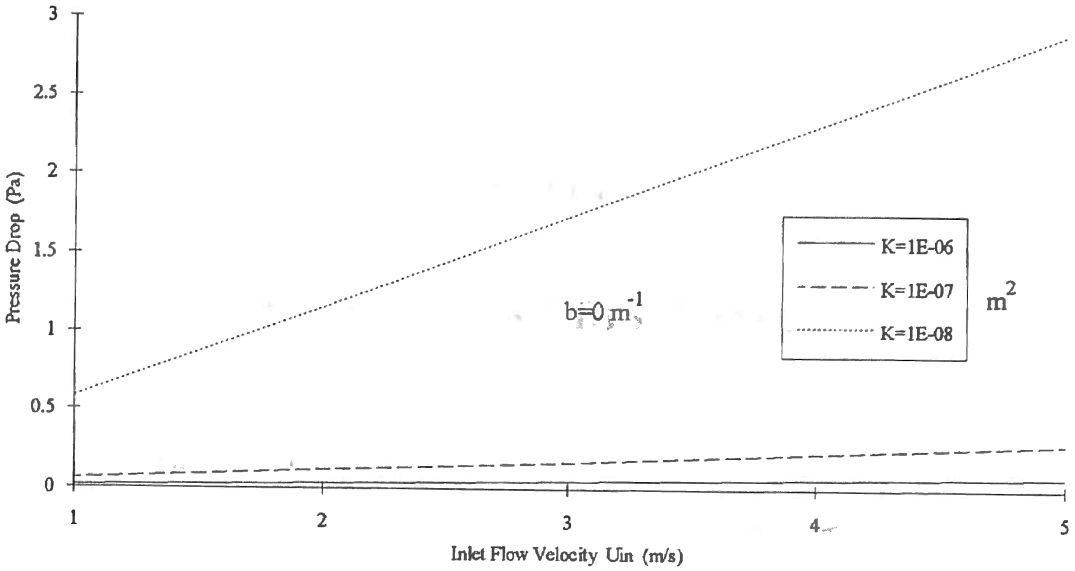

Figure 3.13 Pressure Profile for Changing Flow Velocity with $b=0\,m^{-1}$

CHAPTER IV

RESULTS AND DISCUSSION

4.1 List of Parameters in Calculations

Some important parameters used for calculation have been discussed in Chapter III. There are fourteen different parameter combinations used in the calculations presented in this chapter. Table 4.1 presents the parameters which are the same for all fourteen cases. Table 4.2 lists the parameters used in cases 1 to 4, for which the inlet velocity is varied. These calculations show how the flow field will be affected by inlet velocity.

With other parameters kept the same as case 1, the inertial effect factor b is changed to zero in case 5 and permeability coefficient K is changed in case 6. These calculations show how the inertial factor and permeability affect two dimensional filter fluid flow. The parameters are presented in Table 4.3.

It is understood that the filter is not isotropic when the inertial factor b and permeability coefficient K are not equal in horizontal and vertical directions. Thus, inertial factor b and permeability K are set unequal in two directions with one kept the same. There are four combinations set for the calculations in case 7, 8, 9, 10, in which different Kx and Ky or bx and by are used.

So far, all the cases are calculated under the assumption of one percent turbulent kinetic energy at the inlet. In case 11, thirty percent is used to compare with case 1.

Next, in case 12 the horizontal paper thickness, t_x, of the filter is increased ten times to compare with case 1. The thickness used here is horizontal paper thickness t_x

which has been discussed in Figure 2.6. The t_x in case 1 is 0.0024m for eight nodes inside the filter (8x0.0003m) and in case 12, t_x is 0.024m (8x0.003m). For 15° pleat angle γ, the correspondent paper thickness t_p is about 0.00032m in case 1 and 0.0032 in case 12. This investigation will present some effects of the filter thickness.

It is interesting to know how flow around the filter will be changed when the pleat angle is varied. The paper thickness t_p is kept constant as 2mm in case 13 while the pleat angle γ is varied as 15° and 45° respectively. The comparison of the parameters is shown in Table 4.6.

Finally, there are two adjoining filter pleats set in the computed flow field, which is shown in Figure 2.4 . The case 14 demonstrates that the flow field is not affected much by these simple geometry and boundary conditions.

TABLE 4.1

UNCHANGED PARAMETERS IN FILTER FLOW

CALCULATIONS, CASES 1-13

number of cells in x direction	IBAR	42
number of cells in y direction	JBAR	10
number of nodes inside the filter	Nnode	8
time increment step size	DELT	4×10^{-5} sec
kinematic viscosity	NU	1.5×10^{-5} m^2/sec
pressure iteration criterion	EPSI	5×10^{-2}
scaling factor for convergence	D0	1.0
computing time to be terminated	TWFIN	10^{-2} sec
over relaxation factor	OMG	1.7
donor cell fluxing coefficient	ALPHA	0.80
boundary conditions	Free Slip	

TABLE 4.2

PARAMETERS IN FILTER FLOW CALCULATIONS CASES 1-4

		Case 1	Case 2	Case 3	Case 4
width of cell in x direction	DELX (m)	0.0003	0.0003	0.0003	0.0003
width of cell in y direction	DELY (m)	0.00004	0.00004	0.00004	0.00004
*inlet velocity in x direction	Uin (m/s)	3.0	5.0	7.0	1.0
porous media permeability in x	Kx (m^2)	10^{-8}	10^{-8}	10^{-8}	10^{-8}
porous media permeability in y	Ky (m^2)	10^{-8}	10^{-8}	10^{-8}	10^{-8}
inertial term factor in x	bx (m^{-1})	1147.0	1147.0	1147.0	1147.0
inertial term factor in y	by (m^{-1})	1147.0	1147.0	1147.0	1147.0

* indicates the varied parameter for comparison

TABLE 4.3

PARAMETERS IN FILTER FLOW CALCULATIONS

CASES 5-6

		Case 5	Case 6
width of cell in x direction	DELX (m)	0.0003	0.0003
width of cell in y direction	DELY (m)	0.00004	0.00004
inlet velocity in x direction	Uin (m/s)	3.0	3.0
*porous media permeability in x	Kx (m^2)	10^{-8}	10^{-7}
*porous media permeability in y	Ky (m^2)	10^{-8}	10^{-7}
*inertial term factor in x	bx (m^{-1})	0	1147.0
*inertial term factor in y	by (m^{-1})	0	1147.0

TABLE 4.4

PARAMETERS IN FILTER FLOW CALCULATIONS

CASES 7-10

		Case 7	Case 8	Case 9	Case 10
width of cell in x direction	DELX (m)	0.0003	0.0003	0.0003	0.0003
width of cell in y direction	DELY (m)	0.00004	0.00004	0.00004	0.00004
inlet velocity in x direction	Uin (m/s)	3.0	3.0	3.0	3.0
*porous media permeability in x	Kx (m^2)	10^{-8}	10^{-7}	10^{-8}	10^{-8}
*porous media permeability in y	Ky (m^2)	10^{-7}	10^{-8}	10^{-8}	10^{-8}
*inertial term factor in x	bx (m^{-1})	1147.0	1147.0	547.0	1147.0
*inertial term factor in y	by (m^{-1})	1147.0	1147.0	1147.0	547.0

Case 11:

Table of parameters is same as case 1 but inlet kinetic energy is set as:

$k_{1,j} = \frac{3}{2}(0.3V_{in})^2$ instead of $k_{1,j} = \frac{3}{2}(0.01V_{in})^2$ in case 1.

TABLE 4.5

PARAMETERS IN FILTER FLOW

CALCULATIONS CASE 12

		Case 12
*width of cell in x direction	DELX (m)	0.003
*width of cell in y direction	DELY (m)	0.0004
inlet velocity in x direction	Uin (m/s)	3.0
porous media permeability in x	Kx (m^2)	10^{-8}

TABLE 4.5 (Continued)

		Case 12
porous media permeability in y	Ky (m^2)	10^{-8}
inertial term factor in x	bx (m^{-1})	1147.0
inertial term factor in y	by (m^{-1})	1147.0

TABLE 4.6

PARAMETERS IN DIFFERENT PLEAT ANGLE CASE 13

*Pleat Angle		15°	45°
paper thickness	t_p (m)	0.002	0.002
horizontal paper thickness	t_x (m)	0.01532	0.00523
width of cell in x direction	DELX (m)	0.001915	0.000653
width of cell in y direction	DELY (m)	0.000252	0.000271
inlet velocity in x direction	Uin (m/s)	3.0	3.0
porous media permeability in x	Kx (m^2)	10^{-8}	10^{-8}
porous media permeability in y	Ky (m^2)	10^{-8}	10^{-8}
inertial term factor in x	bx (m^{-1})	1147.0	1147.0
inertial term factor in y	by (m^{-1})	1147.0	1147.0

Case 14:

Table of parameters is same as case 1 but there are two filter pleats:

JBAR = 20

4.2 Results

4.2.1 Velocity Vector Plots

In order to help to view the results and to understand the pattern of flow well, the results are presented in velocity vector plots. The arrow head points in the flow direction and the arrow length represents the velocity magnitude. The filter media region is represented by two tri-angular lines.

Figure 4.1a presents the scaled velocity vector plot of case 1. Here the "scale" means the reference velocity used for the plot. In the scaled plot, the horizontal and vertical velocity plot scales should be the same. In Figure 4.1a, 3m/s, the inlet velocity, is used as reference velocity for both components. Figure 4.1b is a vector plot of velocity which is amplified to show the flow direction variation. Since the vertical velocity plot scale is smaller than the horizontal one, the vertical arrow length looks like it is amplified. Here 3m/s is used as horizontal velocity plot scale and 1m/s is used as vertical velocity scale. When the paper thickness is increased, the variation of velocity magnitude is much larger, hence, the view of vector plot is different. Figure 4.2a and 4.2b show the scaled and amplified vector plot for case 12 in which the horizontal paper thickness t_x is increased ten times thicker than case 1. It is obvious that the vector plot are different under the same plot scale as case 1. Because there is no significant observable difference in of the vector plot in other cases, they are not shown here.

Note that since the horizontal flow field length (42 x 0.0003) is much larger than the vertical height (10 x 0.00004), the angle of the triangular filter pleat, γ, cannot be plotted in scale. It may be observed from the plots that there are three major changes in direction of the flow near and in the filter.

The first is when flow is approaching the triangular filter in the contraction area. Since the flow at lines close to the top or bottom boundary reaches the filter cell first, it

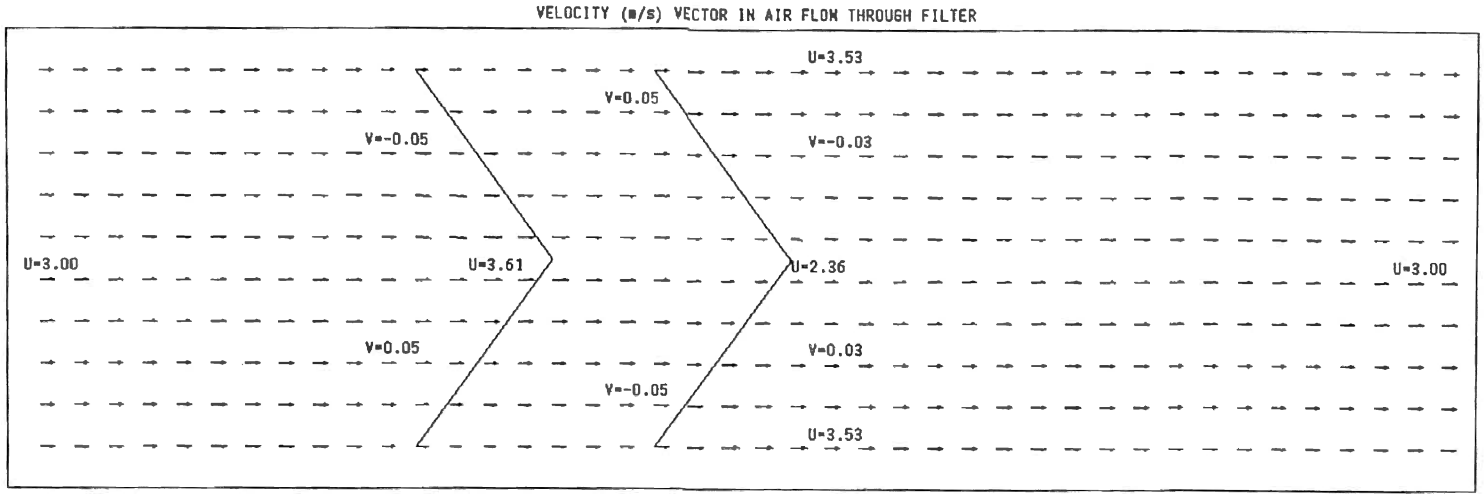

a. Scaled Velocity Vectors

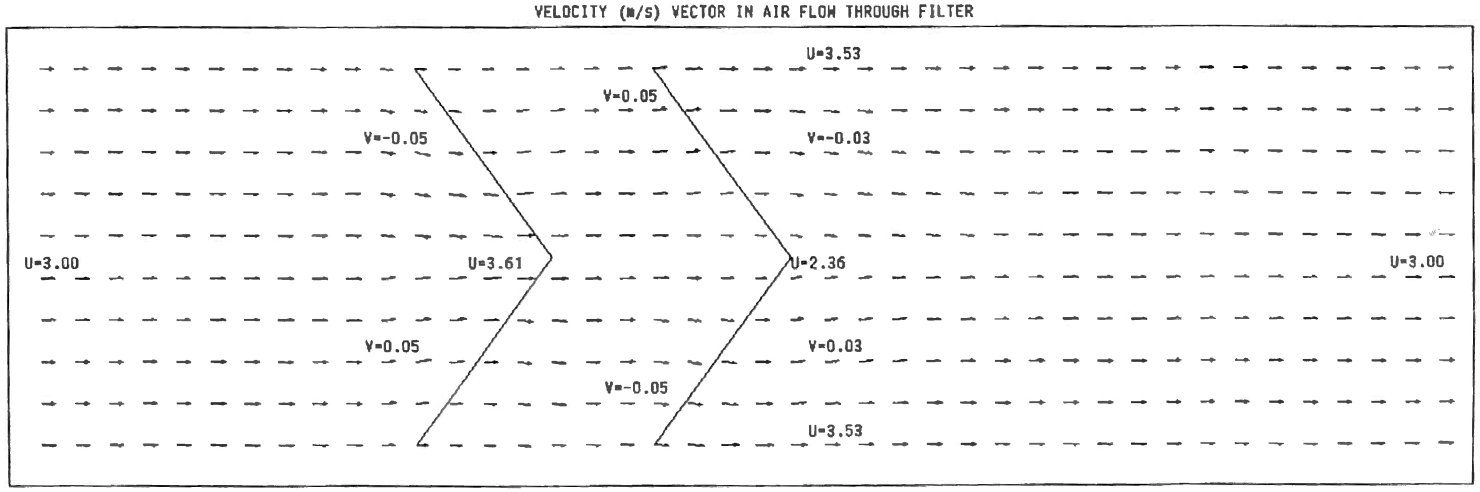

b. Amplified Flow Velocity Vectors

Figure 4.1 Velocity Vector Plots in Case 1

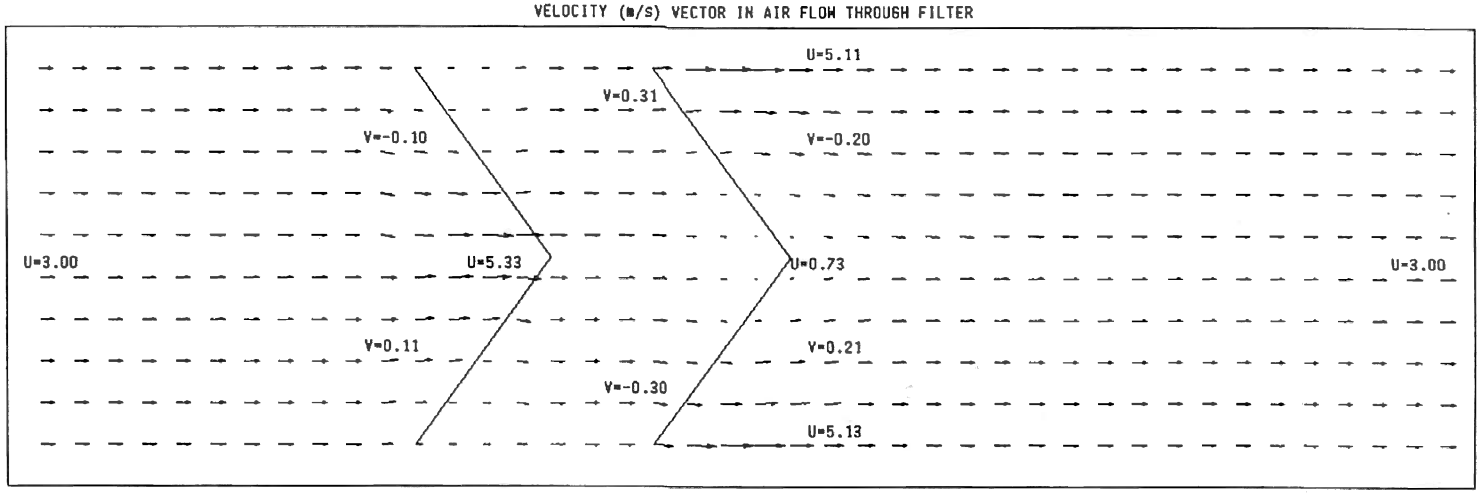

a. Scaled Velocity Vectors

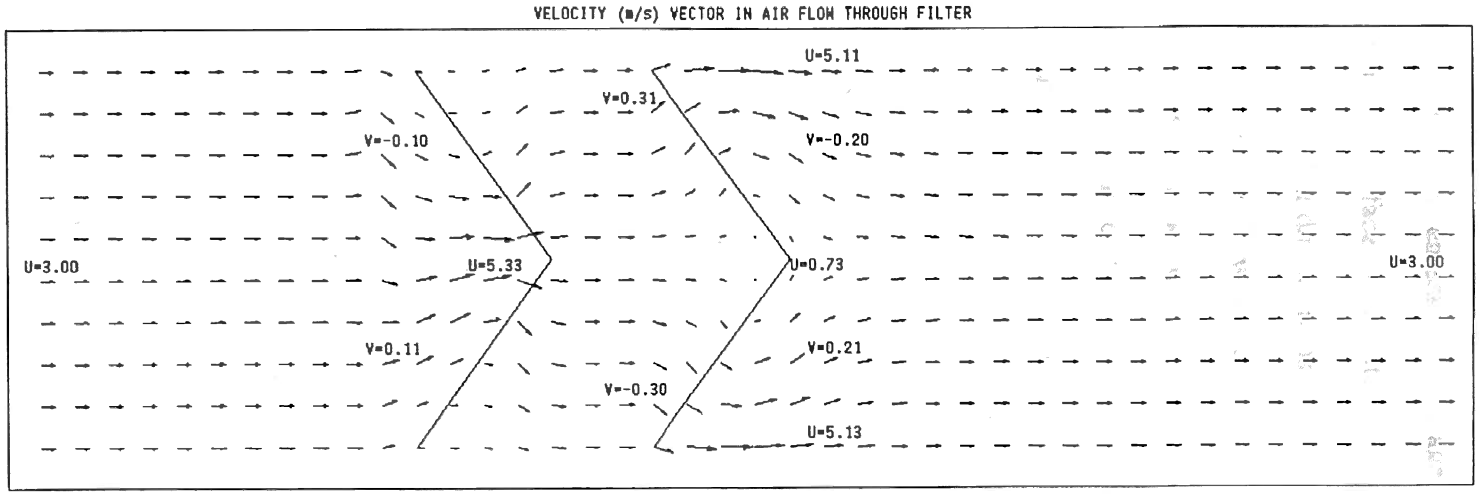

b. Amplified Flow Velocity Vectors

Figure 4.2 Velocity Vector Plots in Case 12

tends to change direction toward the center area where the resistance is smaller. So, the flow looks like flow in a contraction.

The second change in direction occurs when the flow enters the filter again due to the resistance effect. Since the resistance normal to the surface of the filter is smaller than that in other directions, the flow naturally tends to go in that direction instead of others.

The third area of flow direction change is after the flow leaves the filter media. The flow close to the top and bottom boundary mixes with the centerline flow. There are several reasons for this phenomena. One is that the pressure at the center line is smaller than that far from the center line. Another is that the flow velocity at the area near the side wall is greater than that close to the centerline. The high velocity flow area will compensate the low velocity flow area. The non-uniform flows at different lines mix together and eventually become uniform flow. It is obvious that the flow is uniform at the exit in this case.

The changes of the flow are easy to see from the value of the vertical component velocity variation that will be discussed in more detail in section 4.2.3.

4.2.2 Normal Velocity Along Filter Surface

The normal velocity is the flow velocity component on the normal direction which is 90° towards the filter surface. The normal velocity component is calculated with given horizontal and vertical component velocities, and the pleat angle γ which is 15° in the following calculation. Because the flow is not primarily normal but streamwise, the normal component velocity is usually small.

The normal velocity along the filter surface is important to predict the behavior of the flow crossing the pleated filter. This normal velocity can help to predict how dust will accumulate on the filter surface. Figure 4.3 shows the position of normal velocity that has been calculated. The ten points are on the surface of the filter entrance.

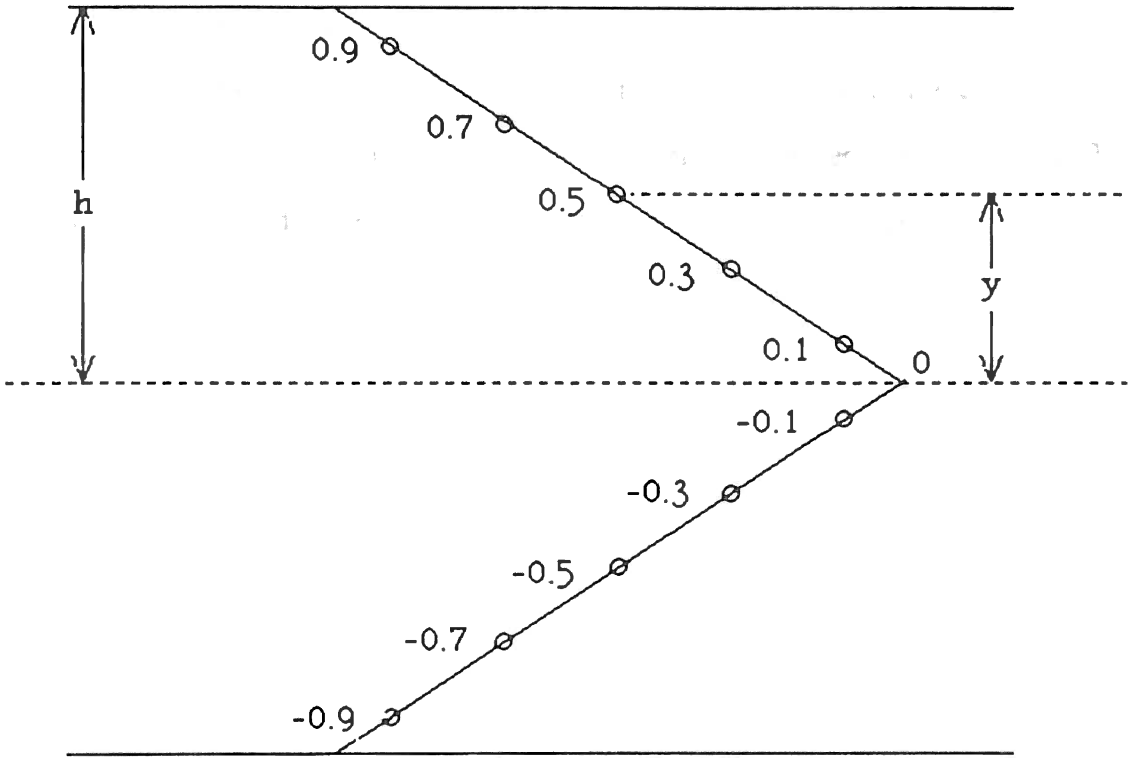

Figure 4.3 Normal Velocity Positions Along Filter Surface in Calculation

Figures 4.4 to Figure 4.9 are results for different inlet flow velocities. There is a limiting velocity, which has different profile shapes when the velocity is below or above it. The limit in this problem is a little below 2m/s. The shape of the profiles at velocity Uin above 2m/s is convex and the profiles are concave in the middle of filter when inlet velocity is below 2m/s. The larger the velocity, the more convex or the smaller the velocity, the more concave.

The reason for this behavior may be that the main flow with higher velocity is not affected much by the contraction region before the flow enters the filter. The flow with lower velocity, and lower momentum, will be affected more strongly.

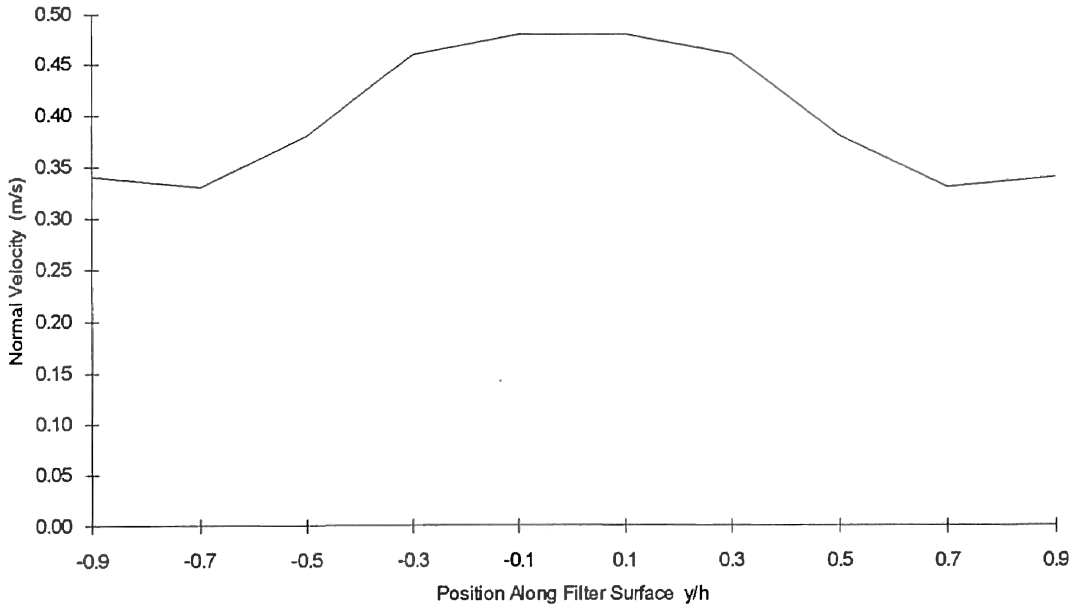

Figure 4.4 Normal Velocity Along Filter Surface at Uin=3m/s (Case 1)

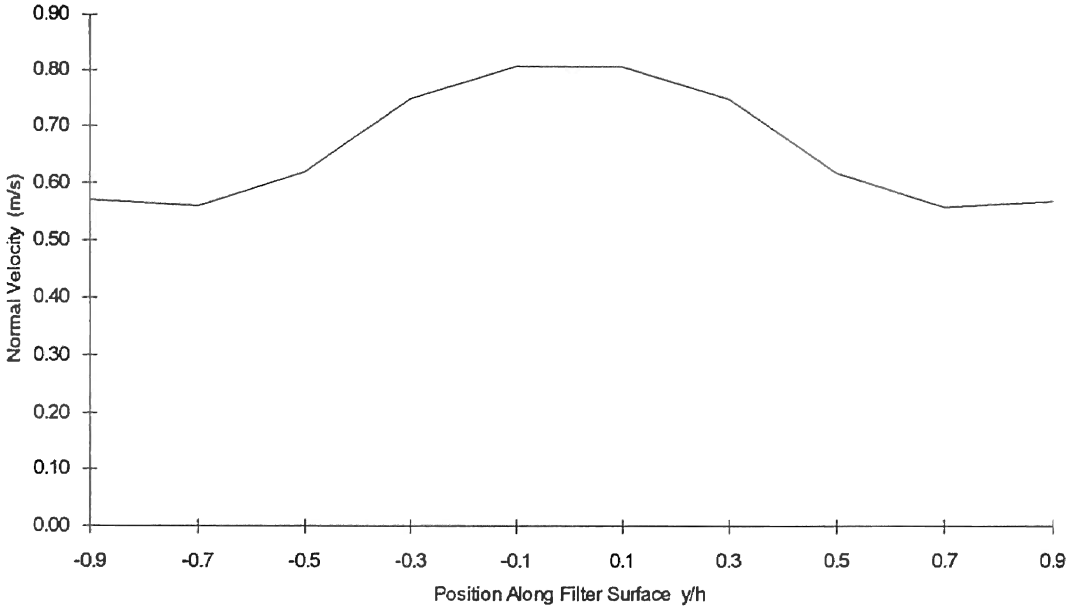

Figure 4.5 Normal Velocity Along Filter Surface at Uin=5m/s (Case 2)

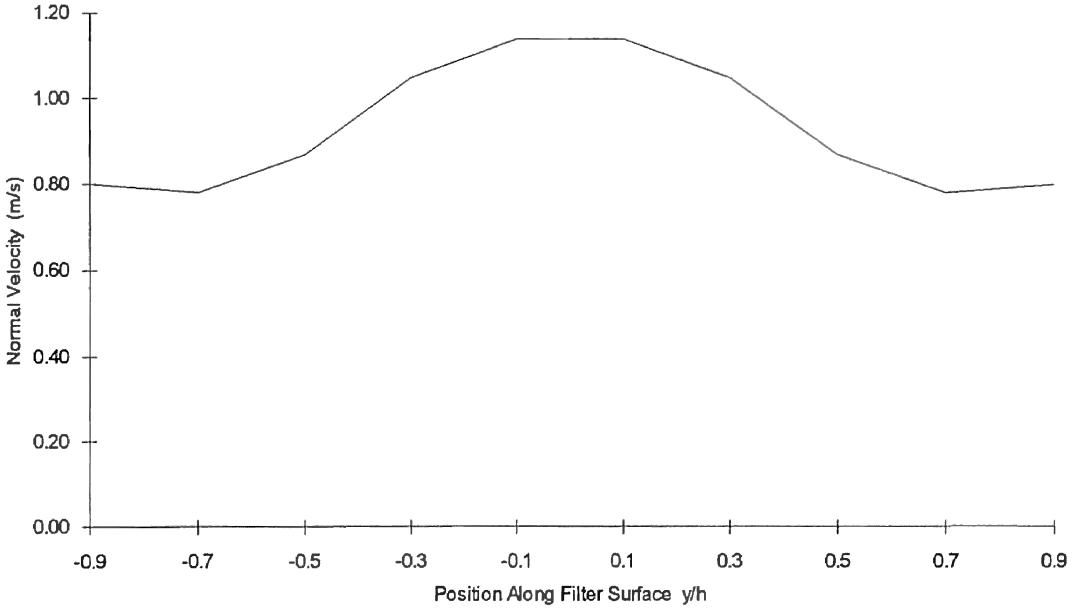

Figure 4.6 Normal Velocity Along Filter Surface at Uin=7m/s (Case 3)

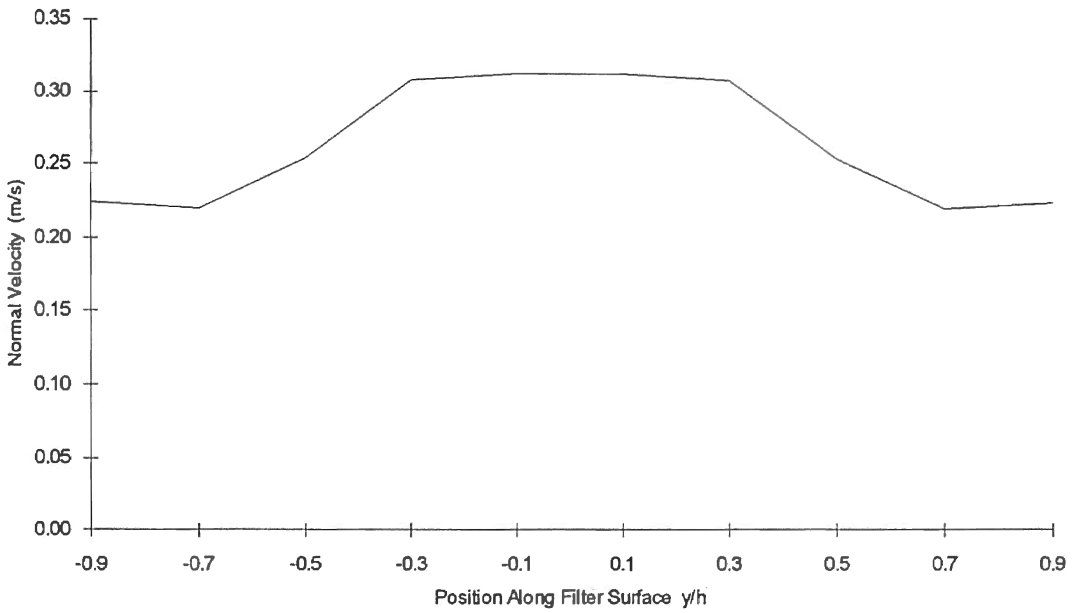

Figure 4.7 Normal Velocity Along Filter Surface at Uin=2m/s

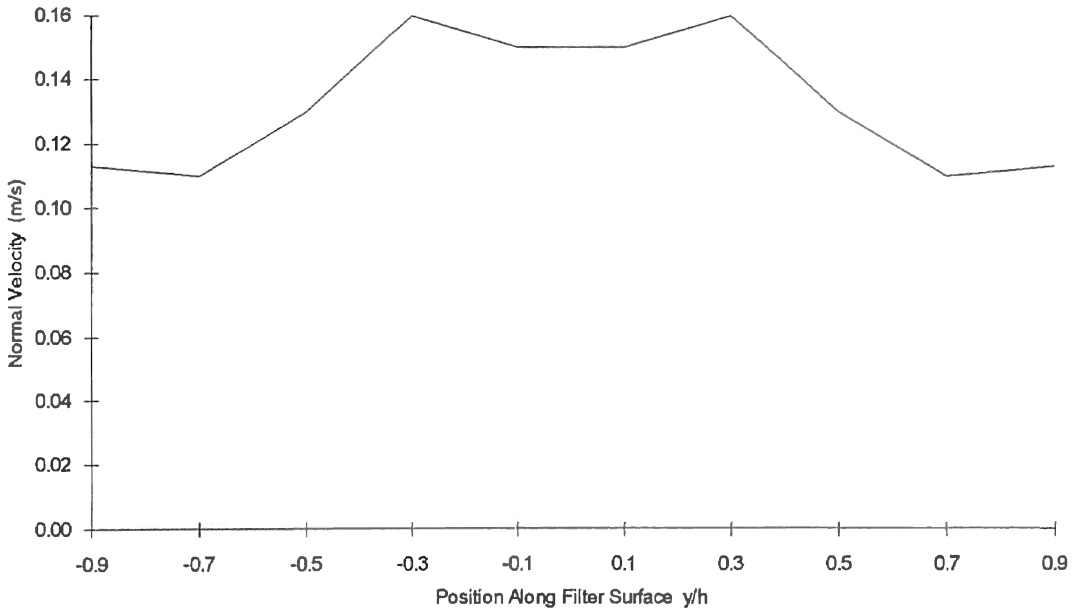

Figure 4.8 Normal Velocity Along Filter Surface at Uin=1m/s (Case 4)

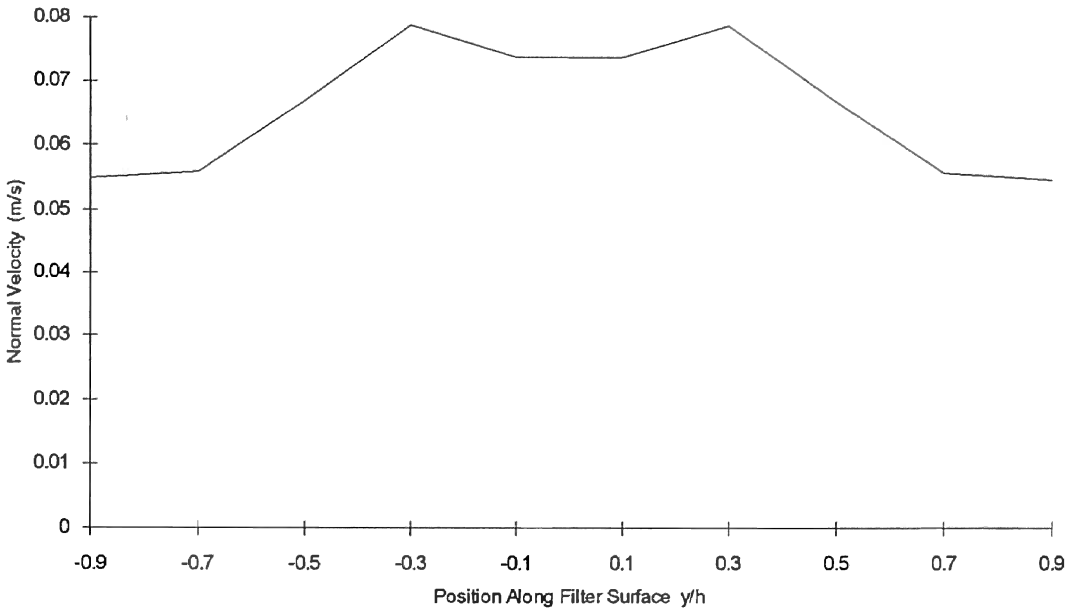

Figure 4.9 Normal Velocity Along Filter Surface at Uin=0.5m/s

It is interesting to compare all the above results to the ideal case of a uniform normal velocity along the filter surface. Figure 4.10 helps to understand the derivation of the uniform normal velocity. As shown in the figure, the normal velocity is based upon the assumption that velocity at each point on the filter surface goes through the filter in the normal direction uniformly. Since the flow rate is constant, the uniform velocity can be calculated with the following equation.

$$U_{uniform} = \frac{U_{in} \cdot W}{2d}$$

Table 4.7 shows uniform normal velocity for different inlet velocities. Then, the non-dimensional velocities are calculated to compare the normal velocities obtained before. The non-dimensional velocity is defined as the ratio of above calculated velocity and uniform normal velocity under each case. The non-dimensional normal velocity curves are drawn in Figure 4.11.

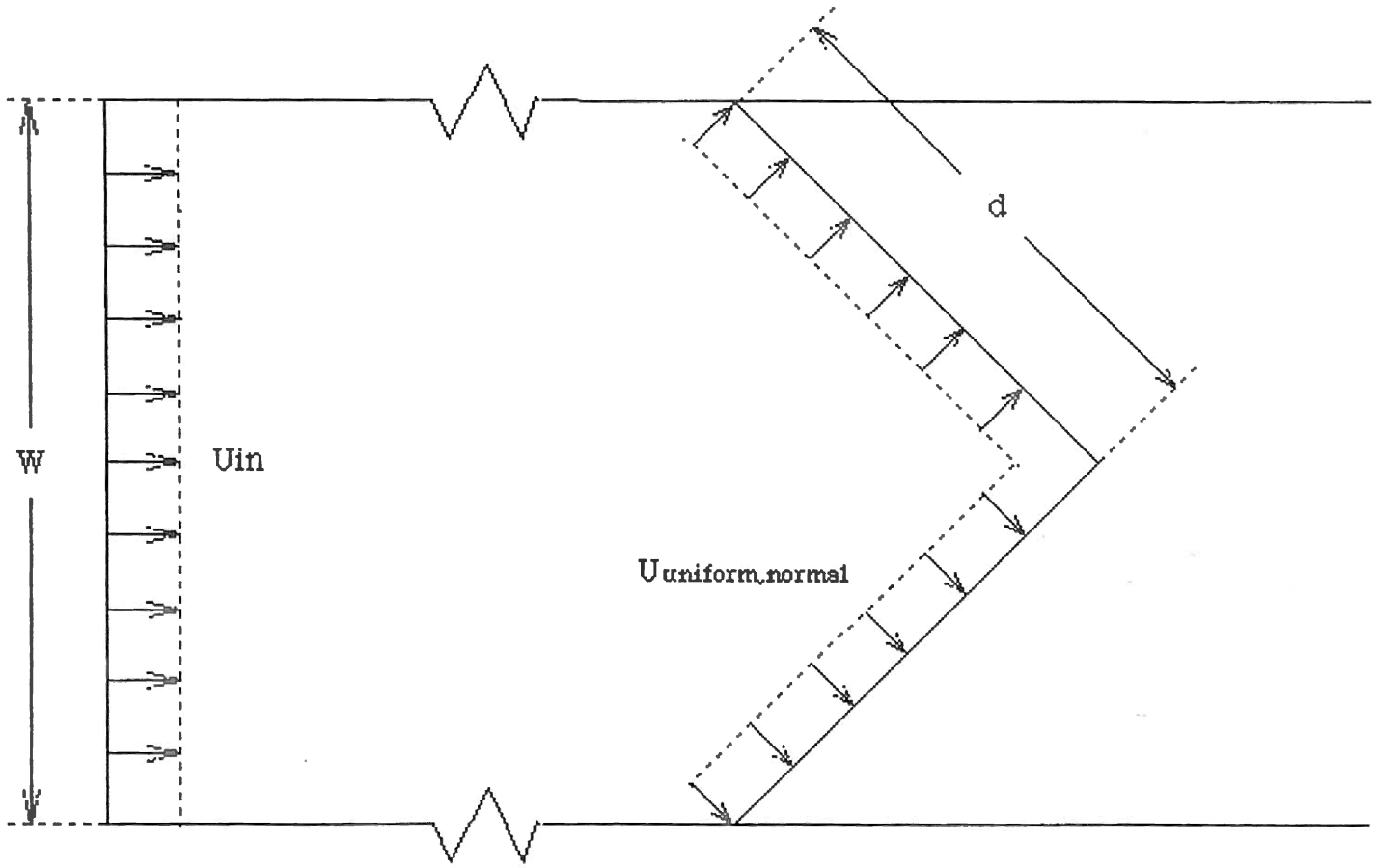

Figure 4.10 Derivation of the Uniform Normal Velocity

$$U_{non-dimension} = \frac{U_{normal}}{U_{uniform,normal}}$$

Figure 4.12 shows the relative magnitude of each case is almost same.

TABLE 4.7

INLET VELOCITY VS. UNIFORM NORMAL VELOCITY ALONG FILER SURFACE

Inlet Velocity (m/s)	Uniform Normal Velocity Along Filter Surface (m/s)
0.5	0.066
1.0	0.132
2.0	0.264
3.0	0.396
5.0	0.660
7.0	0.925

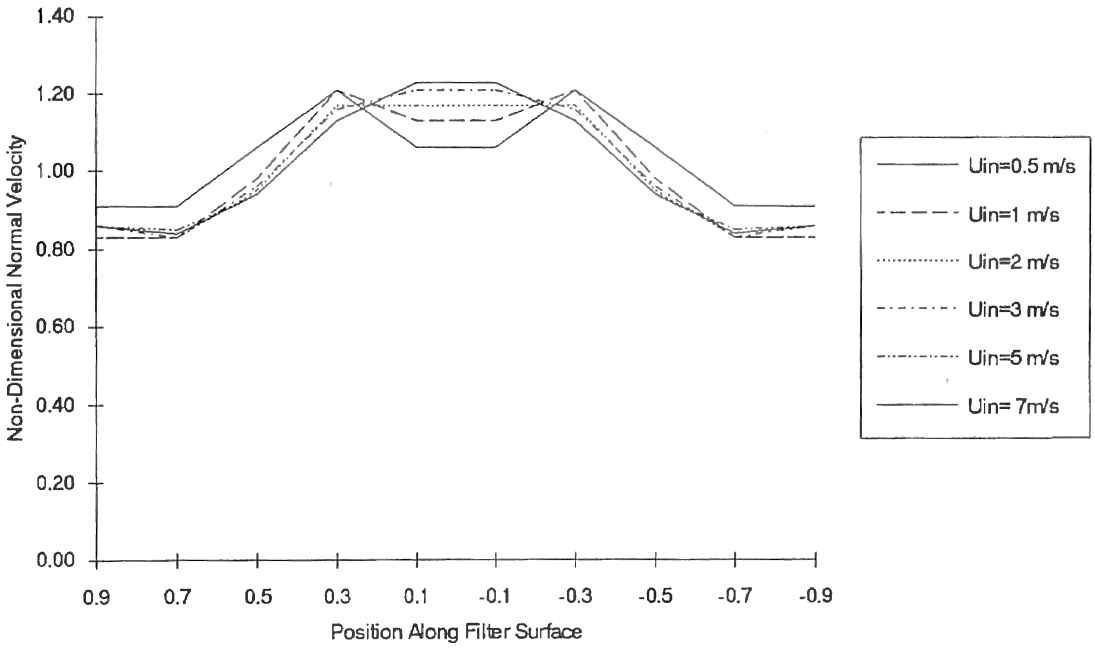

Figure 4.11 Nondimensional Normal Velocity Along Filter Surface at Different Inlet Velocity Uin

4.2.3 Velocity Magnitude

Besides the flow direction changing across the filter, the velocity magnitude changes of the horizontal and vertical components should also be stressed. The results are shown in Figures 4.13 to 4.20. The corresponding position of row number and flow position number are shown on Figure 4.12. There are 10 rows and 42 columns in the flow calculation. The rows are counted from top to bottom. Since the flow is symmetric, there are only five rows included for the plot. The flow position 1 refers to the flow inlet and 42 to outlet. Not all the columns are considered for plotting, because the horizontal velocity equals inlet value at entrance and exit part while vertical velocity always approaches zero. The filter medium distribution is also shown in Figure 4.12. The column nodes 11, 15 and 22 are defined as break points since the velocity profile changes sign of slope there.

(1) Horizontal Velocity

Figures 4.13 to 4.16 are plots of horizontal velocity variations. At the center line (Row 5), the velocity increases after entering filter and decreases from the column 15 where the centerline filter cell starts. It decreases until column 23, the point of exiting the filter, where its value is below the inlet velocity. From there, column 23, the velocity increases again and approaches the inlet flow velocity value. The variation of velocity at Row 4 is the same as Row 5 but for the magnitude. The variation of velocity at Row 2 is similar to Row 1. The magnitude change of the velocity at Row 1 is opposite to Row 5. The decreasing velocity break point of Row 1 is the break point for the increase of Row 5. Flow at Row 3 which is at the middle of the previous four is little different. The direction changes more times than other rows, but its varying magnitude is not that much larger than the other four. The velocity value at all rows eventually approaches the value of inlet. At each point of the flow position, the average velocity of five rows is exactly equal to the inlet value. For example, the average velocity at column 13 is 3m/s in Figure 4.13.

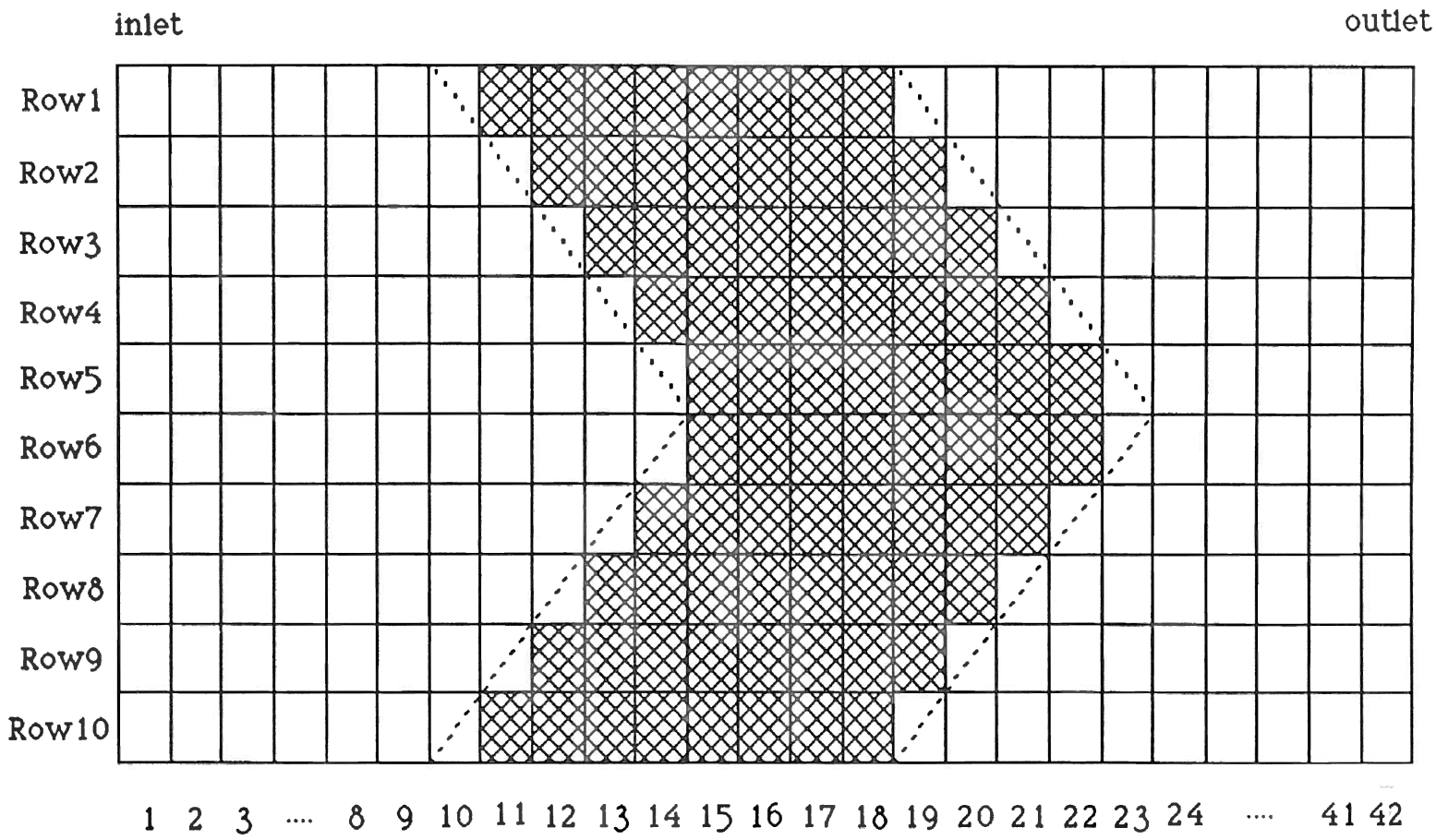

Figure 4.12 Filter Node Positions in Rows and Columns

In Figure 4.13 to 4.15, the inlet velocity is increased. The minimum and maximum values are changed accordingly. It takes a longer distance to reach the uniform flow again for high inlet velocity. Comparing with Figure 4.13, the increasing thickness effect in Figure 4.16 causes the highest velocity magnitude change.

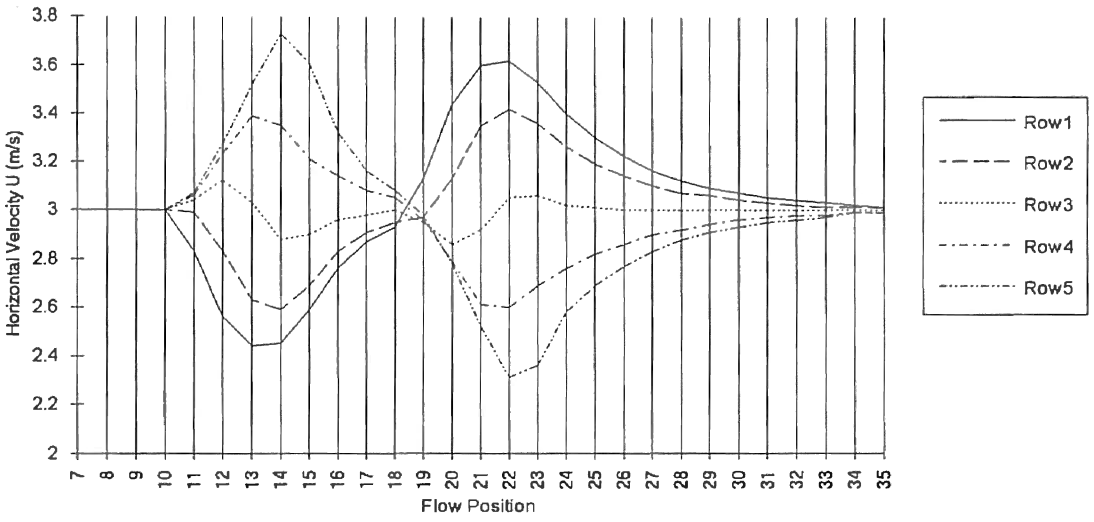

Figure 4.13 Horizontal Velocity Changing Along Horizontal Axis at Uin=3m/s

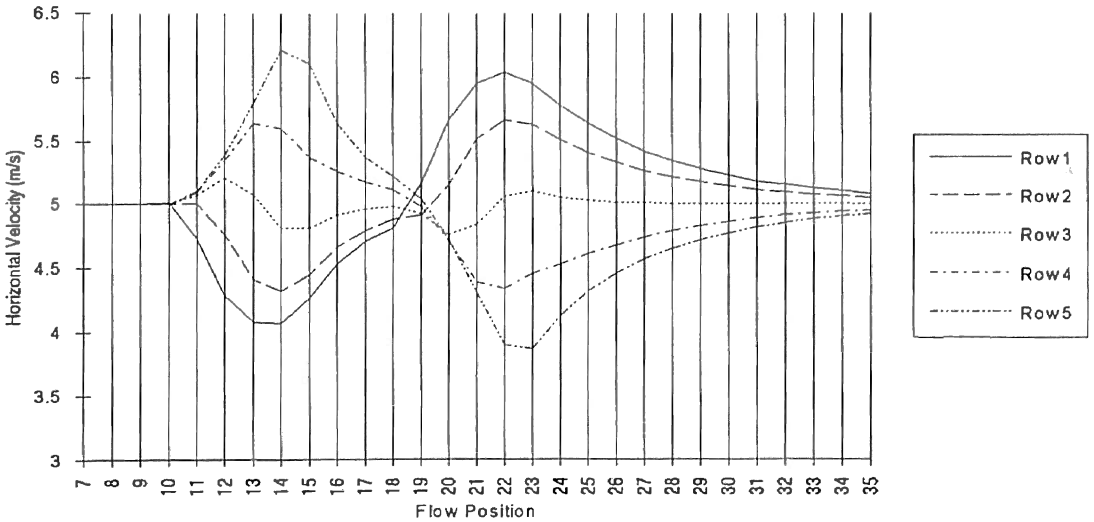

Figure 4.14 Horizontal Velocity Changing Along Horizontal Axis at Uin=5m/s

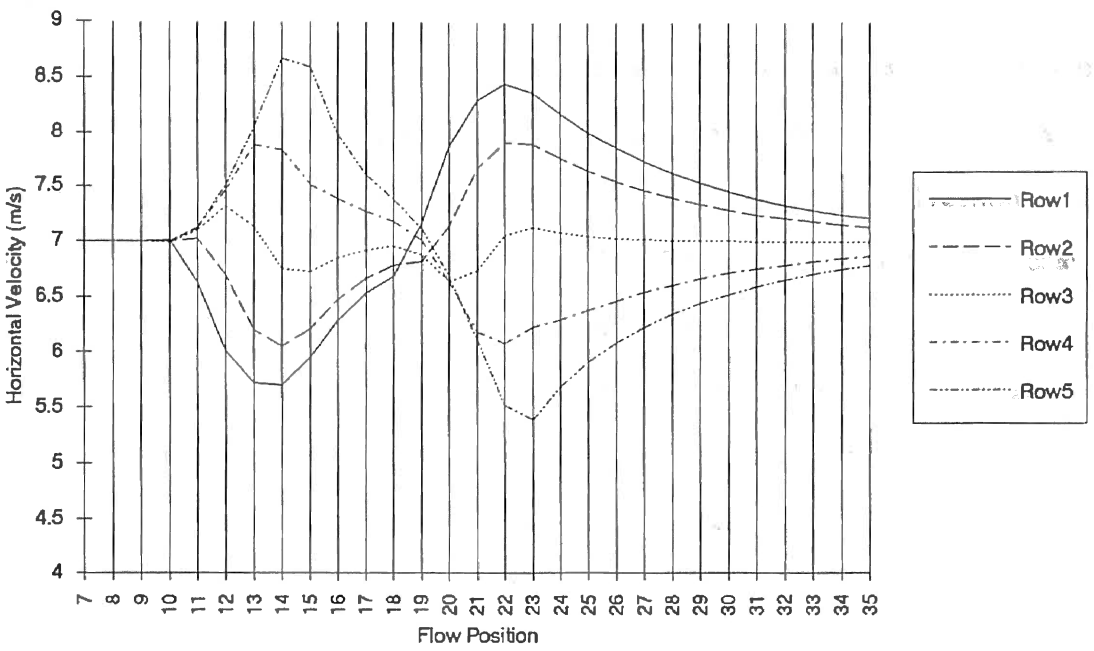

Figure 4.15 Horizontal Velocity Changing Along Horizontal Axis at Uin=7m/s

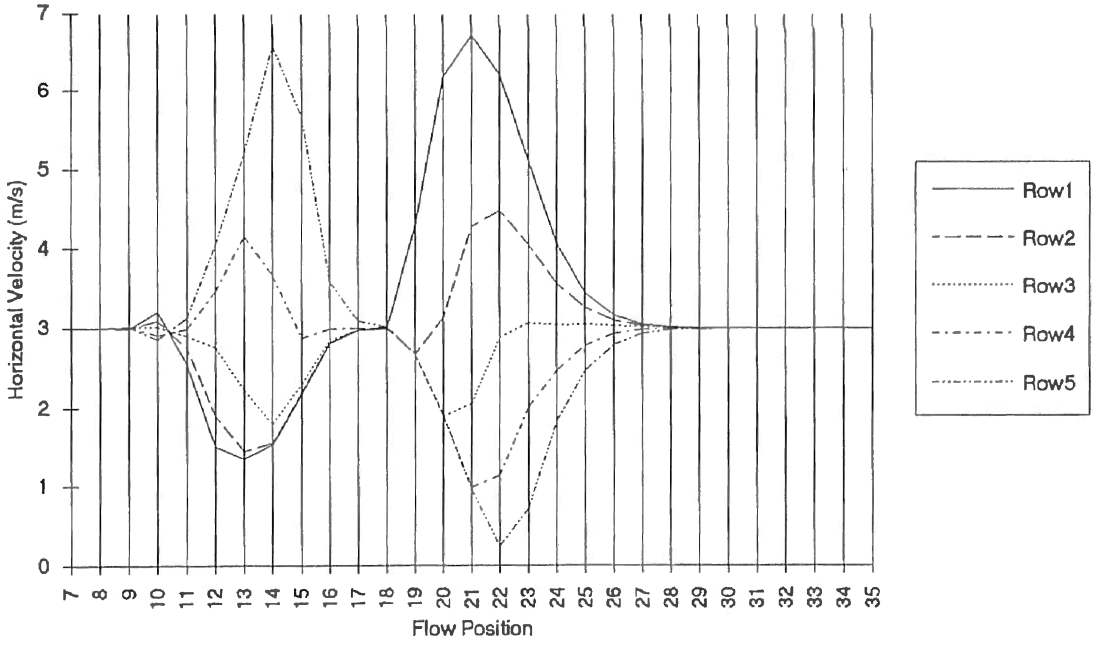

Figure 4.16 Horizontal Velocity Changing Along Horizontal Axis with Filter Ten Times Thicker Than Case 1, (Case 9)

(2) Vertical Velocity

The vertical component velocities also change at the break points discussed before. The positive value refers to upper direction and negative to down. The flow starts to point down before entering the filter and point up until column 15. The direction is again down after column 15 and up again from 18 to 20. The flow vertical direction changes twice, 20 to 23 and 23 to outlet. All five rows run the same way in direction.

The inlet velocity only changes the flow velocity magnitude at each break point. The thickness change of Figure 4.20 shows stronger effect around the filter. The direction starts at column 8 and recovers uniform flow more quickly. The figure also shows the nonuniformity increasing with the thicker filter. This nonuniformity may in turn decrease the efficiency.

However, based on McLaughlin's conclusion[13], one may imagine that the filter efficiency will increase with increasing the thickness of filter. McLaughlin pointed out the collection efficiency increases while the packing density parameter is increased. The packing density parameter β is defined by:

$$\beta = \frac{\pi}{4}(\frac{D}{C})^2$$

where: D is fiber diameter

C is the distance between two fiber centers

Thus, engineers must balance these two factors in their filter thickness design.

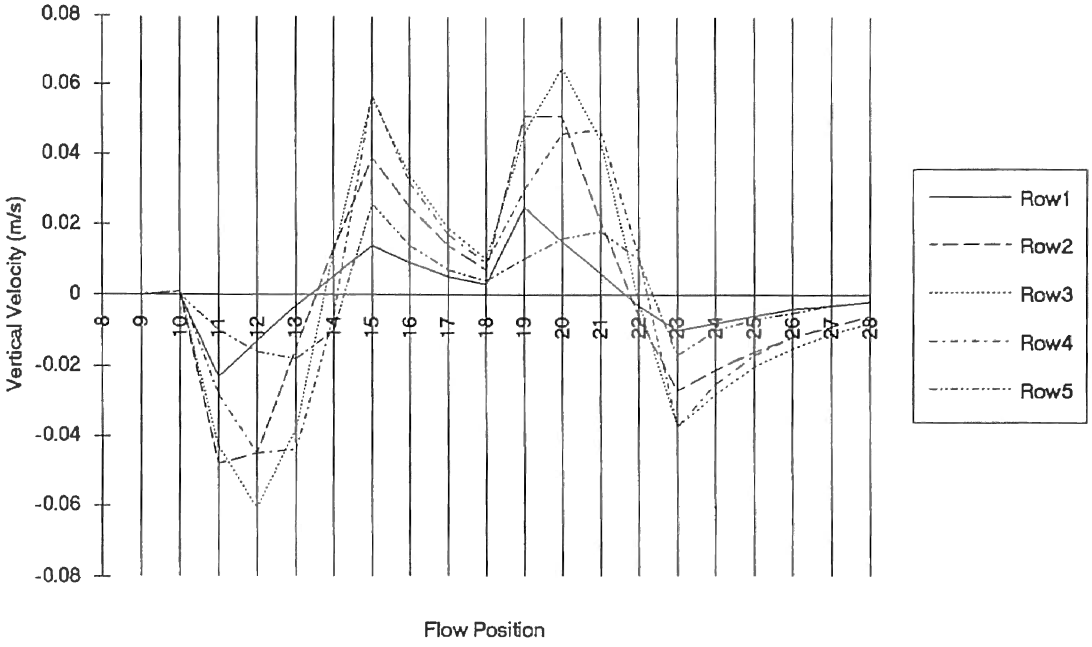

Figure 4.17 Vertical Velocity Changing Along Horizontal Axis at Uin=3m/s

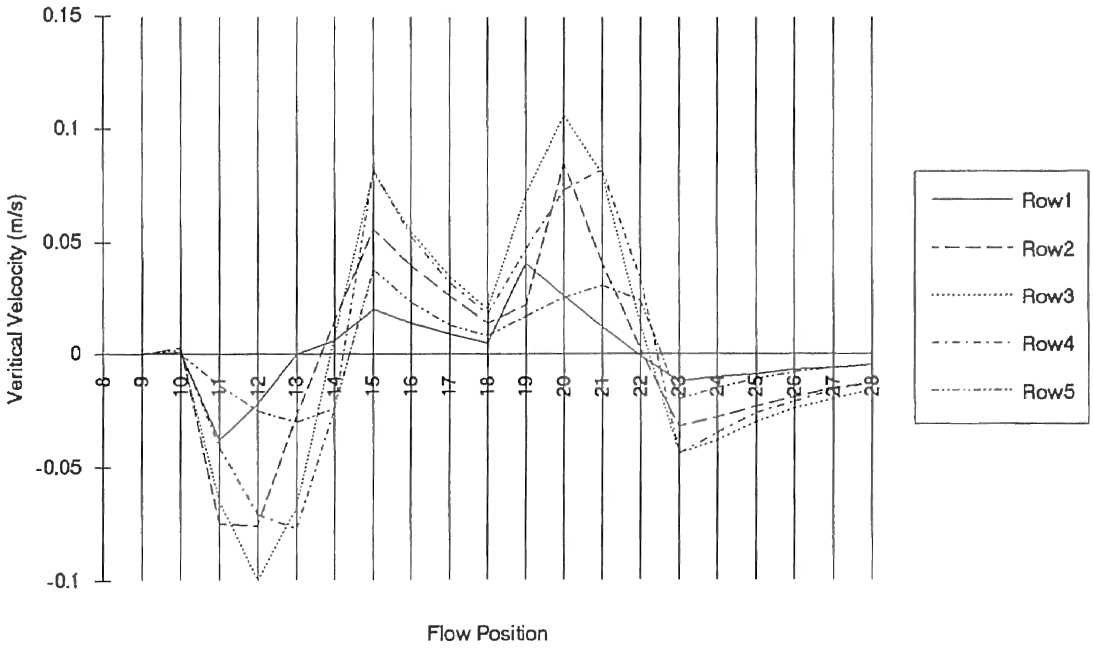

Figure 4.18 Vertical Velocity Changing Along Horizontal Axis at Uin=5m/s

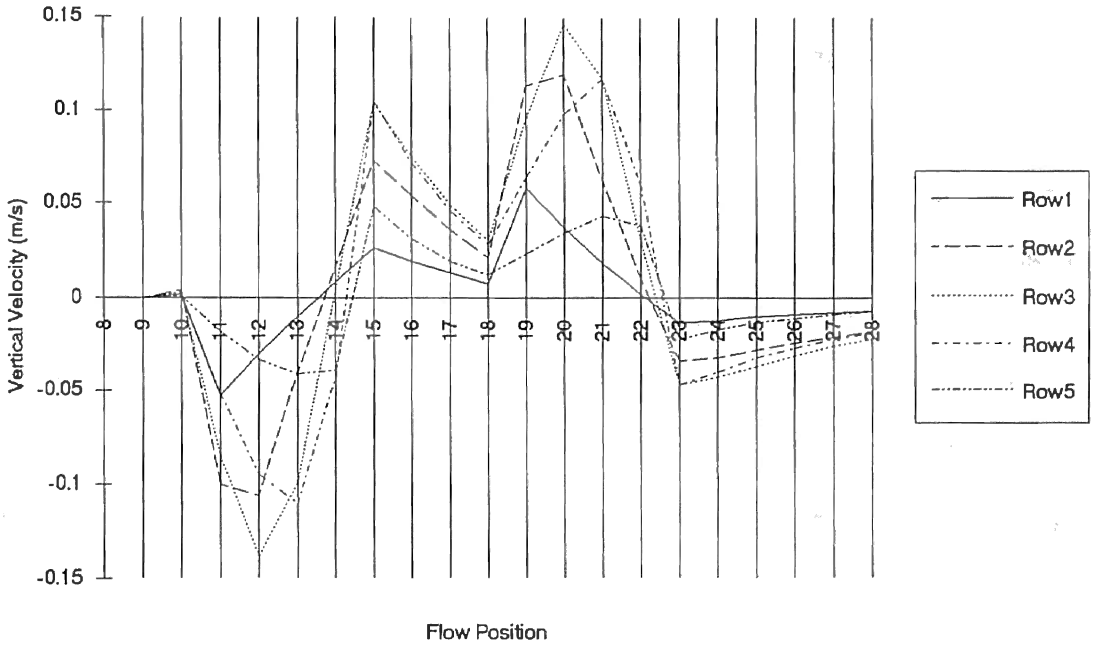

Figure 4.19 Vertical Velocity Changing Along Horizontal Axis at Uin=7m/s

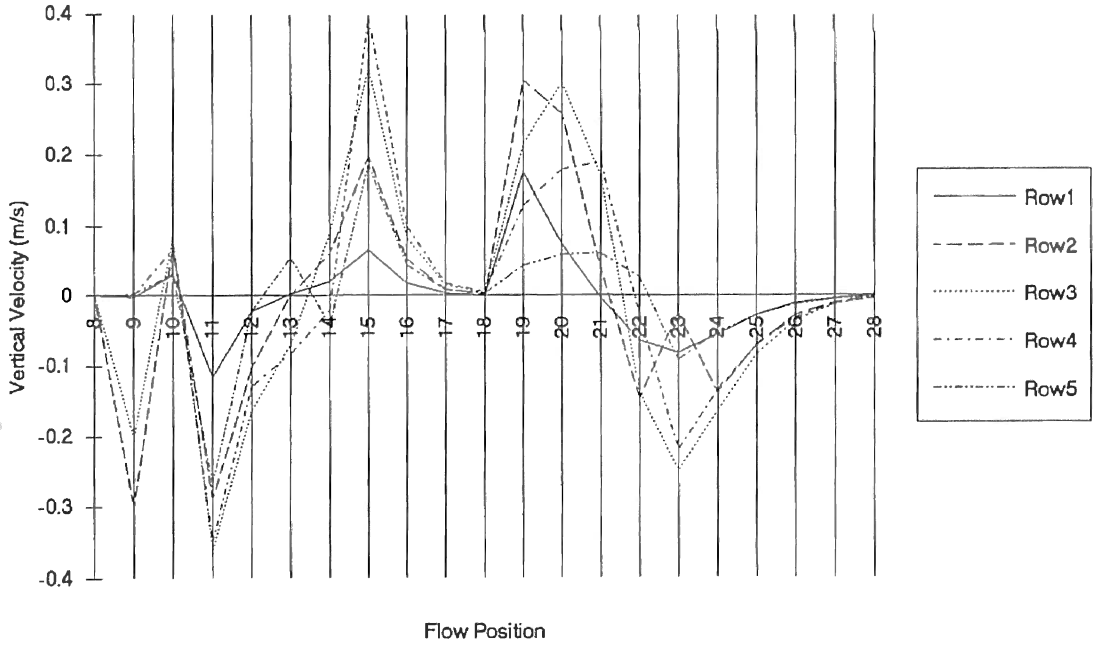

Figure 4.20 Vertical Velocity Changing Along Horizontal Axis

with Filter Ten Times Thicker Than Case 1, (Case 9)

4.2.4 Turbulent Kinetic Energy and Dissipation

Turbulent kinetic energy starts to decay after entering the flow field but the relative decay rate of 1% starting intensity is much smaller than that of 30% starting intensity. It is observed that changing initial turbulent kinetic energy does not affect the velocity field near the filter. The velocity profile of case 10 is not shown, since it is similar to case 1.

Figures 4.21 and 4.22 show the profile of the turbulent kinetic energy in 1% and 30% starting kinetic energy respectively. Figures 4.23 and 4.24 show the profile of turbulent dissipation. In fact, there should be no kinetic energy and dissipation inside the filter, since it is laminar flow there. This means the value of kinetic energy and dissipation should be shut off for calculations inside the filter. These values have to be turned back on after the flow leaves the filter. This requirement gives the problem of what starting value should be used at the flow leaving the filter.

For convenient calculation, the kinetic energy and turbulent dissipation values are not shut off and kept through the entire flow domain. The results for pressure drop and the velocity field are compared in this convenient calculation and the case with k and ε shut off. The results are very close with about 4% error, because the turbulent effect is not strong in the entire flow calculation domain. That is why the turbulent effect can be neglected. Figure 4.24 and 4.25 are the viscous dissipation for cases 1 and 5. The curves appear similar to the curves of kinetic energy.

4.2.5 Total Pressure Drop

Total pressure drop is defined as the pressure difference between inlet and outlet. The values of twelve cases are plotted in Figure 4.25. Pressure drop increases while the velocity increases. This is shown in bars number 1, 2, 3, 4.

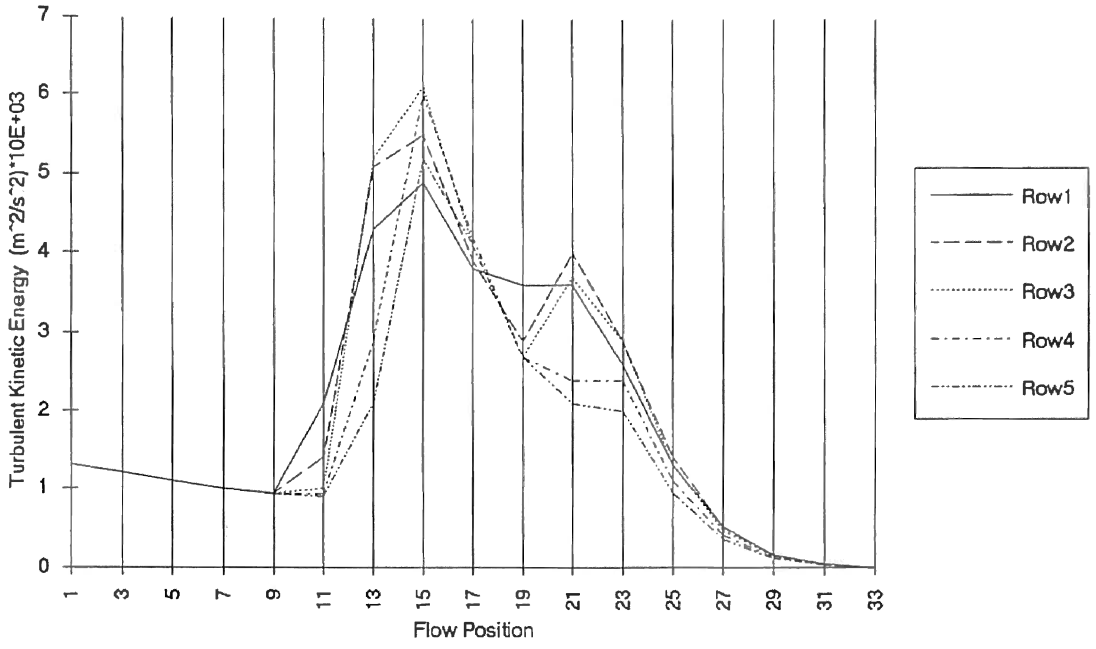

Figure 4.21 Turbulent Kinetic Energy Changing Along Horizontal Axis at Uin=3m/s with 1% Starting Turbulent Intensity (Case 1)

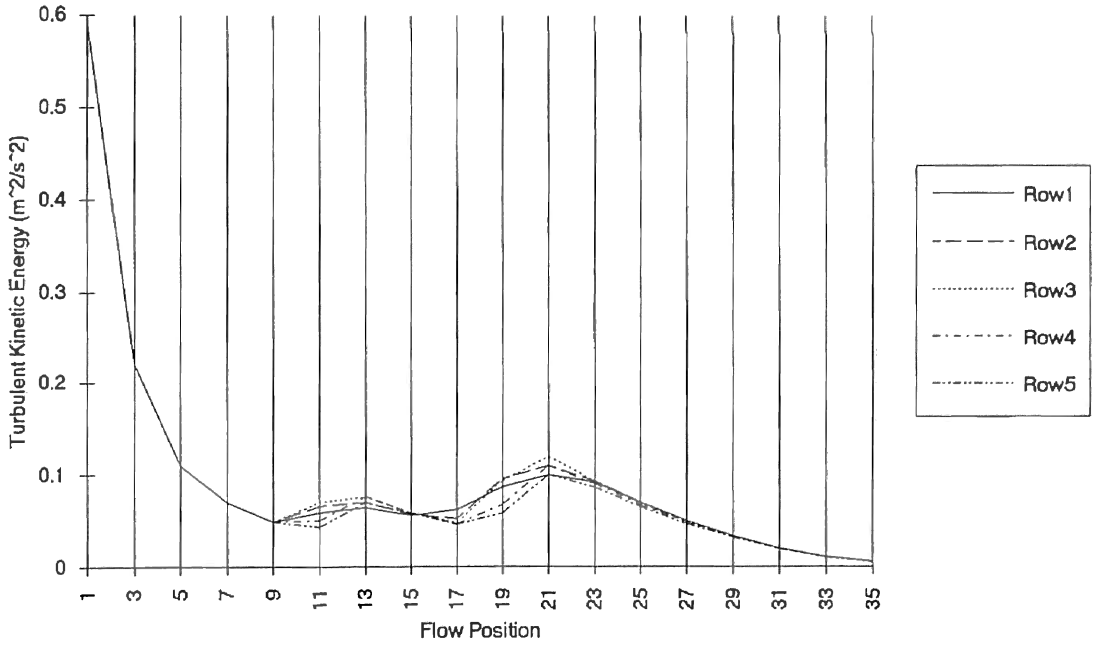

Figure 4.22 Turbulent Kinetic Energy Changing Along Horizontal Axis at Uin=3m/s with 30% Starting Turbulent Intensity (Case 11)

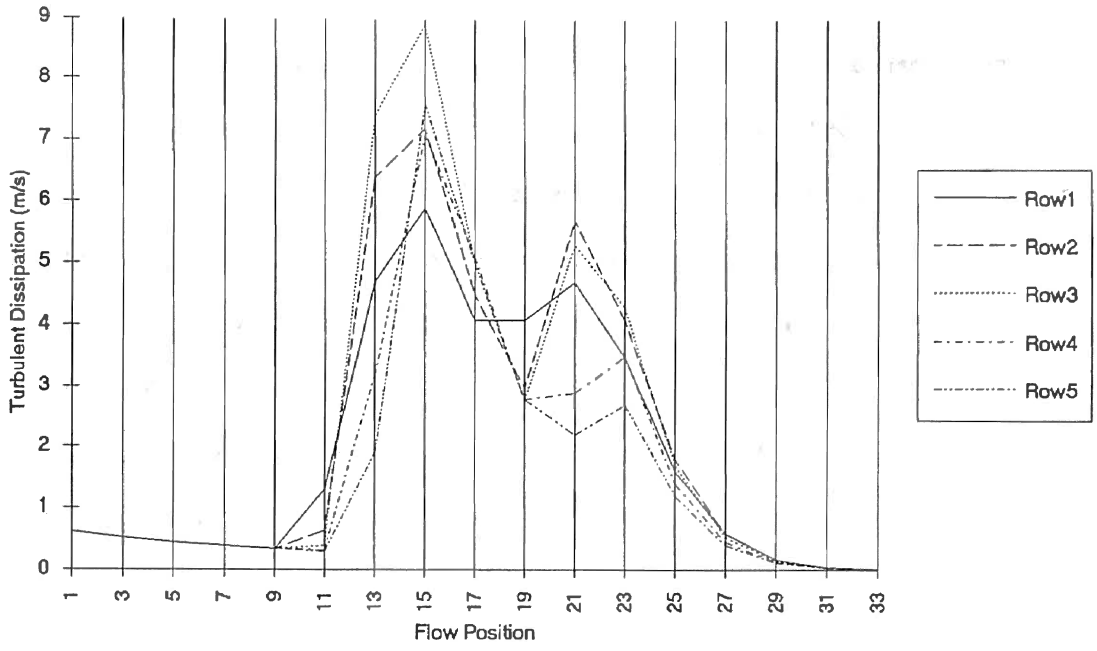

Figure 4.23 Turbulent Dissipation Changing Along Horizontal Axis at Uin=3m/s 1% Starting Turbulent Intensity (Case 1)

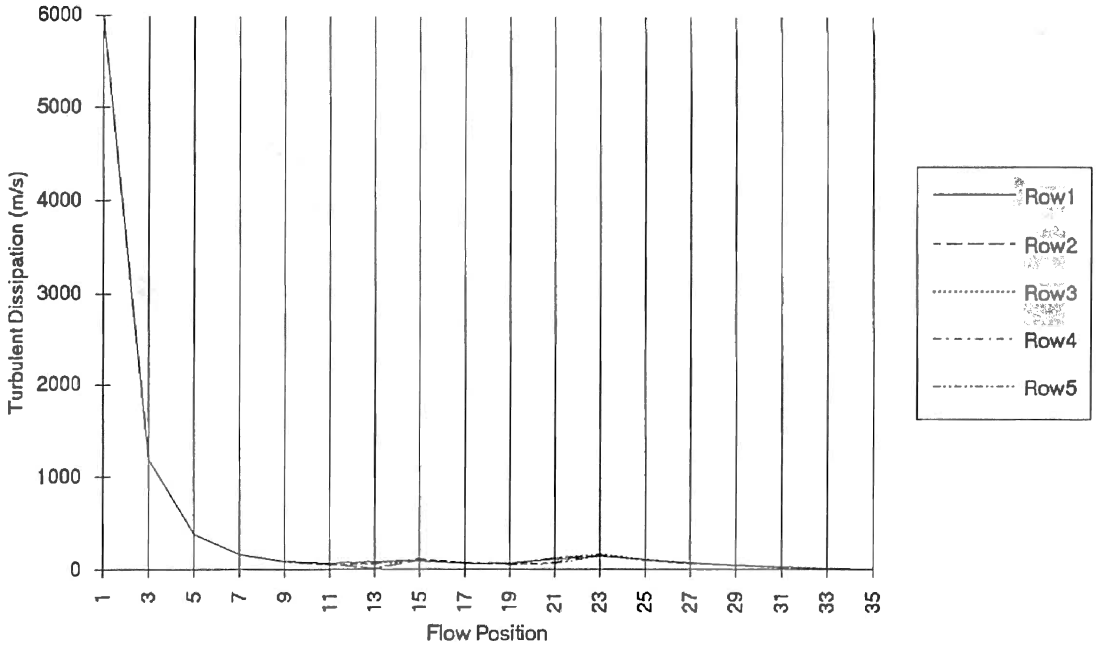

Figure 4.24 Turbulent Dissipation Changing Along Horizontal Axis with 30% Starting Turbulent Intensity (Case 11)

The lower inertial factor value b and higher K value may cause lower pressure drop. The bars 7, 8, 9 and 10 compare the non-isotropic effect of K and b values. Bars 7 and 10 show that there is not a big effect when Ky and by are varied. However, the horizontal component values Kx and bx, do have much effect on the flow distribution. The effect can be seen from bars 8 and 9, and results from the fact that the major flow direction is horizontal.

The starting turbulent intensity also does not strongly affect the pressure. It is sensible that the thicker the filter, the bigger the pressure drop. This is easy to see from bar 12.

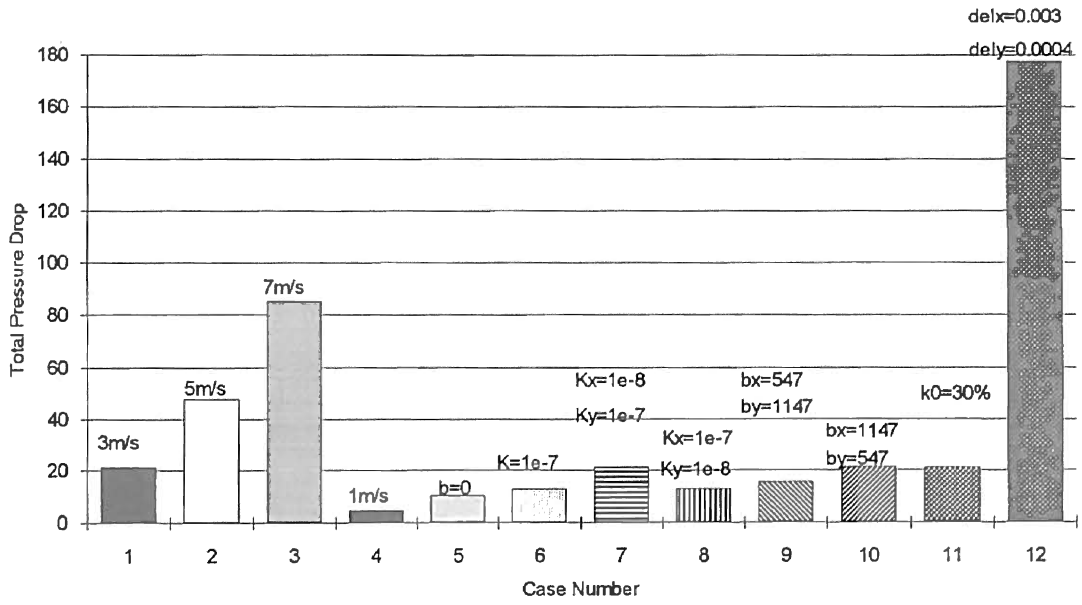

Figure 4.25 Total Pressure Drop Across Filter in All Cases (b in m^{-1}, K in m^2)

4.2.6 The Effect of Pleat Angle

Even for constant paper thickness t_p, the horizontal paper thickness t_x can be very different for different pleat angle γ (see Figure 2.6 for definitions of t_x and t_p). For t_p of 2mm, the t_x of 15° (t_x=15.3mm) pleat angle is about three times bigger than that of 45°

(t_x=5.22mm) pleat angle. Thus, increasing the pleat angle is equivalent to decreasing the horizontal paper thickness. This change will in turn alter the horizontal component velocity distribution. This conclusion can be verified by comparing Figures 4.26 and 4.27. The variation of the vertical component velocity is a little larger than that with smaller pleat angle, since the smaller the pleat angle, the smaller the vertical flow domain size. The results can be seen from Figures 4.28 and 4.29. It is easy to understand that the vertical component velocity will not change in the flat sheet filter paper flow field. The more filter pleats, the smaller the pleat angle, and the bigger vertical flow fluctuation effect between the pleats. The interesting question is whether this vertical velocity variation will affect the distribution of the dust. It is presumed that the vertical velocity will have an effect, but it is hard to predict how much. The effect of pleat angle or number of pleats must be considered in filter design.

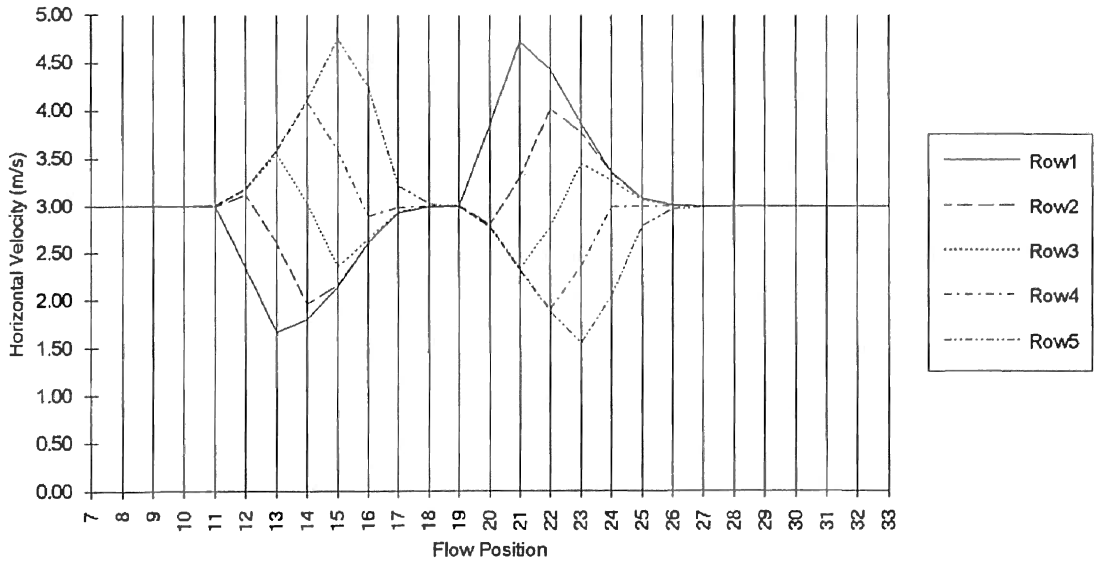

Figure 4.26 Horizontal Velocity in Pleat Angle of 15°

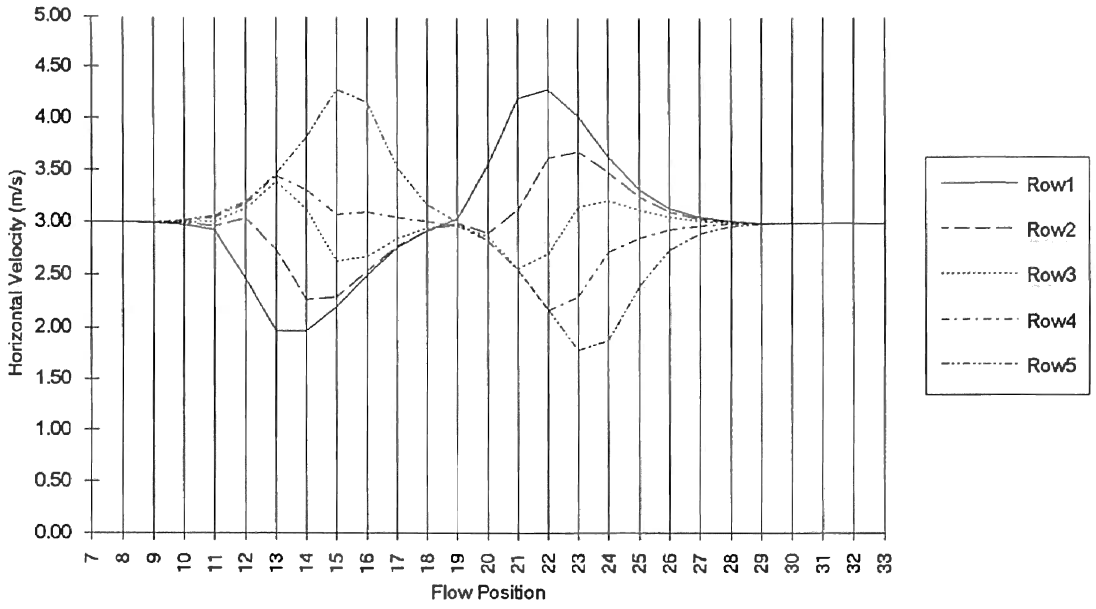

Figure 4.27 Horizontal Velocity in Pleat Angle of 45°

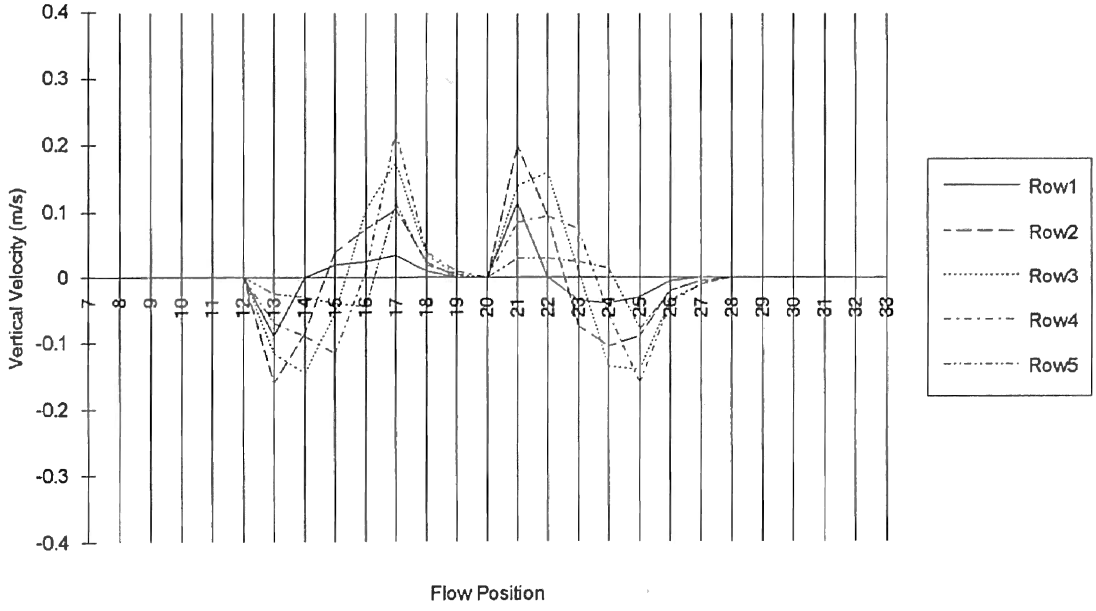

Figure 4.28 Vertical Velocity in Pleat Angle of 15°

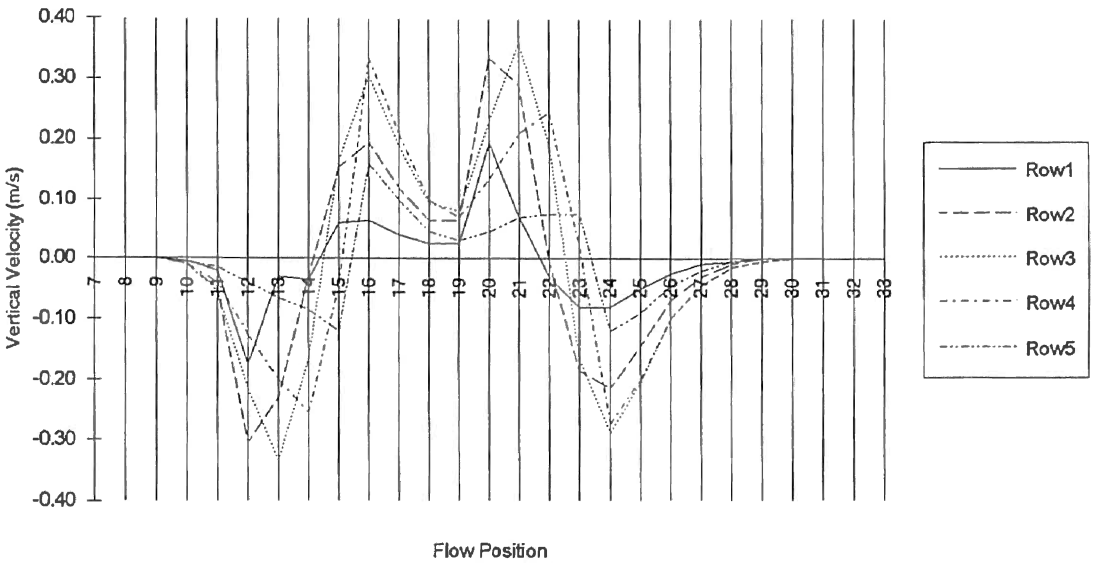

Figure 4.29 Vertical Velocity in Pleat Angle of 45°

4.2.7 One More Filter Pleat in the Flow Domain

So far, results have been presented for computations with only one filter pleat in the flow domain. Practically, there are many pleats in a filter. Are they going to affect each other in the flow? This question is investigated by setting one more filter pleat in the flow field. The filter pleat grid setup is shown in Figure 2.4. Figure 4.30 shows the vector velocity plot of two pleats.

From the plot and values, one can tell the flow is still symmetric around the centerline of each pleat. The flow seems not to be affected much in this kind of problem setup. The major factors are from the filter. The upper and lower parts of the flow keep their own track like there are no other neighbors. This is due to the perfect uniform inlet flow assumption. If the inlet flow is non-uniform, the two parts of the flow will affect each other.

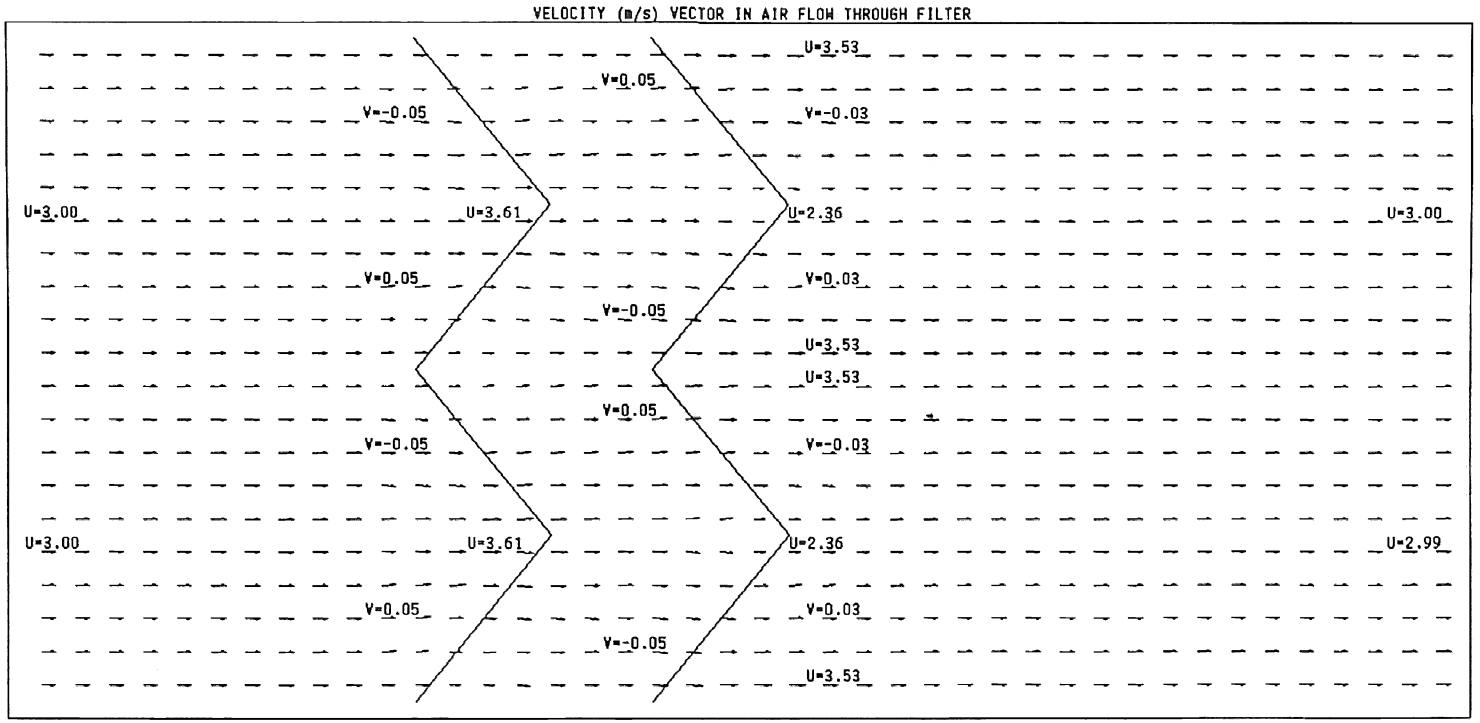

Figure 4.27 Velocity Vector Plot of Two Filter Pleats in Case 13

4.2.8 Grid Independence Study

For a reliable CFD program calculation, the results should not be dependent on the grid size. In order to compare the results for different grid size, three types of grid are used for comparison: coarse, medium, and fine. Table 4.8 lists the parameters.

One must notice that these comparisons have to be under same horizontal paper thickness t_x of the filter. This means that the overall thickness of the filter must be the same even when one changes the grid size.

The total pressure drop across the filter is calculated with five inlet velocity values, 1, 3, 5, 7 and 9m/s. The pressure comparison is plotted in Figure 4.31.

The velocity comparison is performed on the center line. The inlet velocity is 3m/s. The plots are shown in Figures 4.32. The results of the medium grid are very close to those of the fine grid. The values of other lines are also observed and compared. The same conclusion is that the values of the medium grid are very close to those of the fine grid. The fine grid gives the most accurate results. The results of medium grid are also sufficiently accurate compared with those of the fine grid. The grid size used in this thesis is in the medium grid range.

TABLE 4.8

GRID SIZE INDEPENDENCE STUDY

Grid Size Definition	Grid Number	Grid Number Inside the Filter	Δx (m)	Δy (m)
Coarse	24×6	3	0.0008	0.00004
Medium	48×12	6	0.0004	0.00002
Fine	96×24	12	0.0002	0.00001

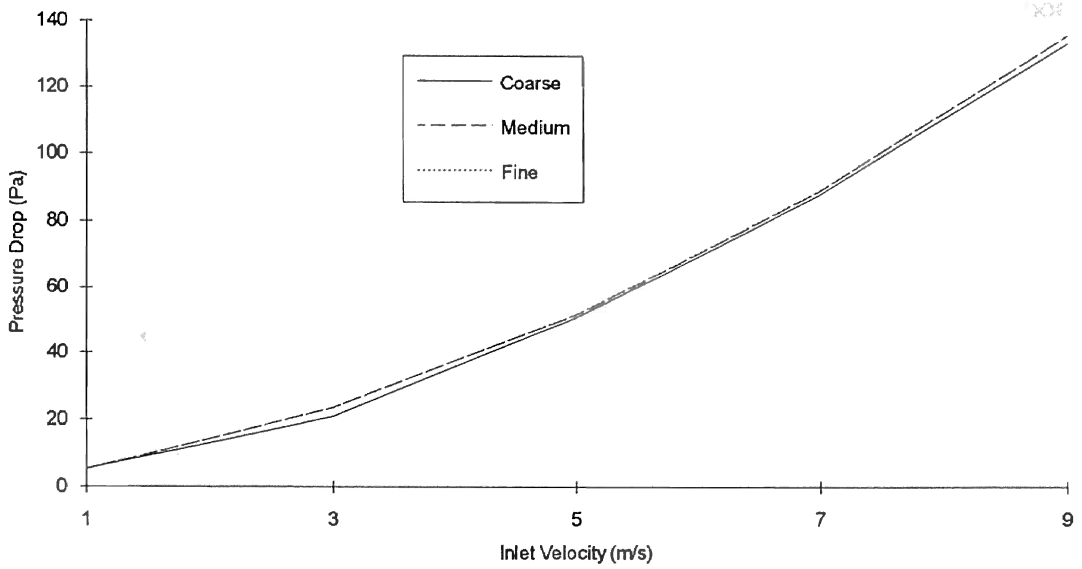

Figure 4.31 Pressure Profile of Grid Size Independence Study

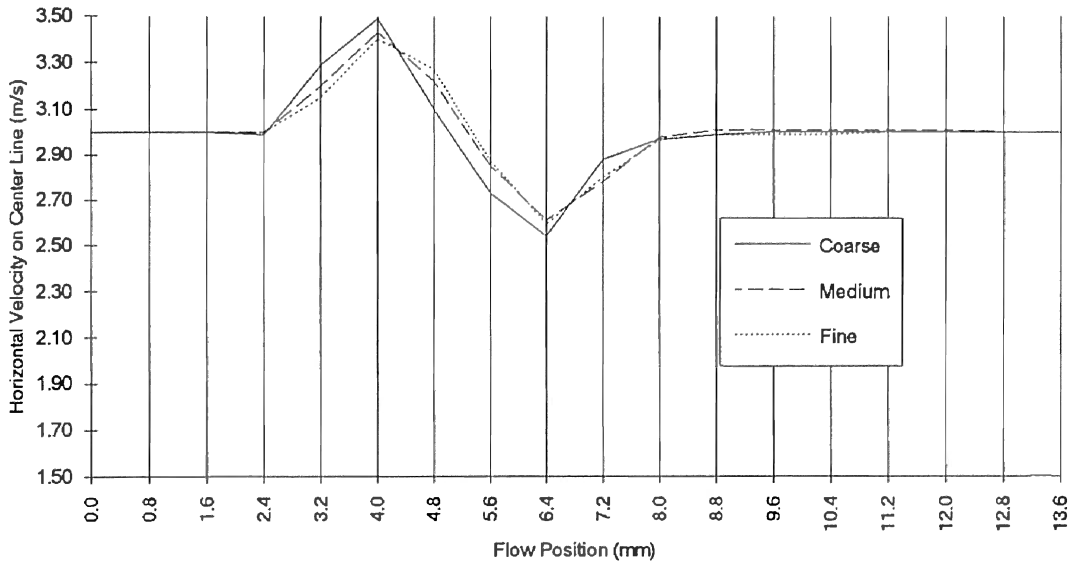

Figure 4.32 Center Line Horizontal Velocity of Grid Size Independence Study

From Figure 4.31 and 4.32, one can conclude that this filter calculation is not grid dependent and results are reliable. Nevertheless the fine grid will give more accurate results.

4.3 Discussion

The pleats of a real pleated filter are not triangular shape but look like those in Figure 4.33. The velocity flow will vary when it is approaching the filter. Contraction flow will occur when the flow enters filter pleats. The expansion flow occurs inside the filter and the contraction flow happens again after the flow leaves the filter. Thus, the flow at the outlet of the filter is not uniform, but eventually will recover uniform flow with the same velocity value of inlet. The nonuniformity only occurs near the filter region which is small compared with the main flow in the housing. More specifically, for the conditions studied, one can say that the horizontal velocity magnitude varies about 5%-15% and the vertical velocity magnitude varies less than 5%. These percentage values are calculated using the difference between the velocity value and uniform inlet value, divided by the uniform inlet flow velocity. So, the nonuniformity is not very significant from this point of view.

The influence of multiple pleats will be present in the real filter flow with nonuniform inlet conditions. This influence will not be strong, in fact, will vanish, with uniform inlet flow conditions.

The anisotropy of the filter in the main flow direction will cause different pressure drops at different point on the filter. This effect may worsen the dust distribution and decrease the filter efficiency and life, since the pressure drop at one point may be very high and at others very low.

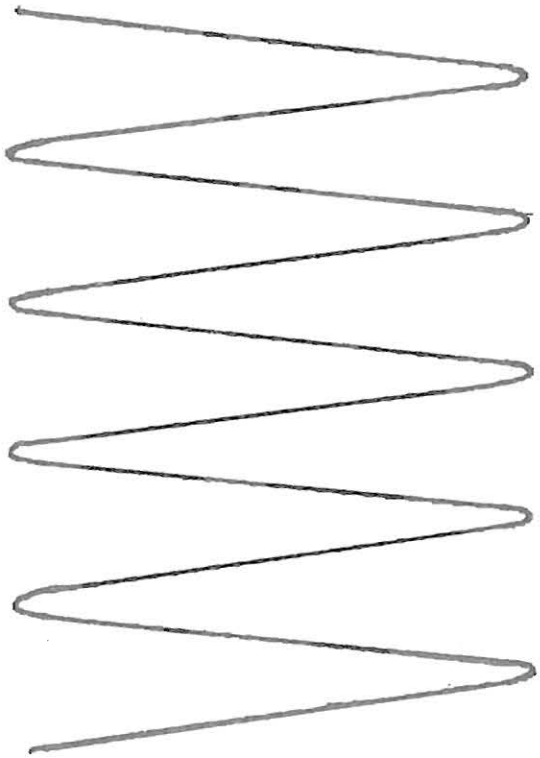

Figure 4.33 Pleat Shape of Real Filter

There is no big difference between the flat sheet paper filter which is used for design and the real pleated filter in the velocity field. With uniform inlet flow, the velocity field of flat sheet paper filter will be always uniform, and pleated filter will be a little bit nonuniform near the filter, as discussed above, but uniform far upstream and downstream.

4.4 Conclusions

[1] The flow direction and magnitude varies several times approaching, passing through and leaving the filter. This shows that the filter pleat shape is an important factor to determine the flow field very close to the filter, and in turn the performance of the filter. However, one may notice that the variations are not very large.

[2] The flow entering and leaving the pleated filter surface is not normal to the surface. Different flow velocities will cause different normal velocity distributions along the filter surface. For better filter performance, one may prefer the higher inlet flow velocity, since the higher velocity may help to distribute the dust more uniformly. It is believed that the higher the uniformity of the distribution, the higher filter efficiency will be.

[3] The horizontal paper thickness, t_x, of the filter will effectively change the flow velocity magnitude distribution. The engineers must consider this effect when they try to increase the filter thickness. The thickness may cause higher flow non-uniformity, perhaps thereby decreasing the filter efficiency. However, of course, the higher thickness filter is expected to filter more dust than a thin filter at the same flow conditions. Also, high filter thickness will greatly increase pressure drop across the filter, reducing the air filter life time and increasing the performance cost as well as the material cost.

[4] The calculations show that the turbulent effect is not important to the filter. For these simple calculations with perfectly uniform inlet velocity and free boundary conditions, the turbulent effect is negligible. The velocity field with turbulent effect assumption is almost the same as that for a non-turbulent condition.

[5] The inertial factor, b, and permeability coefficient, K, do not strongly affect the velocity magnitude variation. But variation of the horizontal values of b and K may cause more significant effects on the pressure drop.

[6] The pleat angle may strongly affect the flow velocity distribution around the filter pleat. The smaller angle with the same paper thickness will cause higher vertical component velocity fluctuations. One the other hand. the bigger angle may cause stronger horizontal velocity changes.

4.5 Recommendations

There are several ways that to improve the application of CFD discussed in this thesis.

[1] Specify more realistic boundaries. Solid boundary walls always are present in a filter flow. The log law can be used to model the flow close to the wall.

[2] Model the real shape of the pleated filter. By inspecting the air filter in detail, one may observe that the pleated filter is not exactly like the triangle that has been modeled in this thesis. Since the filter geometry is very important in affecting the flow direction, especially on the normal velocity distribution along the filter surface, modeling the realistic filter shape becomes important.

[3] Use 3-Dimensional simulation. Generally, the flow field is in three dimensions instead of two dimensions. In the boundary conditions and flow field geometry specified in this thesis, the flow field has to be symmetric and the two-dimensional model is good enough. To model the practical case, however, the calculation should be in three dimensions, especially if the flow domain is not symmetric.

[4] Specify more realistic flow domain geometry. Actually, the practical filter flow domain is not symmetric, like the diffuser-shaped test housing specified in SAE J726 standard. The more general case in the vehicle usually does not have straight walls.

[5] Specify more pleats in the flow domain. It was found that more pleats do not affect each other in this very symmetric flow domain. If the flow domain is not symmetric, the upstream flow distribution ahead of the filter should cause some difference between the symmetric flow domain and asymmetric domains.

[6] Use some parameter combinations that apply to actual filters. The parameter combinations used in this thesis are not for any particular filter and filter field. The filter thickness, the material permeability K (including nonisotropic cases), flow inertial factor b, flow domain size, etc. all need to be modified for some particular filter calculation.

[7] Since the flow fields are symmetric, a more efficient way to perform calculations is to use half the area of the flow domain used for the present computations. Using the whole domain was a good way to check if the result was symmetric.

[8] Use experimental methods to prove or partially prove the results. Although the experimental method can not obtain the information inside the filter, the velocity distribution very close to the filter should be capable of measurement by some special technique, like the Laser Doppler Anemometer. If one can not use LDA to measure deep in the pleats, one still can measure predictions upstream and downstream. The validations of the assumptions and basic equations used should be checked by a comparison of results between calculation and experiment.

The recommendations listed here are the work needed to be done to improve this research.

REFERENCES

1. Busnaina, A.A. and Lilley, D.G. (1981): " Numerical Simulation of Swirling Flow in A Cyclone Chamber," Proceedings of ASME Fluids Engineering/Applied Mechanics Conference, Boulder, Colorado, June 22-24.
2. Chambers, F.W. and Dougherty, R.L. (1992): "First Year's Progress Report for OCAST Applied Research Project, AR2-040, Contract No. 4331", School of Mechanical and Aerospace Engineering, Oklahoma State University.
3. Cheikhrouhou, M. and Sigli, D. (1988): "Influence of the Structure of Fabric Filters on the Velocity and Stress Fields of Filtration Flows in Their Vicinity," Textile Research Journal, No.7, July, pp. 371-379.
4. Chen, C.Y. (1990): "An Analytical and Experimental Study of Pressure Drop and Flow Characteristics of a Heavy-Duty Air Filter," PhD Thesis, Department of Mechanical Engineering, University of Rhode Island, Kingston, R.I.
5. Collins, M.W. & Ciofalo, M. (1991): "Computational Fluid Dynamics and Its Application to Transport Processes," J. Chem. Tech. Biotechnol, Vol.52, pp. 5-47.
6. Fletcher, C. A. J. (1989): Computational Techniques for Fluid Dynamics, Springer-Verlag, Berlin, Volume I, Fundamental and General Techniques, 2nd Edition.
7. Gurumoorthy, V. (1990): "Computational Fluid Dynamics Modeling of an Air Induction System," Masters Thesis, Department of Mechanical Engineering, University of Rhode Island, Kingston, R.I.

8. Harlow, F.H. and Welch, J.E. (1965): "Numerical Calculation of Time-Dependent Viscous Incompressible Flow of Fluid with Free Surface," The Physics of Fluids., Vol.8, No.12, pp. 2182-2189.

9. Hinze, J.O. (1975): Turbulence, McGraw Hill, New York.

10. Hirt, C.W., Nichols, B.D., and Romero, N.C. (1975): "SOLA-A Numerical Solution Algorithm for Transient Fluid Flows," Los Alamos Scientific Laboratory Report LA-5852, April.

11. Jaroszczyk, T., Ptak, T. J., Fallon, S. L., and Wake, J. (1993): "Particulate and Odor Control in Car Ventilation Systems," SAE Technical Paper Series 930014, SAE International Congress and Exposition. Detroit, Michigan, March 1-5.

12. Lilley, D.G. and Vatistas, G. (1978): "Flow Prediction in Cyclone Chambers," Presented at Combustion Institute/Canadian Section Meeting, Ottawa, Canada, May 4-5.

13. McLaughlin, C., McComber, P. and Gakwaya, A. (1986): "Numerical Calculation of Particle Collection by a Row of Cylinders in a Viscous Fluid," The Canadian Journal of Chemical Engineering, Vol. 64, pp. 205-210.

14. Nagano, Y. and Hishida, M. (1987): "Improved Form of the k-ε Model for Wall Turbulent Shear Flows," Transactions of the ASME, J. of Fluids Engineering, Vol.109, pp. 156-160.

15. Patankar, V. S. (1980): Numerical Heat Transfer and Fluid Flow, Hemisphere Publishing Corporation, New York.

16. Rodi, W. (1980): " Turbulence Models for Environmental Problems," Prediction Methods for Turbulent Flows, Hemisphere Publishing Corporation, New York, Wolfgang Kollman, Editor, pp. 259-349.

17. Rodman, C. A. (1979): "Filter Media Performance and Fibre Morphology," Proceedings of the Second World Filtration Congress, London, pp. 257-267.

18. Rodman, C. A. and Lessmann, R. C. (1988): "Automotive Nonwoven Filter Media: Their Constructions and Filter Mechanisms," TAPPI Journal, Vol.71, No.4, pp.161-168

19. Spielman, A. L. (1977):"Partical Capture From Low-Speed Laminar Flows," Ann. Rev. Fluid Mech., pp. 297-319.

20. Vafai, K. and Tien, C.L. (1981): "Boundary and Inertia Effects on Flow and Heat Transfer in Porous Media," Int. J. Heat and Mass Transfer, Vol.24, pp. 195-203.

21. Weathers, J. (1992): "A Study of Computational Fluid Dynamics in Room Air Flow," Masters Thesis, School of Mechanical and Aerospace Engineering, Oklahoma State University, May.

22. White, F.M. (1974): Viscous Fluid Flow, First Edition, McGraw Hill, New York.

23. Zia, M., M. Faghri and R. C. Lessmann (1990): "The Effect of Different Flow Field Models on Aerosol Particle Capture in Nonwoven Fibrous Filters," Proceedings of Third Annual Meeting of the American Filtration Society, Washington, D. C., March.

APPENDICES

APPENDIX A

VELOCITY DATA OF CALCULATION CASES IN CHAPTER IV

In order to help readers to check the calculation results, the raw data of horizontal velocity and vertical velocity are presented in this Appendix. The two triangular lines show the position of the filter. The pleat angle and the flow domain size is not in scale. Finally, the vector plots for different pleat angles are added to view the effect of variation of pleat angle.

U VELOCITY (m/s) MATRIX IN AIR FLOW THROUGH FILTER

3.0	3.0	3.0	3.0	3.0	3.0	3.0	3.0	3.0	3.0	2.8	2.6	2.4	2.4	2.6	2.8	2.9	2.9	3.1	3.4	3.6	3.6	3.5	3.4	3.3	3.2	3.2	3.1	3.1	3.1	3.0	3.0	3.0	3.0	3.0	3.0	3.0	3.0	3.0	3.0	3.0
3.0	3.0	3.0	3.0	3.0	3.0	3.0	3.0	3.0	3.0	3.0	2.8	2.6	2.6	2.7	2.8	2.9	3.0	3.0	3.1	3.3	3.4	3.4	3.3	3.2	3.1	3.1	3.1	3.1	3.0	3.0	3.0	3.0	3.0	3.0	3.0	3.0	3.0	3.0	3.0	3.0
3.0	3.0	3.0	3.0	3.0	3.0	3.0	3.0	3.0	3.0	3.0	3.1	3.0	2.9	2.9	3.0	3.0	3.0	3.0	2.9	2.9	3.1	3.1	3.0	3.0	3.0	3.0	3.0	3.0	3.0	3.0	3.0	3.0	3.0	3.0	3.0	3.0	3.0	3.0	3.0	3.0
3.0	3.0	3.0	3.0	3.0	3.0	3.0	3.0	3.0	3.0	3.1	3.2	3.4	3.4	3.2	3.1	3.1	3.0	3.0	2.8	2.6	2.6	2.7	2.8	2.8	2.9	2.9	2.9	2.9	3.0	3.0	3.0	3.0	3.0	3.0	3.0	3.0	3.0	3.0	3.0	3.0
3.0	3.0	3.0	3.0	3.0	3.0	3.0	3.0	3.0	3.0	3.1	3.3	3.5	3.7	3.6	3.3	3.2	3.1	3.0	2.8	2.5	2.3	2.4	2.6	2.7	2.8	2.8	2.9	2.9	2.9	3.0	3.0	3.0	3.0	3.0	3.0	3.0	3.0	3.0	3.0	3.0
3.0	3.0	3.0	3.0	3.0	3.0	3.0	3.0	3.0	3.0	3.1	3.3	3.5	3.7	3.6	3.3	3.2	3.1	3.0	2.8	2.5	2.3	2.4	2.6	2.7	2.8	2.8	2.9	2.9	2.9	3.0	3.0	3.0	3.0	3.0	3.0	3.0	3.0	3.0	3.0	3.0
3.0	3.0	3.0	3.0	3.0	3.0	3.0	3.0	3.0	3.0	3.1	3.2	3.4	3.4	3.2	3.1	3.1	3.0	3.0	2.8	2.6	2.6	2.7	2.8	2.8	2.9	2.9	2.9	2.9	3.0	3.0	3.0	3.0	3.0	3.0	3.0	3.0	3.0	3.0	3.0	3.0
3.0	3.0	3.0	3.0	3.0	3.0	3.0	3.0	3.0	3.0	3.1	3.0	2.9	2.9	3.0	3.0	3.0	3.0	2.9	2.9	3.1	3.1	3.0	3.0	3.0	3.0	3.0	3.0	3.0	3.0	3.0	3.0	3.0	3.0	3.0	3.0	3.0	3.0	3.0	3.0	3.0
3.0	3.0	3.0	3.0	3.0	3.0	3.0	3.0	3.0	3.0	2.8	2.6	2.6	2.7	2.8	2.9	3.0	3.0	3.1	3.3	3.4	3.4	3.3	3.2	3.1	3.1	3.1	3.1	3.0	3.0	3.0	3.0	3.0	3.0	3.0	3.0	3.0	3.0	3.0	3.0	3.0
3.0	3.0	3.0	3.0	3.0	3.0	3.0	3.0	3.0	3.0	2.8	2.6	2.4	2.4	2.6	2.8	2.9	2.9	3.1	3.4	3.6	3.6	3.5	3.4	3.3	3.2	3.2	3.1	3.1	3.1	3.0	3.0	3.0	3.0	3.0	3.0	3.0	3.0	3.0	3.0	3.0

Figure A.1 Data of Horizontal Velocity of Case 1 (Table 4.2) in Chapter IV

V VELOCITY (m/s) MATRIX IN AIR FLOW THROUGH FILTER

0.00	0.00	0.00	0.00	-0.00	0.00	-0.02	-0.01	-0.00	0.01	0.01	0.01	0.01	0.00	0.03	0.02	0.01	-0.00	-0.01	-0.01	-0.01	-0.00	-0.00	-0.00	-0.00	-0.00
0.00	0.00	0.00	0.00	-0.00	0.00	-0.05	-0.05	-0.01	0.01	0.04	0.02	0.01	0.01	0.05	0.05	0.02	-0.01	-0.03	-0.02	-0.02	-0.01	-0.01	-0.01	-0.00	-0.00
0.00	0.00	0.00	0.00	-0.00	0.00	-0.04	-0.06	-0.04	0.01	0.06	0.03	0.02	0.01	0.05	0.07	0.04	-0.00	-0.04	-0.03	-0.02	-0.01	-0.01	-0.01	-0.01	-0.00
0.00	0.00	0.00	0.00	-0.00	0.00	-0.03	-0.05	-0.04	-0.01	0.06	0.03	0.02	0.01	0.03	0.05	0.05	0.01	-0.04	-0.02	-0.02	-0.01	-0.01	-0.01	-0.00	-0.00
0.00	0.00	0.00	0.00	-0.00	0.00	-0.01	-0.02	-0.02	-0.01	0.03	0.01	0.01	0.00	0.01	0.02	0.02	0.01	-0.02	-0.01	-0.01	-0.00	-0.00	-0.00	-0.00	-0.00
0.00	0.00	0.00	0.00	0.00	-0.00	0.01	0.02	0.02	0.01	-0.03	-0.01	-0.01	-0.00	-0.01	-0.02	-0.02	-0.01	0.02	0.01	0.01	0.00	0.00	0.00	0.00	0.00
0.00	0.00	0.00	0.00	0.00	-0.00	0.03	0.05	0.04	0.01	-0.06	-0.03	-0.02	-0.01	-0.03	-0.05	-0.05	-0.01	0.04	0.02	0.02	0.01	0.01	0.01	0.00	0.00
0.00	0.00	0.00	-0.00	0.00	-0.00	0.04	0.06	0.04	-0.01	-0.06	-0.03	-0.02	-0.01	-0.05	-0.07	-0.04	0.00	0.04	0.03	0.02	0.01	0.01	0.01	0.01	0.00
0.00	0.00	0.00	-0.00	0.00	-0.00	0.05	0.05	0.01	-0.01	-0.04	-0.02	-0.01	-0.01	-0.05	-0.05	-0.02	0.01	0.03	0.02	0.02	0.01	0.01	0.01	0.00	0.00
0.00	0.00	0.00	0.00	0.00	-0.00	0.02	0.01	0.00	-0.01	-0.01	-0.01	-0.01	-0.00	-0.03	-0.02	-0.01	0.00	0.01	0.01	0.01	0.00	0.00	0.00	0.00	0.00

Figure A.2 Data of Vertical Velocity of Case 1 (Table 4.2) in Chapter IV

U VELOCITY (m/s) MATRIX IN AIR FLOW THROUGH FILTER

5.0	5.0	5.0	5.0	5.0	5.0	5.0	5.0	5.0	5.0	4.7	4.3	4.1	4.1	4.3	4.5	4.7	4.8	5.2	5.7	6.0	6.0	5.9	5.8	5.6	5.5	5.4	5.3	5.3	5.2	5.2	5.1	5.1	5.1	5.1	5.1	5.1	5.0	5.0	5.0	5.0	5.0
5.0	5.0	5.0	5.0	5.0	5.0	5.0	5.0	5.0	5.0	5.0	4.8	4.4	4.3	4.5	4.7	4.8	4.9	4.9	5.1	5.5	5.7	5.6	5.5	5.4	5.3	5.3	5.2	5.2	5.1	5.1	5.1	5.1	5.1	5.0	5.0	5.0	5.0	5.0	5.0	5.0	5.0
5.0	5.0	5.0	5.0	5.0	5.0	5.0	5.0	5.0	5.0	5.1	5.2	5.1	4.8	4.8	4.9	5.0	5.0	4.9	4.8	4.8	5.1	5.1	5.1	5.0	5.0	5.0	5.0	5.0	5.0	5.0	5.0	5.0	5.0	5.0	5.0	5.0	5.0	5.0	5.0	5.0	5.0
5.0	5.0	5.0	5.0	5.0	5.0	5.0	5.0	5.0	5.0	5.1	5.4	5.6	5.6	5.4	5.3	5.2	5.1	5.0	4.7	4.4	4.3	4.5	4.5	4.6	4.7	4.7	4.8	4.8	4.9	4.9	4.9	4.9	4.9	5.0	5.0	5.0	5.0	5.0	5.0	5.0	5.0
5.0	5.0	5.0	5.0	5.0	5.0	5.0	5.0	5.0	5.0	5.1	5.4	5.8	6.2	6.1	5.6	5.4	5.2	5.0	4.7	4.3	3.9	3.9	4.1	4.3	4.5	4.6	4.7	4.7	4.8	4.8	4.9	4.9	4.9	4.9	4.9	4.9	5.0	5.0	5.0	5.0	5.0
5.0	5.0	5.0	5.0	5.0	5.0	5.0	5.0	5.0	5.0	5.1	5.4	5.8	6.2	6.1	5.6	5.4	5.2	5.0	4.7	4.3	3.9	3.9	4.1	4.3	4.5	4.6	4.6	4.7	4.8	4.8	4.8	4.9	4.9	4.9	4.9	4.9	5.0	5.0	5.0	5.0	5.0
5.0	5.0	5.0	5.0	5.0	5.0	5.0	5.0	5.0	5.0	5.1	5.4	5.6	5.6	5.4	5.3	5.2	5.1	5.0	4.7	4.4	4.3	4.5	4.5	4.6	4.7	4.7	4.8	4.8	4.9	4.9	4.9	4.9	4.9	5.0	5.0	5.0	5.0	5.0	5.0	5.0	5.0
5.0	5.0	5.0	5.0	5.0	5.0	5.0	5.0	5.0	5.0	5.1	5.2	5.1	4.8	4.8	4.9	5.0	5.0	4.9	4.8	4.8	5.1	5.1	5.0	5.0	5.0	5.0	5.0	5.0	5.0	5.0	5.0	5.0	5.0	5.0	5.0	5.0	5.0	5.0	5.0	5.0	5.0
5.0	5.0	5.0	5.0	5.0	5.0	5.0	5.0	5.0	5.0	5.0	4.8	4.4	4.3	4.5	4.7	4.8	4.9	4.9	5.1	5.5	5.7	5.6	5.5	5.4	5.3	5.3	5.2	5.2	5.1	5.1	5.1	5.1	5.1	5.1	5.0	5.0	5.0	5.0	5.0	5.0	5.0
5.0	5.0	5.0	5.0	5.0	5.0	5.0	5.0	5.0	5.0	4.7	4.3	4.1	4.1	4.3	4.5	4.7	4.8	5.2	5.7	6.0	6.0	6.0	5.8	5.6	5.5	5.4	5.4	5.3	5.2	5.2	5.2	5.1	5.1	5.1	5.1	5.1	5.0	5.0	5.0	5.0	5.0

Figure A.3 Data of Horizontal Velocity of Case 2 (Table 4.2) in Chapter IV

V VELOCITY (m/s) MATRIX IN AIR FLOW THROUGH FILTER

0.00	0.00	-0.00	0.00	-0.04	-0.02	-0.01	0.01	0.02	0.01	0.01	0.00	0.04	0.03	0.01	-0.00	-0.01	-0.01	-0.01	-0.01	-0.01	-0.00	-0.00	-0.00
0.00	0.00	-0.00	0.00	-0.08	-0.08	-0.03	0.01	0.06	0.04	0.03	0.01	0.08	0.08	0.04	0.00	-0.03	-0.03	-0.02	-0.02	-0.02	-0.01	-0.01	-0.01
0.00	0.00	-0.00	0.00	-0.06	-0.10	-0.07	0.01	0.08	0.06	0.03	0.02	0.07	0.11	0.08	0.01	-0.04	-0.04	-0.03	-0.02	-0.02	-0.02	-0.01	-0.01
0.00	0.00	-0.00	0.00	-0.04	-0.07	-0.08	-0.02	0.08	0.05	0.03	0.02	0.05	0.07	0.08	0.03	-0.04	-0.03	-0.03	-0.02	-0.02	-0.01	-0.01	-0.01
0.00	0.00	-0.00	0.00	-0.01	-0.02	-0.03	-0.02	0.04	0.02	0.01	0.01	0.02	0.03	0.03	0.02	-0.02	-0.01	-0.01	-0.01	-0.01	-0.01	-0.00	-0.00
0.00	0.00	0.00	-0.00	0.01	0.03	0.03	0.02	-0.04	-0.02	-0.01	-0.01	-0.02	-0.02	-0.03	-0.02	0.02	0.01	0.01	0.01	0.01	0.00	0.00	0.00
0.00	-0.00	0.00	-0.00	0.04	0.07	0.08	0.02	-0.08	-0.05	-0.03	-0.02	-0.05	-0.07	-0.08	-0.03	0.04	0.03	0.03	0.02	0.02	0.01	0.01	0.01
0.00	-0.00	0.00	-0.00	0.06	0.10	0.07	-0.01	-0.08	-0.06	-0.03	-0.02	-0.07	-0.11	-0.08	-0.01	0.04	0.04	0.03	0.02	0.02	0.02	0.01	0.01
0.00	-0.00	0.00	-0.00	0.08	0.08	0.03	-0.01	-0.06	-0.04	-0.03	-0.01	-0.08	-0.08	-0.04	-0.00	0.03	0.03	0.02	0.02	0.02	0.01	0.01	0.01
0.00	-0.00	0.00	-0.00	0.04	0.02	0.01	-0.01	-0.02	-0.01	-0.01	-0.00	-0.04	-0.03	-0.01	0.00	0.01	0.01	0.01	0.01	0.01	0.00	0.00	0.00

Figure A.4 Data of Vertical Velocity of Case 2 (Table 4.2) in Chapter IV

U VELOCITY (m/s) MATRIX IN AIR FLOW THROUGH FILTER

7.0	7.0	7.0	7.0	7.0	7.0	7.0	7.0	7.0	7.0	6.6	6.0	5.7	5.7	6.0	6.3	6.5	6.7	7.2	7.9	8.3	8.4	8.4	8.2	8.0	7.9	7.7	7.6	7.5	7.5	7.4	7.3	7.3	7.2	7.2	7.2	7.1	7.1	7.1	7.1	7.1	7.1
7.0	7.0	7.0	7.0	7.0	7.0	7.0	7.0	7.0	7.0	7.0	6.7	6.2	6.1	6.2	6.5	6.7	6.8	6.8	7.1	7.7	7.9	7.9	7.8	7.6	7.6	7.5	7.4	7.3	7.3	7.2	7.2	7.2	7.2	7.1	7.1	7.1	7.1	7.1	7.1	7.0	7.0
7.0	7.0	7.0	7.0	7.0	7.0	7.0	7.0	7.0	7.0	7.1	7.3	7.1	6.7	6.7	6.9	6.9	7.0	6.9	6.6	6.7	7.1	7.1	7.1	7.0	7.0	7.0	7.0	7.0	7.0	7.0	7.0	7.0	7.0	7.0	7.0	7.0	7.0	7.0	7.0	7.0	7.0
7.0	7.0	7.0	7.0	7.0	7.0	7.0	7.0	7.0	7.0	7.1	7.5	7.9	7.8	7.5	7.4	7.3	7.2	7.0	6.6	6.2	6.1	6.2	6.3	6.4	6.5	6.5	6.6	6.7	6.7	6.8	6.8	6.8	6.8	6.9	6.9	6.9	6.9	6.9	6.9	6.9	7.0
7.0	7.0	7.0	7.0	7.0	7.0	7.0	7.0	7.0	7.0	7.1	7.5	8.1	8.7	8.6	8.0	7.6	7.4	7.1	6.7	6.1	5.6	5.4	5.7	5.9	6.1	6.2	6.4	6.5	6.5	6.6	6.7	6.7	6.8	6.8	6.8	6.8	6.9	6.9	6.9	6.9	6.9
7.0	7.0	7.0	7.0	7.0	7.0	7.0	7.0	7.0	7.0	7.1	7.5	8.1	8.7	8.6	8.0	7.6	7.4	7.1	6.7	6.1	5.5	5.4	5.7	5.9	6.1	6.2	6.3	6.4	6.5	6.6	6.7	6.7	6.8	6.8	6.8	6.8	6.9	6.9	6.9	6.9	6.9
7.0	7.0	7.0	7.0	7.0	7.0	7.0	7.0	7.0	7.0	7.1	7.5	7.9	7.8	7.5	7.4	7.3	7.2	7.0	6.6	6.2	6.1	6.2	6.3	6.4	6.5	6.5	6.6	6.7	6.7	6.8	6.8	6.8	6.8	6.9	6.9	6.9	6.9	6.9	6.9	6.9	7.0
7.0	7.0	7.0	7.0	7.0	7.0	7.0	7.0	7.0	7.0	7.1	7.3	7.1	6.7	6.7	6.8	6.9	7.0	6.9	6.6	6.7	7.0	7.1	7.1	7.0	7.0	7.0	7.0	7.0	7.0	7.0	7.0	7.0	7.0	7.0	7.0	7.0	7.0	7.0	7.0	7.0	7.0
7.0	7.0	7.0	7.0	7.0	7.0	7.0	7.0	7.0	7.0	7.0	6.7	6.2	6.1	6.2	6.5	6.7	6.8	6.8	7.1	7.7	7.9	7.9	7.8	7.6	7.5	7.5	7.4	7.3	7.3	7.2	7.2	7.2	7.2	7.1	7.1	7.1	7.1	7.1	7.1	7.1	7.0
7.0	7.0	7.0	7.0	7.0	7.0	7.0	7.0	7.0	7.0	6.6	6.0	5.7	5.7	6.0	6.3	6.5	6.7	7.2	7.9	8.3	8.5	8.4	8.2	8.0	7.9	7.8	7.6	7.6	7.5	7.4	7.3	7.3	7.3	7.2	7.2	7.2	7.1	7.1	7.1	7.1	7.1

Figure A.5 Data of Horizontal Velocity of Case 3 (Table 4.2) in Chapter IV

V VELOCITY (m/s) MATRIX IN AIR FLOW THROUGH FILTER

0.00	0.00	-0.00	0.00	-0.05	-0.03	-0.01	0.01	0.03	0.02	0.01	0.01	0.06	0.04	0.02	0.00	-0.01	-0.01	-0.01	-0.01	-0.01	-0.01	-0.01	-0.00
0.00	0.00	-0.00	0.00	-0.10	-0.11	-0.04	0.02	0.07	0.05	0.04	0.02	0.11	0.12	0.06	0.01	-0.03	-0.03	-0.03	-0.02	-0.02	-0.02	-0.02	-0.01
0.00	0.00	-0.00	0.00	-0.08	-0.14	-0.10	0.00	0.10	0.07	0.05	0.03	0.10	0.15	0.12	0.03	-0.05	-0.04	-0.04	-0.03	-0.03	-0.02	-0.02	-0.02
0.00	0.00	-0.00	0.00	-0.05	-0.09	-0.11	-0.04	0.11	0.07	0.05	0.03	0.06	0.10	0.12	0.06	-0.05	-0.04	-0.03	-0.03	-0.02	-0.02	-0.02	-0.01
0.00	0.00	-0.00	0.00	-0.02	-0.03	-0.04	-0.04	0.05	0.03	0.02	0.01	0.02	0.03	0.04	0.04	-0.02	-0.02	-0.01	-0.01	-0.01	-0.01	-0.01	-0.01
0.00	-0.00	0.00	-0.00	0.02	0.03	0.04	0.04	-0.05	-0.03	-0.02	-0.01	-0.02	-0.03	-0.04	-0.04	0.02	0.02	0.01	0.01	0.01	0.01	0.01	0.00
0.00	-0.00	0.00	-0.00	0.05	0.10	0.11	0.04	-0.11	-0.07	-0.05	-0.03	-0.06	-0.10	-0.12	-0.06	0.05	0.04	0.03	0.03	0.02	0.02	0.02	0.01
0.00	-0.00	0.00	-0.00	0.08	0.14	0.10	-0.00	-0.10	-0.07	-0.05	-0.03	-0.10	-0.15	-0.12	-0.03	0.05	0.04	0.04	0.03	0.03	0.02	0.02	0.02
0.00	-0.00	0.00	-0.00	0.10	0.11	0.04	-0.02	-0.07	-0.05	-0.04	-0.02	-0.11	-0.12	-0.06	-0.01	0.03	0.03	0.03	0.02	0.02	0.02	0.02	0.01
0.00	-0.00	0.00	-0.00	0.05	0.03	0.01	-0.01	-0.03	-0.02	-0.01	-0.01	-0.06	-0.04	-0.02	-0.00	0.01	0.01	0.01	0.01	0.01	0.01	0.01	0.00

Figure A.6 Data of Vertical Velocity of Case 3 (Table 4.2) in Chapter IV

U VELOCITY (m/s) MATRIX IN AIR FLOW THROUGH FILTER

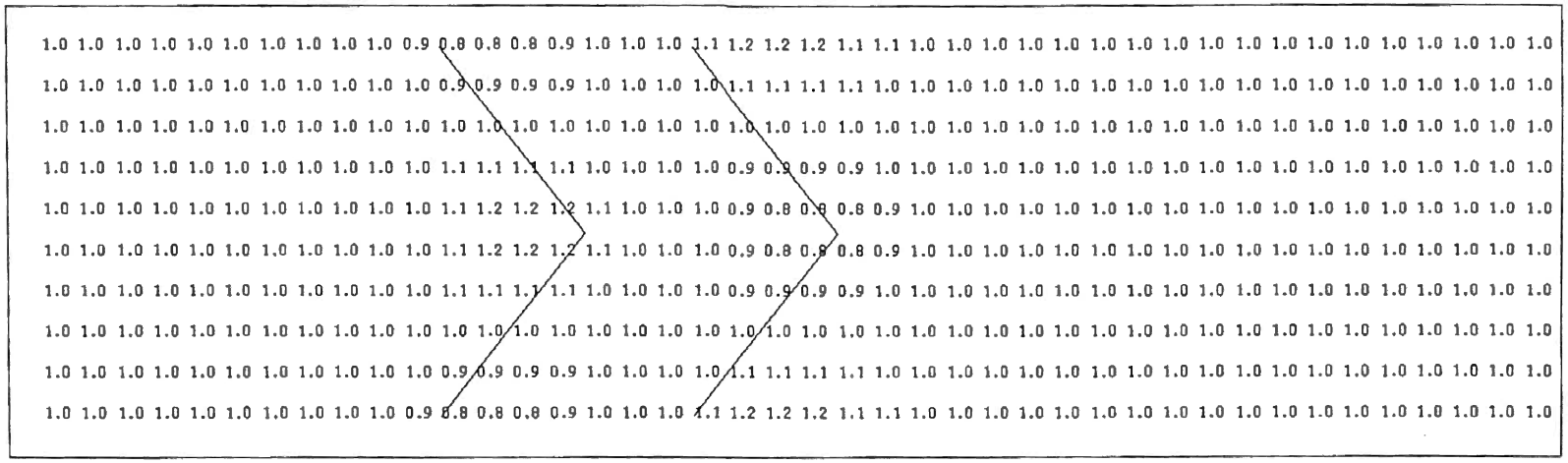

Figure A.7 Data of Horizontal Velocity of Case 4 (Table 4.2) in Chapter IV

V VELOCITY (m/s) MATRIX IN AIR FLOW THROUGH FILTER

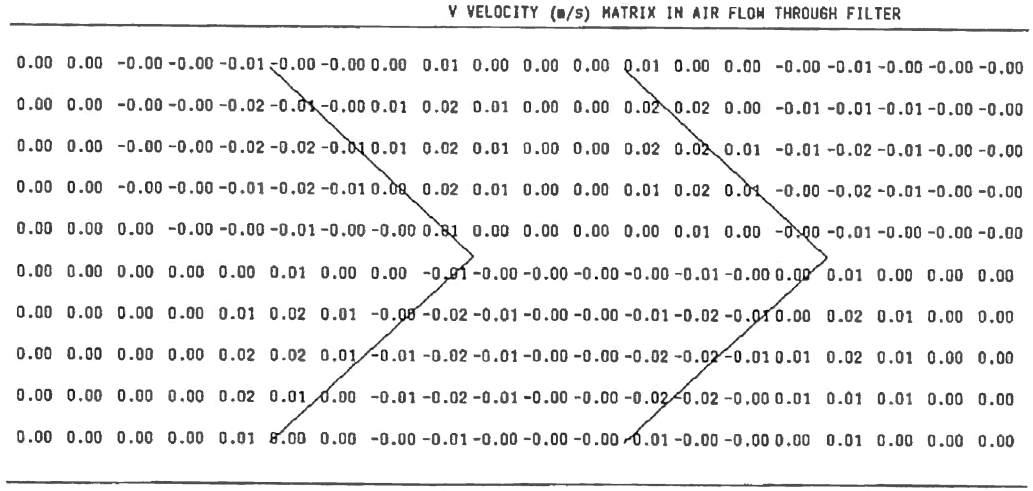

Figure A.8 Data of Vertical Velocity of Case 4 (Table 4.2) in Chapter IV

U VELOCITY (m/s) MATRIX IN AIR FLOW THROUGH FILTER

3.0	3.0	3.0	3.0	3.0	3.0	3.0	3.0	3.0	3.0	2.9	2.8	2.7	2.7	2.7	2.8	2.9	2.9	3.0	3.2	3.3	3.3	3.3	3.2	3.2	3.1	3.1	3.1	3.1	3.0	3.0	3.0	3.0	3.0	3.0	3.0	3.0	3.0	3.0	3.0	3.0	3.0
3.0	3.0	3.0	3.0	3.0	3.0	3.0	3.0	3.0	3.0	3.0	2.9	2.8	2.8	2.8	2.9	2.9	2.9	3.0	3.1	3.2	3.2	3.2	3.1	3.1	3.1	3.1	3.0	3.0	3.0	3.0	3.0	3.0	3.0	3.0	3.0	3.0	3.0	3.0	3.0	3.0	3.0
3.0	3.0	3.0	3.0	3.0	3.0	3.0	3.0	3.0	3.0	3.0	3.1	3.0	3.0	3.0	3.0	3.0	3.0	3.0	2.9	3.0	3.0	3.0	3.0	3.0	3.0	3.0	3.0	3.0	3.0	3.0	3.0	3.0	3.0	3.0	3.0	3.0	3.0	3.0	3.0	3.0	3.0
3.0	3.0	3.0	3.0	3.0	3.0	3.0	3.0	3.0	3.0	3.0	3.1	3.2	3.2	3.1	3.1	3.1	3.1	3.0	2.9	2.8	2.8	2.8	2.9	2.9	2.9	2.9	3.0	3.0	3.0	3.0	3.0	3.0	3.0	3.0	3.0	3.0	3.0	3.0	3.0	3.0	3.0
3.0	3.0	3.0	3.0	3.0	3.0	3.0	3.0	3.0	3.0	3.0	3.1	3.3	3.4	3.4	3.2	3.1	3.1	3.0	2.9	2.8	2.6	2.6	2.8	2.8	2.9	2.9	2.9	3.0	3.0	3.0	3.0	3.0	3.0	3.0	3.0	3.0	3.0	3.0	3.0	3.0	3.0
3.0	3.0	3.0	3.0	3.0	3.0	3.0	3.0	3.0	3.0	3.0	3.1	3.3	3.4	3.4	3.2	3.1	3.1	3.0	2.9	2.8	2.6	2.6	2.8	2.8	2.9	2.9	2.9	3.0	3.0	3.0	3.0	3.0	3.0	3.0	3.0	3.0	3.0	3.0	3.0	3.0	3.0
3.0	3.0	3.0	3.0	3.0	3.0	3.0	3.0	3.0	3.0	3.0	3.1	3.2	3.2	3.1	3.1	3.1	3.1	3.0	2.9	2.8	2.8	2.8	2.9	2.9	2.9	2.9	3.0	3.0	3.0	3.0	3.0	3.0	3.0	3.0	3.0	3.0	3.0	3.0	3.0	3.0	3.0
3.0	3.0	3.0	3.0	3.0	3.0	3.0	3.0	3.0	3.0	3.0	3.1	3.0	3.0	3.0	3.0	3.0	3.0	3.0	2.9	3.0	3.0	3.0	3.0	3.0	3.0	3.0	3.0	3.0	3.0	3.0	3.0	3.0	3.0	3.0	3.0	3.0	3.0	3.0	3.0	3.0	3.0
3.0	3.0	3.0	3.0	3.0	3.0	3.0	3.0	3.0	3.0	3.0	2.9	2.8	2.8	2.8	2.9	2.9	2.9	3.0	3.1	3.2	3.2	3.2	3.1	3.1	3.1	3.1	3.0	3.0	3.0	3.0	3.0	3.0	3.0	3.0	3.0	3.0	3.0	3.0	3.0	3.0	3.0
3.0	3.0	3.0	3.0	3.0	3.0	3.0	3.0	3.0	3.0	2.9	2.8	2.7	2.7	2.7	2.8	2.9	2.9	3.0	3.2	3.3	3.3	3.3	3.2	3.2	3.1	3.1	3.1	3.0	3.0	3.0	3.0	3.0	3.0	3.0	3.0	3.0	3.0	3.0	3.0	3.0	3.0

Figure A.9 Data of Horizontal Velocity of Case 5 (Table 4.3) in Chapter IV

V VELOCITY (m/s) MATRIX IN AIR FLOW THROUGH FILTER

0.00	0.00	-0.00	0.00	-0.01	-0.01	-0.00	0.00	0.01	0.00	0.00	0.00	0.01	0.01	0.00	-0.00	-0.00	-0.00	-0.00	-0.00	-0.00	-0.00
0.00	0.00	-0.00	0.00	-0.02	-0.03	-0.01	0.00	0.02	0.01	0.01	0.01	0.03	0.03	0.01	-0.00	-0.01	-0.01	-0.01	-0.01	-0.00	-0.00
0.00	0.00	-0.00	0.00	-0.02	-0.03	-0.02	0.00	0.02	0.02	0.01	0.01	0.03	0.04	0.03	0.00	-0.02	-0.01	-0.01	-0.01	-0.01	-0.00
0.00	0.00	-0.00	0.00	-0.01	-0.02	-0.02	-0.01	0.02	0.02	0.01	0.01	0.02	0.03	0.03	0.01	-0.02	-0.01	-0.01	-0.01	-0.00	-0.00
0.00	0.00	-0.00	0.00	-0.00	-0.01	-0.01	-0.01	0.01	0.01	0.00	0.00	0.01	0.01	0.01	0.01	-0.01	-0.01	-0.00	-0.00	-0.00	-0.00
0.00	0.00	0.00	-0.00	0.00	0.01	0.01	0.01	-0.01	-0.01	-0.00	-0.00	-0.01	-0.01	-0.01	-0.01	0.01	0.01	0.00	0.00	0.00	0.00
0.00	0.00	0.00	-0.00	0.01	0.02	0.02	0.01	-0.02	-0.02	-0.01	-0.01	-0.02	-0.03	-0.03	-0.01	0.02	0.01	0.01	0.01	0.00	0.00
0.00	0.00	0.00	-0.00	0.02	0.03	0.02	-0.00	-0.02	-0.02	-0.01	-0.01	-0.03	-0.04	-0.03	-0.00	0.02	0.02	0.01	0.01	0.01	0.00
0.00	0.00	0.00	-0.00	0.02	0.03	0.01	-0.00	-0.02	-0.01	-0.01	-0.01	-0.03	-0.03	-0.01	0.00	0.01	0.01	0.01	0.01	0.00	0.00
0.00	0.00	0.00	-0.00	0.01	0.01	0.00	-0.00	-0.01	-0.00	-0.00	-0.00	-0.01	-0.01	-0.00	0.00	0.00	0.00	0.00	0.00	0.00	0.00

Figure A.10 Data of Vertical Velocity of Case 5 (Table 4.3) in Chapter IV

U VELOCITY (m/s) MATRIX IN AIR FLOW THROUGH FILTER

3.0	3.0	3.0	3.0	3.0	3.0	3.0	3.0	3.0	3.0	2.9	2.7	2.6	2.6	2.7	2.8	2.9	2.9	3.1	3.3	3.4	3.4	3.3	3.3	3.2	3.1	3.1	3.1	3.1	3.0	3.0	3.0	3.0	3.0	3.0	3.0	3.0	3.0	3.0	3.0	3.0	3.0
3.0	3.0	3.0	3.0	3.0	3.0	3.0	3.0	3.0	3.0	3.0	2.9	2.8	2.7	2.8	2.9	2.9	3.0	3.0	3.1	3.2	3.3	3.2	3.2	3.1	3.1	3.1	3.0	3.0	3.0	3.0	3.0	3.0	3.0	3.0	3.0	3.0	3.0	3.0	3.0	3.0	3.0
3.0	3.0	3.0	3.0	3.0	3.0	3.0	3.0	3.0	3.0	3.0	3.1	3.0	2.9	2.9	3.0	3.0	3.0	3.0	2.9	3.0	3.0	3.0	3.0	3.0	3.0	3.0	3.0	3.0	3.0	3.0	3.0	3.0	3.0	3.0	3.0	3.0	3.0	3.0	3.0	3.0	3.0
3.0	3.0	3.0	3.0	3.0	3.0	3.0	3.0	3.0	3.0	3.0	3.1	3.2	3.2	3.1	3.1	3.1	3.0	3.0	2.9	2.8	2.8	2.8	2.8	2.9	2.9	2.9	3.0	3.0	3.0	3.0	3.0	3.0	3.0	3.0	3.0	3.0	3.0	3.0	3.0	3.0	3.0
3.0	3.0	3.0	3.0	3.0	3.0	3.0	3.0	3.0	3.0	3.0	3.2	3.3	3.5	3.4	3.2	3.1	3.1	3.0	2.9	2.7	2.6	2.6	2.7	2.8	2.9	2.9	2.9	2.9	3.0	3.0	3.0	3.0	3.0	3.0	3.0	3.0	3.0	3.0	3.0	3.0	3.0
3.0	3.0	3.0	3.0	3.0	3.0	3.0	3.0	3.0	3.0	3.0	3.2	3.3	3.5	3.4	3.2	3.1	3.1	3.0	2.9	2.7	2.6	2.6	2.7	2.8	2.9	2.9	2.9	2.9	3.0	3.0	3.0	3.0	3.0	3.0	3.0	3.0	3.0	3.0	3.0	3.0	3.0
3.0	3.0	3.0	3.0	3.0	3.0	3.0	3.0	3.0	3.0	3.0	3.1	3.2	3.2	3.1	3.1	3.1	3.0	3.0	2.9	2.8	2.8	2.8	2.8	2.9	2.9	2.9	3.0	3.0	3.0	3.0	3.0	3.0	3.0	3.0	3.0	3.0	3.0	3.0	3.0	3.0	3.0
3.0	3.0	3.0	3.0	3.0	3.0	3.0	3.0	3.0	3.0	3.0	3.1	3.0	2.9	2.9	3.0	3.0	3.0	3.0	2.9	3.0	3.0	3.0	3.0	3.0	3.0	3.0	3.0	3.0	3.0	3.0	3.0	3.0	3.0	3.0	3.0	3.0	3.0	3.0	3.0	3.0	3.0
3.0	3.0	3.0	3.0	3.0	3.0	3.0	3.0	3.0	3.0	3.0	2.9	2.8	2.7	2.8	2.9	2.9	3.0	3.0	3.1	3.2	3.3	3.2	3.2	3.1	3.1	3.1	3.0	3.0	3.0	3.0	3.0	3.0	3.0	3.0	3.0	3.0	3.0	3.0	3.0	3.0	3.0
3.0	3.0	3.0	3.0	3.0	3.0	3.0	3.0	3.0	3.0	2.9	2.7	2.6	2.6	2.7	2.8	2.9	2.9	3.1	3.3	3.4	3.4	3.3	3.3	3.2	3.1	3.1	3.1	3.1	3.0	3.0	3.0	3.0	3.0	3.0	3.0	3.0	3.0	3.0	3.0	3.0	3.0

Figure A.11 Data of Horizontal Velocity of Case 6 (Table 4.3) in Chapter IV

V VELOCITY (m/s) MATRIX IN AIR FLOW THROUGH FILTER

0.00	0.00	-0.00	0.00	-0.01	-0.01	-0.00	0.00	0.01	0.01	0.00	0.00	0.02	0.01	0.00	-0.00	-0.01	-0.00	-0.00	-0.00	-0.00	-0.00	-0.00	-0.00
0.00	0.00	-0.00	0.00	-0.03	-0.03	-0.01	0.01	0.02	0.02	0.01	0.01	0.03	0.03	0.01	-0.00	-0.02	-0.01	-0.01	-0.01	-0.01	-0.00	-0.00	-0.00
0.00	0.00	-0.00	0.00	-0.03	-0.04	-0.02	0.01	0.03	0.02	0.01	0.01	0.03	0.04	0.03	-0.00	-0.02	-0.02	-0.01	-0.01	-0.01	-0.01	-0.00	-0.00
0.00	0.00	-0.00	0.00	-0.02	-0.03	-0.03	-0.01	0.03	0.02	0.01	0.01	0.02	0.03	0.03	0.01	-0.02	-0.02	-0.01	-0.01	-0.01	-0.00	-0.00	-0.00
0.00	0.00	-0.00	0.00	-0.01	-0.01	-0.01	-0.01	0.02	0.01	0.00	0.00	0.01	0.01	0.01	0.01	-0.01	-0.01	-0.00	-0.00	-0.00	-0.00	-0.00	-0.00
0.00	0.00	0.00	-0.00	0.01	0.01	0.01	0.01	-0.02	-0.01	-0.00	-0.00	-0.01	-0.01	-0.01	-0.01	0.01	0.01	0.00	0.00	0.00	0.00	0.00	0.00
0.00	0.00	0.00	-0.00	0.02	0.03	0.03	0.01	-0.03	-0.02	-0.01	-0.01	-0.02	-0.03	-0.03	-0.01	0.02	0.02	0.01	0.01	0.01	0.00	0.00	0.00
0.00	0.00	0.00	-0.00	0.03	0.04	0.02	-0.01	-0.03	-0.02	-0.01	-0.01	-0.03	-0.04	-0.03	-0.00	0.02	0.02	0.01	0.01	0.01	0.01	0.00	0.00
0.00	0.00	0.00	-0.00	0.03	0.03	0.01	-0.01	-0.02	-0.02	-0.01	-0.01	-0.03	-0.03	-0.01	0.00	0.02	0.01	0.01	0.01	0.01	0.00	0.00	0.00
0.00	0.00	0.00	-0.00	0.01	0.01	0.00	-0.00	-0.01	-0.01	-0.00	-0.00	-0.02	-0.01	-0.00	0.00	0.01	0.00	0.00	0.00	0.00	0.00	0.00	0.00

Figure A.12 Data of Vertical Velocity of Case 6 (Table 4.3) in Chapter IV

U VELOCITY (m/s) MATRIX IN AIR FLOW THROUGH FILTER

3.0	3.0	3.0	3.0	3.0	3.0	3.0	3.0	3.0	3.0	2.8	2.6	2.4	2.4	2.6	2.8	2.9	2.9	3.1	3.4	3.6	3.6	3.5	3.4	3.3	3.2	3.2	3.1	3.1	3.1	3.0	3.0	3.0	3.0	3.0	3.0	3.0	3.0	3.0	3.0	3.0	3.0
3.0	3.0	3.0	3.0	3.0	3.0	3.0	3.0	3.0	3.0	3.0	2.8	2.6	2.6	2.7	2.8	2.9	3.0	3.0	3.1	3.3	3.4	3.4	3.3	3.2	3.1	3.1	3.1	3.1	3.0	3.0	3.0	3.0	3.0	3.0	3.0	3.0	3.0	3.0	3.0	3.0	3.0
3.0	3.0	3.0	3.0	3.0	3.0	3.0	3.0	3.0	3.0	3.0	3.1	3.0	2.9	2.9	3.0	3.0	3.0	3.0	2.9	2.9	3.1	3.1	3.0	3.0	3.0	3.0	3.0	3.0	3.0	3.0	3.0	3.0	3.0	3.0	3.0	3.0	3.0	3.0	3.0	3.0	3.0
3.0	3.0	3.0	3.0	3.0	3.0	3.0	3.0	3.0	3.0	3.1	3.2	3.4	3.4	3.2	3.1	3.1	3.0	3.0	2.8	2.6	2.6	2.7	2.8	2.8	2.9	2.9	2.9	2.9	3.0	3.0	3.0	3.0	3.0	3.0	3.0	3.0	3.0	3.0	3.0	3.0	3.0
3.0	3.0	3.0	3.0	3.0	3.0	3.0	3.0	3.0	3.0	3.1	3.3	3.5	3.7	3.6	3.3	3.2	3.1	3.0	2.8	2.5	2.3	2.4	2.6	2.7	2.8	2.8	2.9	2.9	2.9	3.0	3.0	3.0	3.0	3.0	3.0	3.0	3.0	3.0	3.0	3.0	3.0
3.0	3.0	3.0	3.0	3.0	3.0	3.0	3.0	3.0	3.0	3.1	3.3	3.5	3.7	3.6	3.3	3.2	3.1	3.0	2.8	2.5	2.3	2.4	2.6	2.7	2.8	2.8	2.9	2.9	2.9	3.0	3.0	3.0	3.0	3.0	3.0	3.0	3.0	3.0	3.0	3.0	3.0
3.0	3.0	3.0	3.0	3.0	3.0	3.0	3.0	3.0	3.0	3.1	3.2	3.4	3.4	3.2	3.1	3.1	3.0	3.0	2.8	2.6	2.6	2.7	2.8	2.8	2.9	2.9	2.9	2.9	3.0	3.0	3.0	3.0	3.0	3.0	3.0	3.0	3.0	3.0	3.0	3.0	3.0
3.0	3.0	3.0	3.0	3.0	3.0	3.0	3.0	3.0	3.0	3.0	3.1	3.0	2.9	2.9	3.0	3.0	3.0	3.0	2.9	2.9	3.1	3.1	3.0	3.0	3.0	3.0	3.0	3.0	3.0	3.0	3.0	3.0	3.0	3.0	3.0	3.0	3.0	3.0	3.0	3.0	3.0
3.0	3.0	3.0	3.0	3.0	3.0	3.0	3.0	3.0	3.0	3.0	2.8	2.6	2.6	2.7	2.8	2.9	3.0	3.0	3.1	3.3	3.4	3.4	3.3	3.2	3.1	3.1	3.1	3.1	3.0	3.0	3.0	3.0	3.0	3.0	3.0	3.0	3.0	3.0	3.0	3.0	3.0
3.0	3.0	3.0	3.0	3.0	3.0	3.0	3.0	3.0	3.0	2.8	2.6	2.4	2.4	2.6	2.8	2.9	2.9	3.1	3.4	3.6	3.6	3.5	3.4	3.3	3.2	3.2	3.1	3.1	3.1	3.0	3.0	3.0	3.0	3.0	3.0	3.0	3.0	3.0	3.0	3.0	3.0

Figure A.13 Data of Horizontal Velocity of Case 7 (Table 4.4) in Chapter IV

V VELOCITY (m/s) MATRIX IN AIR FLOW THROUGH FILTER

0.00	0.00	0.00	-0.00	0.00	-0.02	-0.01	-0.00	0.01	0.01	0.01	0.01	0.00	0.03	0.02	0.01	-0.00	-0.01	-0.01	-0.01	-0.00	-0.00	-0.00	-0.00	-0.00
0.00	0.00	0.00	-0.00	0.00	-0.05	-0.05	-0.01	0.01	0.04	0.02	0.01	0.01	0.05	0.05	0.02	-0.01	-0.03	-0.02	-0.02	-0.01	-0.01	-0.01	-0.00	-0.00
0.00	0.00	0.00	-0.00	0.00	-0.04	-0.06	-0.04	0.01	0.06	0.03	0.02	0.01	0.05	0.07	0.04	-0.00	-0.04	-0.03	-0.02	-0.01	-0.01	-0.01	-0.01	-0.00
0.00	0.00	0.00	-0.00	0.00	-0.03	-0.05	-0.04	-0.01	0.06	0.03	0.02	0.01	0.03	0.05	0.05	0.01	-0.04	-0.02	-0.02	-0.01	-0.01	-0.01	-0.00	-0.00
0.00	0.00	0.00	-0.00	0.00	-0.01	-0.02	-0.02	-0.01	0.03	0.01	0.01	0.00	0.01	0.02	0.02	0.01	-0.02	-0.01	-0.01	-0.00	-0.00	-0.00	-0.00	-0.00
0.00	0.00	0.00	0.00	-0.00	0.01	0.02	0.02	0.01	-0.03	-0.01	-0.01	-0.00	-0.01	-0.02	-0.02	-0.01	0.02	0.01	0.01	0.00	0.00	0.00	0.00	0.00
0.00	0.00	-0.00	0.00	-0.00	0.03	0.05	0.04	0.01	-0.06	-0.03	-0.02	-0.01	-0.03	-0.05	-0.05	-0.01	0.04	0.02	0.02	0.01	0.01	0.01	0.00	0.00
0.00	0.00	-0.00	0.00	-0.00	0.04	0.06	0.04	-0.01	-0.06	-0.03	-0.02	-0.01	-0.05	-0.07	-0.04	0.00	0.04	0.03	0.02	0.01	0.01	0.01	0.01	0.00
0.00	0.00	-0.00	0.00	-0.00	0.05	0.05	0.01	-0.01	-0.04	-0.02	-0.01	-0.01	-0.05	-0.05	-0.02	0.01	0.03	0.02	0.02	0.01	0.01	0.01	0.00	0.00
0.00	0.00	0.00	0.00	-0.00	0.02	0.01	0.00	-0.01	-0.01	-0.01	-0.01	-0.00	-0.03	-0.02	-0.01	0.00	0.01	0.01	0.01	0.00	0.00	0.00	0.00	0.00

Figure A.14 Data of Vertical Velocity of Case 7 (Table 4.4) in Chapter IV

U VELOCITY (m/s) MATRIX IN AIR FLOW THROUGH FILTER

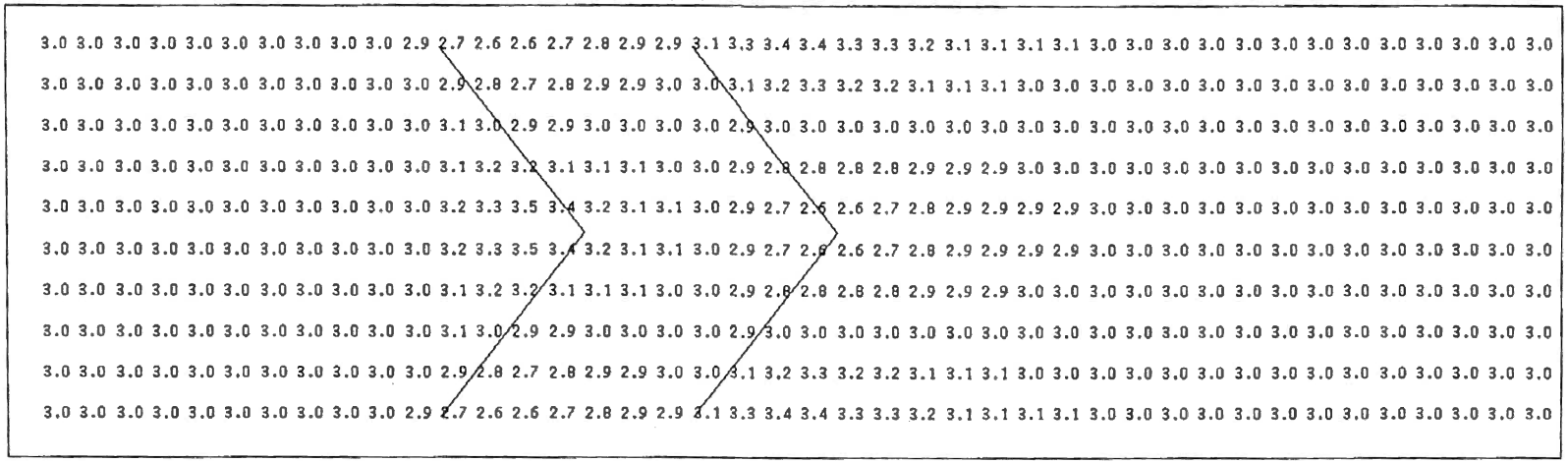

Figure A.15 Data of Horizontal Velocity of Case 8 (Table 4.4) in Chapter IV

V VELOCITY (m/s) MATRIX IN AIR FLOW THROUGH FILTER

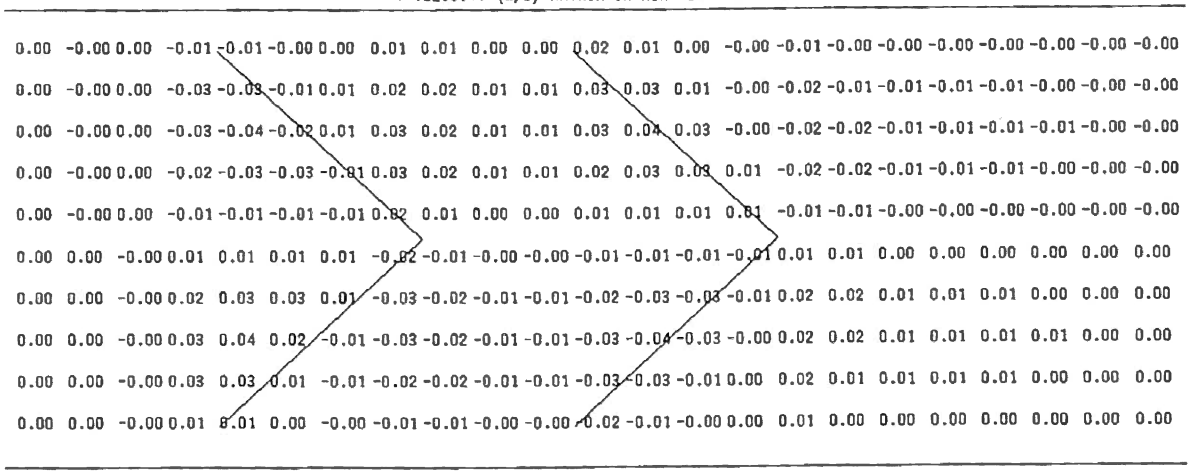

Figure A.16 Data of Vertical Velocity of Case 8 (Table 4.4) in Chapter IV

U VELOCITY (m/s) MATRIX IN AIR FLOW THROUGH FILTER

3.0	3.0	3.0	3.0	3.0	3.0	3.0	3.0	3.0	3.0	2.9	2.7	2.6	2.6	2.7	2.8	2.9	2.9	3.1	3.3	3.4	3.5	3.4	3.3	3.2	3.2	3.1	3.1	3.1	3.1	3.0	3.0	3.0	3.0	3.0	3.0	3.0	3.0	3.0	3.0	3.0
3.0	3.0	3.0	3.0	3.0	3.0	3.0	3.0	3.0	3.0	3.0	2.9	2.7	2.7	2.7	2.8	2.9	2.9	3.0	3.1	3.3	3.3	3.3	3.2	3.1	3.1	3.1	3.1	3.0	3.0	3.0	3.0	3.0	3.0	3.0	3.0	3.0	3.0	3.0	3.0	3.0
3.0	3.0	3.0	3.0	3.0	3.0	3.0	3.0	3.0	3.0	3.0	3.1	3.0	2.9	2.9	3.0	3.0	3.0	3.0	2.9	2.9	3.0	3.0	3.0	3.0	3.0	3.0	3.0	3.0	3.0	3.0	3.0	3.0	3.0	3.0	3.0	3.0	3.0	3.0	3.0	3.0
3.0	3.0	3.0	3.0	3.0	3.0	3.0	3.0	3.0	3.0	3.0	3.2	3.3	3.3	3.2	3.1	3.1	3.1	3.0	2.9	2.7	2.7	2.8	2.8	2.9	2.9	2.9	2.9	3.0	3.0	3.0	3.0	3.0	3.0	3.0	3.0	3.0	3.0	3.0	3.0	3.0
3.0	3.0	3.0	3.0	3.0	3.0	3.0	3.0	3.0	3.0	3.1	3.2	3.4	3.6	3.5	3.3	3.2	3.1	3.0	2.8	2.6	2.5	2.5	2.7	2.8	2.8	2.9	2.9	2.9	2.9	3.0	3.0	3.0	3.0	3.0	3.0	3.0	3.0	3.0	3.0	3.0
3.0	3.0	3.0	3.0	3.0	3.0	3.0	3.0	3.0	3.0	3.1	3.2	3.4	3.6	3.5	3.3	3.2	3.1	3.0	2.8	2.6	2.5	2.5	2.7	2.8	2.8	2.9	2.9	2.9	2.9	3.0	3.0	3.0	3.0	3.0	3.0	3.0	3.0	3.0	3.0	3.0
3.0	3.0	3.0	3.0	3.0	3.0	3.0	3.0	3.0	3.0	3.0	3.2	3.3	3.3	3.2	3.1	3.1	3.1	3.0	2.9	2.7	2.7	2.8	2.8	2.9	2.9	2.9	2.9	3.0	3.0	3.0	3.0	3.0	3.0	3.0	3.0	3.0	3.0	3.0	3.0	3.0
3.0	3.0	3.0	3.0	3.0	3.0	3.0	3.0	3.0	3.0	3.0	3.1	3.0	2.9	2.9	3.0	3.0	3.0	3.0	2.9	2.9	3.0	3.0	3.0	3.0	3.0	3.0	3.0	3.0	3.0	3.0	3.0	3.0	3.0	3.0	3.0	3.0	3.0	3.0	3.0	3.0
3.0	3.0	3.0	3.0	3.0	3.0	3.0	3.0	3.0	3.0	2.9	2.7	2.7	2.7	2.8	2.9	2.9	3.0	3.1	3.3	3.3	3.3	3.2	3.1	3.1	3.1	3.1	3.0	3.0	3.0	3.0	3.0	3.0	3.0	3.0	3.0	3.0	3.0	3.0	3.0	3.0
3.0	3.0	3.0	3.0	3.0	3.0	3.0	3.0	3.0	2.9	2.7	2.6	2.6	2.7	2.8	2.9	2.9	3.1	3.3	3.4	3.5	3.4	3.3	3.2	3.2	3.1	3.1	3.1	3.1	3.0	3.0	3.0	3.0	3.0	3.0	3.0	3.0	3.0	3.0	3.0	3.0

Figure A.17 Data of Horizontal Velocity of Case 9 (Table 4.4) in Chapter IV

V VELOCITY (m/s) MATRIX IN AIR FLOW THROUGH FILTER

0.00	0.00	0.00	-0.00	0.00	-0.02	-0.01	-0.00	0.00	0.01	0.01	0.00	0.00	0.02	0.01	0.01	-0.00	-0.01	-0.01	-0.00	-0.00	-0.00	-0.00	-0.00	-0.00																
0.00	0.00	0.00	-0.00	0.00	-0.04	-0.04	-0.01	0.01	0.03	0.02	0.01	0.01	0.04	0.04	0.02	-0.00	-0.02	-0.02	-0.01	-0.01	-0.01	-0.00	-0.00	-0.00																
0.00	0.00	0.00	-0.00	0.00	-0.03	-0.05	-0.03	0.01	0.04	0.03	0.02	0.01	0.04	0.05	0.04	0.00	-0.03	-0.02	-0.02	-0.01	-0.01	-0.01	-0.00	-0.00																
0.00	0.00	0.00	-0.00	0.00	-0.02	-0.04	-0.03	-0.01	0.04	0.02	0.01	0.01	0.02	0.04	0.04	0.01	-0.03	-0.02	-0.01	-0.01	-0.01	-0.01	-0.00	-0.00																
0.00	0.00	0.00	-0.00	0.00	-0.01	-0.01	-0.01	-0.01	0.02	0.01	0.01	0.00	0.01	0.01	0.01	0.01	-0.01	-0.01	-0.01	-0.00	-0.00	-0.00	-0.00	-0.00																
0.00	0.00	0.00	0.00	-0.00	0.01	0.01	0.01	0.01	-0.02	-0.01	-0.01	-0.00	-0.01	-0.01	-0.01	-0.01	0.01	0.01	0.01	0.00	0.00	0.00	0.00	0.00																
0.00	0.00	0.00	0.00	-0.00	0.02	0.04	0.03	0.01	-0.04	-0.02	-0.01	-0.01	-0.02	-0.04	-0.04	-0.01	0.03	0.02	0.01	0.01	0.01	0.01	0.00	0.00																
0.00	0.00	0.00	0.00	-0.00	0.03	0.05	0.03	-0.01	-0.04	-0.03	-0.02	-0.01	-0.04	-0.05	-0.04	-0.00	0.03	0.02	0.02	0.01	0.01	0.01	0.00	0.00																
0.00	0.00	0.00	0.00	-0.00	0.04	0.04	0.01	-0.01	-0.03	-0.02	-0.01	-0.01	-0.04	-0.04	-0.02	0.00	0.02	0.02	0.01	0.01	0.01	0.01	0.00	0.00																
0.00	0.00	0.00	0.00	-0.00	0.02	0.01	0.00	-0.00	-0.01	-0.01	-0.00	-0.00	-0.02	-0.01	-0.01	0.00	0.01	0.01	0.00	0.00	0.00	0.00	0.00	0.00																

Figure A.18 Data of Vertical Velocity of Case 9 (Table 4.4) in Chapter IV

U VELOCITY (m/s) MATRIX IN AIR FLOW THROUGH FILTER

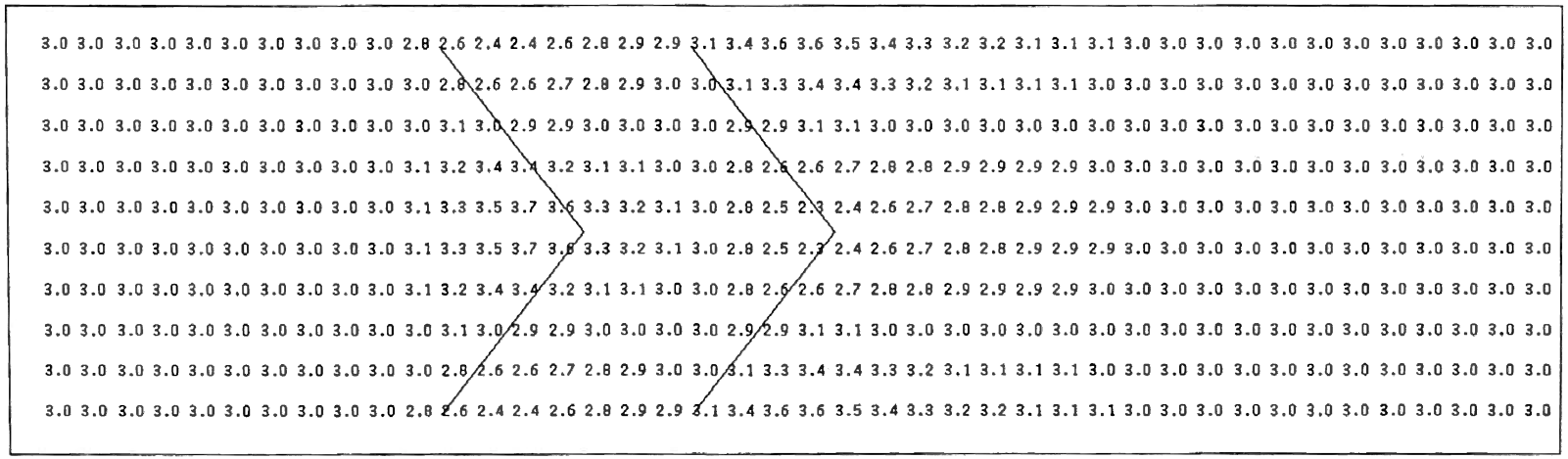

Figure A.19 Data of Horizontal Velocity of Case 10 (Table 4.4) in Chapter IV

V VELOCITY (m/s) MATRIX IN AIR FLOW THROUGH FILTER

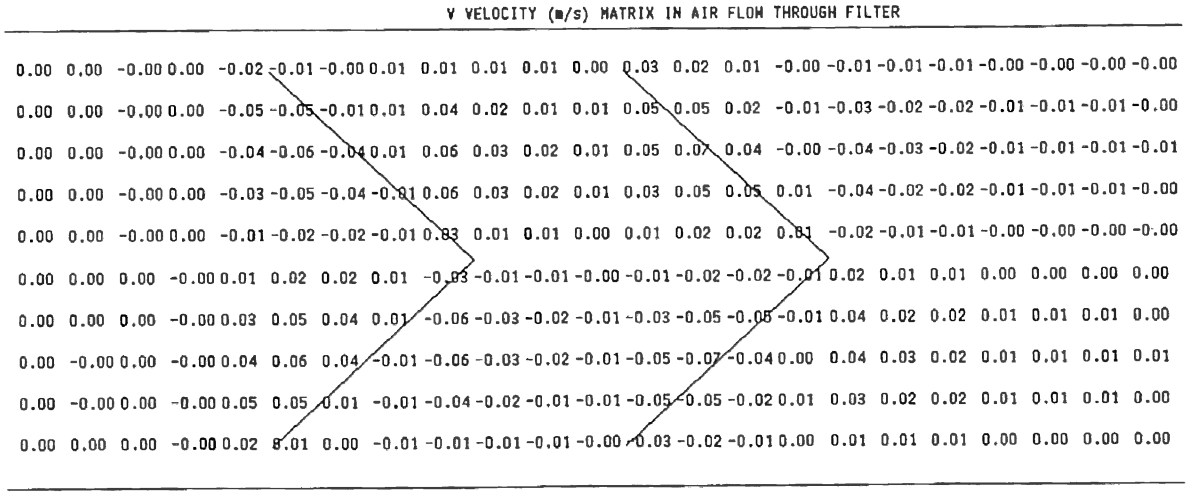

Figure A.20 Data of Vertical Velocity of Case 10 (Table 4.4) in Chapter IV

U VELOCITY (m/s) MATRIX IN AIR FLOW THROUGH FILTER

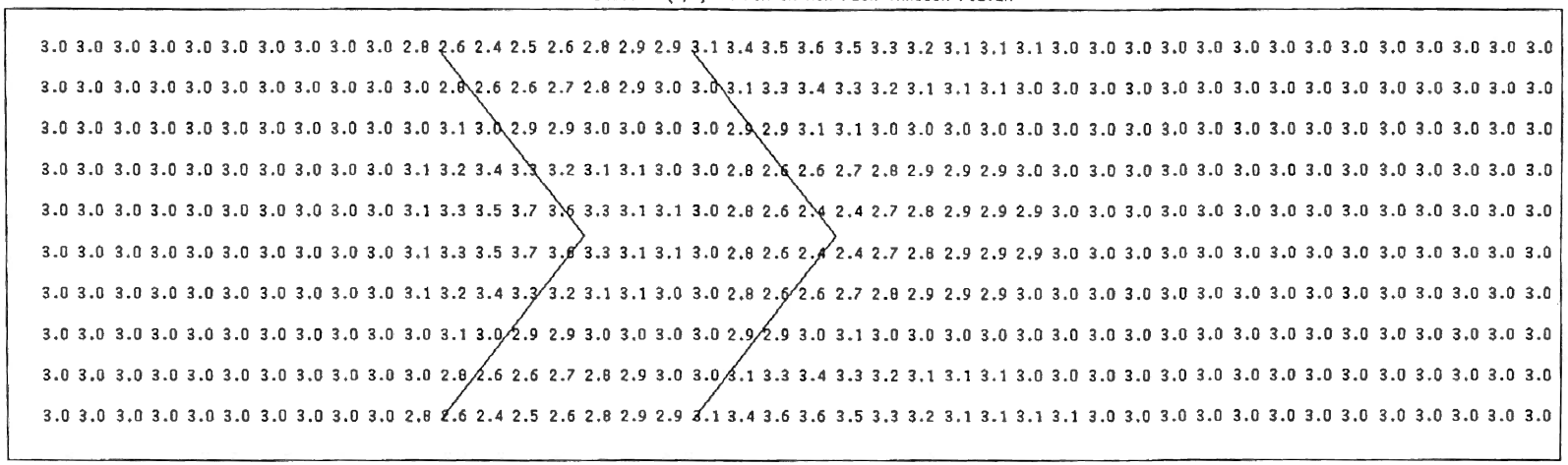

Figure A.21 Data of Horizontal Velocity of Case 11 in Chapter IV

V VELOCITY (m/s) MATRIX IN AIR FLOW THROUGH FILTER

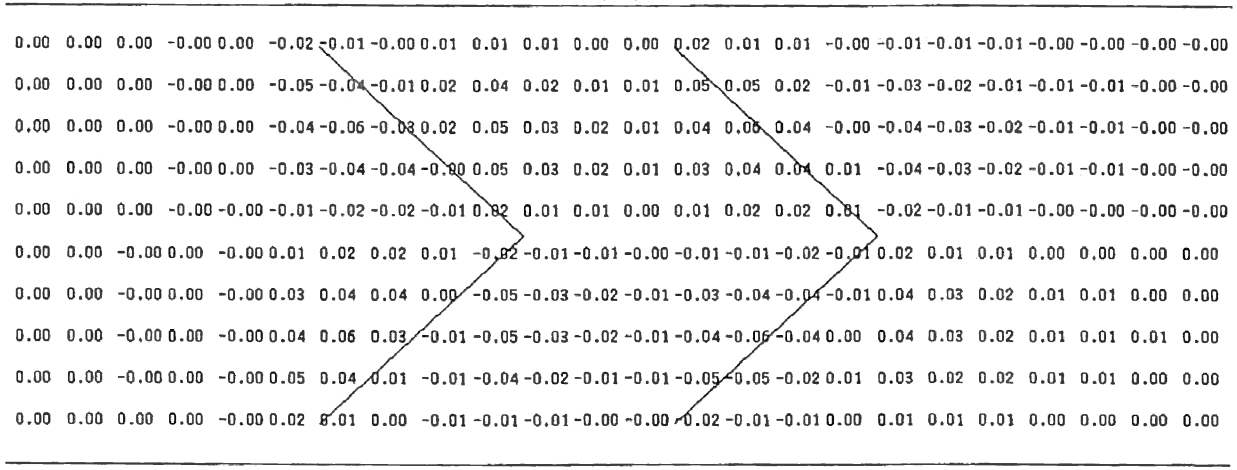

Figure A.22 Data of Vertical Velocity of Case 11 in Chapter IV

U VELOCITY (m/s) MATRIX IN AIR FLOW THROUGH FILTER

3.0	3.0	3.0	3.0	3.0	3.0	3.0	3.0	3.0	3.2	2.6	1.5	1.4	1.5	2.2	2.8	3.0	3.0	4.3	6.2	6.7	6.2	5.1	4.1	3.4	3.2	3.0	3.0	3.0	3.0	3.0	3.0	3.0	3.0	3.0	3.0	3.0	3.0
3.0	3.0	3.0	3.0	3.0	3.0	3.0	3.0	3.0	3.1	2.7	1.9	1.4	1.6	2.2	2.8	3.0	3.0	2.7	3.1	4.3	4.5	4.1	3.6	3.3	3.1	3.0	3.0	3.0	3.0	3.0	3.0	3.0	3.0	3.0	3.0	3.0	3.0
3.0	3.0	3.0	3.0	3.0	3.0	3.0	3.0	3.0	2.9	2.8	2.2	1.8	2.3	2.8	3.0	3.0	3.0	2.7	1.9	2.1	2.9	3.1	3.0	3.0	3.0	3.0	3.0	3.0	3.0	3.0	3.0	3.0	3.0	3.0	3.0	3.0	3.0
3.0	3.0	3.0	3.0	3.0	3.0	3.0	3.0	3.0	2.9	3.0	3.5	4.2	3.7	2.9	3.0	3.0	3.0	2.7	1.9	1.0	1.1	2.0	2.5	2.8	2.9	3.0	3.0	3.0	3.0	3.0	3.0	3.0	3.0	3.0	3.0	3.0	3.0
3.0	3.0	3.0	3.0	3.0	3.0	3.0	3.0	3.0	2.9	3.1	4.1	5.2	6.6	5.7	3.6	3.1	3.0	2.7	1.9	1.0	0.2	0.7	1.8	2.5	2.8	2.9	3.0	3.0	3.0	3.0	3.0	3.0	3.0	3.0	3.0	3.0	3.0
3.0	3.0	3.0	3.0	3.0	3.0	3.0	3.0	3.0	2.9	3.3	4.4	5.2	6.2	5.3	3.5	3.1	3.0	2.7	1.9	1.0	0.2	0.7	1.8	2.5	2.8	2.9	3.0	3.0	3.0	3.0	3.0	3.0	3.0	3.0	3.0	3.0	3.0
3.0	3.0	3.0	3.0	3.0	3.0	3.0	3.0	3.0	3.5	4.3	4.5	3.6	2.8	3.0	3.0	3.0	2.7	1.9	1.0	1.1	2.0	2.5	2.8	2.9	3.0	3.0	3.0	3.0	3.0	3.0	3.0	3.0	3.0	3.0	3.0	3.0	3.0
3.0	3.0	3.0	3.0	3.0	3.0	3.0	3.0	3.0	3.1	3.5	3.7	2.7	1.9	2.3	2.8	3.0	3.0	2.7	1.9	2.1	2.9	3.1	3.1	3.0	3.0	3.0	3.0	3.0	3.0	3.0	3.0	3.0	3.0	3.0	3.0	3.0	3.0
3.0	3.0	3.0	3.0	3.0	3.0	3.0	3.0	3.0	3.0	2.5	1.7	1.6	2.2	2.8	3.0	3.0	2.7	3.1	4.3	4.5	4.1	3.6	3.3	3.1	3.0	3.0	3.0	3.0	3.0	3.0	3.0	3.0	3.0	3.0	3.0	3.0	3.0
3.0	3.0	3.0	3.0	3.0	3.0	3.0	3.0	3.0	3.0	2.3	1.5	1.4	1.6	2.2	2.8	3.0	3.0	4.3	6.2	6.7	6.2	5.1	4.1	3.4	3.1	3.0	3.0	3.0	3.0	3.0	3.0	3.0	3.0	3.0	3.0	3.0	3.0

Figure A.23 Data of Horizontal Velocity of Case 12 (Table 4.5) in Chapter IV

V VELOCITY (m/s) MATRIX IN AIR FLOW THROUGH FILTER

0.00	0.00	0.00	0.00	-0.00	0.03	-0.12	-0.02	0.00	0.02	0.07	0.02	0.00	-0.00	0.18	0.08	-0.00	-0.06	-0.08	-0.06	-0.03	-0.01	-0.00	-0.00	-0.00
0.00	0.00	0.00	0.00	-0.00	0.07	-0.29	-0.18	0.00	0.06	0.20	0.05	0.01	0.00	0.31	0.26	0.04	-0.15	-0.20	-0.14	-0.07	-0.03	-0.01	-0.00	-0.00
0.00	0.00	0.00	0.00	-0.00	0.08	-0.36	-0.16	-0.07	0.09	0.32	0.08	0.01	0.00	0.22	0.30	0.17	-0.14	-0.25	-0.16	-0.08	-0.04	-0.01	-0.00	-0.00
0.00	0.00	0.00	0.00	-0.00	0.07	-0.35	-0.13	-0.08	-0.02	0.39	0.10	0.02	0.00	0.13	0.18	0.19	-0.03	-0.22	-0.13	-0.07	-0.03	-0.01	-0.00	-0.00
0.00	0.00	0.00	0.00	0.00	0.03	-0.27	-0.02	0.06	-0.04	0.19	0.05	0.01	0.00	0.04	0.06	0.06	0.03	-0.09	-0.05	-0.03	-0.01	-0.01	-0.00	-0.00
0.00	0.00	0.00	0.00	0.00	-0.00	-0.14	0.11	0.19	0.14	-0.23	-0.06	-0.01	-0.00	-0.04	-0.06	-0.07	-0.03	0.10	0.06	0.03	0.01	0.01	0.00	0.00
0.00	0.00	0.00	0.00	0.00	-0.02	0.01	0.21	0.25	0.08	-0.40	-0.10	-0.02	-0.00	-0.13	-0.18	-0.20	0.02	0.22	0.14	0.07	0.03	0.01	0.00	0.00
0.00	0.00	0.00	0.00	0.00	-0.01	0.12	0.22	0.15	-0.05	-0.32	-0.09	-0.02	-0.00	-0.21	-0.30	-0.18	0.14	0.25	0.17	0.09	0.04	0.01	0.00	0.00
0.00	0.00	0.00	0.00	-0.00	0.00	0.17	0.11	0.02	-0.04	-0.20	-0.05	-0.01	0.00	-0.30	-0.26	-0.05	0.15	0.21	0.14	0.07	0.03	0.01	0.00	0.00
0.00	0.00	0.00	0.00	0.00	0.00	0.09	0.01	-0.00	-0.02	-0.07	-0.02	-0.00	0.00	-0.18	-0.08	0.00	0.06	0.08	0.06	0.03	0.01	0.00	0.00	0.00

Figure A.24 Data of Vertical Velocity of Case 12 (Table 4.5) in Chapter IV

U VELOCITY (m/s) MATRIX IN AIR FLOW THROUGH FILTER

3.00	3.00	3.00	3.00	3.00	3.00	3.00	3.00	3.00	3.00	2.36	1.72	1.87	2.20	2.63	2.93	2.99	3.00	3.82	4.62	4.33	3.80	3.33	3.07	3.01	3.00	3.00	3.00	3.00	3.00	3.00	3.00	3.00	3.00	3.00	3.00	3.00
3.00	3.00	3.00	3.00	3.00	3.00	3.00	3.00	3.00	2.99	3.12	2.62	2.01	2.21	2.64	2.94	2.99	3.01	2.81	3.30	3.97	3.73	3.31	3.06	3.01	3.00	3.00	3.00	3.00	3.00	3.00	3.00	3.00	3.00	3.00	3.00	3.00
3.00	3.00	3.00	3.00	3.00	3.00	3.00	3.00	3.00	3.00	3.17	3.53	3.03	2.38	2.67	2.95	2.99	3.00	2.79	2.36	2.81	3.44	3.25	3.05	3.01	3.00	3.00	3.00	3.00	3.00	3.00	3.00	3.00	3.00	3.00	3.00	3.00
3.00	3.00	3.00	3.00	3.00	3.00	3.00	3.00	3.00	3.01	3.18	3.56	4.04	3.55	2.89	2.99	3.00	3.00	2.79	2.36	1.95	2.40	3.01	3.00	3.00	3.00	3.00	3.00	3.00	3.00	3.00	3.00	3.00	3.00	3.00	3.00	3.00
3.00	3.00	3.00	3.00	3.00	3.00	3.00	3.00	3.00	3.01	3.18	3.57	4.05	4.65	4.16	3.19	3.02	2.99	2.79	2.36	1.94	1.63	2.09	2.82	2.97	3.00	3.00	3.00	3.00	3.00	3.00	3.00	3.00	3.00	3.00	3.00	3.00
3.00	3.00	3.00	3.00	3.00	3.00	3.00	3.00	3.00	3.01	3.18	3.57	4.05	4.65	4.16	3.19	3.02	2.99	2.79	2.36	1.94	1.63	2.10	2.82	2.97	3.00	3.00	3.00	3.00	3.00	3.00	3.00	3.00	3.00	3.00	3.00	3.00
3.00	3.00	3.00	3.00	3.00	3.00	3.00	3.00	3.00	3.01	3.18	3.56	4.04	3.58	2.89	2.99	3.00	3.00	2.79	2.36	1.95	2.40	3.01	3.00	3.00	3.00	3.00	3.00	3.00	3.00	3.00	3.00	3.00	3.00	3.00	3.00	3.00
3.00	3.00	3.00	3.00	3.00	3.00	3.00	3.00	3.00	3.00	3.17	3.53	3.03	2.39	2.67	2.95	2.99	3.00	2.80	2.36	2.80	3.45	3.25	3.05	3.01	3.00	3.00	3.00	3.00	3.00	3.00	3.00	3.00	3.00	3.00	3.00	3.00
3.00	3.00	3.00	3.00	3.00	3.00	3.00	3.00	3.00	2.99	3.12	2.62	2.01	2.22	2.64	2.94	2.99	3.01	2.81	3.30	3.97	3.73	3.31	3.06	3.01	3.00	3.00	3.00	3.00	3.00	3.00	3.00	3.00	3.00	3.00	3.00	3.00
3.00	3.00	3.00	3.00	3.00	3.00	3.00	3.00	3.00	2.99	2.35	1.72	1.87	2.20	2.64	2.93	2.99	3.00	3.82	4.62	4.33	3.80	3.33	3.07	3.01	3.00	3.00	3.00	3.00	3.00	3.00	3.00	3.00	3.00	3.00	3.00	3.00

Figure A.25 Data of Horizontal Velocity of Case 13 (Table 4.6, 15°) in Chapter IV

V VELOCITY (m/s) MATRIX IN AIR FLOW THROUGH FILTER

0.000	0.000	0.000	0.000	0.000	0.000	0.000	0.000	-0.000	-0.000	-0.084	0.001	0.018	0.025	0.033	0.007	0.001	0.000	0.108	-0.003	-0.035	-0.035	-0.027	-0.007	-0.001	-0.000	-0.[illegible]
0.000	0.000	0.000	0.000	0.000	0.000	-0.000	0.000	-0.000	-0.001	-0.150	-0.082	0.040	0.073	0.098	0.020	0.003	0.002	0.188	0.086	-0.074	-0.097	-0.081	-0.019	-0.003	-0.000	-0.[illegible]
0.000	0.000	0.000	0.000	0.000	0.000	0.000	0.000	-0.000	-0.003	-0.110	-0.141	-0.047	0.102	0.162	0.032	0.004	0.004	0.133	0.149	0.009	-0.129	-0.130	-0.030	-0.005	-0.001	-0.[illegible]
0.000	0.000	0.000	0.000	0.000	0.000	0.000	0.000	-0.000	-0.002	-0.065	-0.087	-0.105	0.010	0.204	0.039	0.005	0.003	0.079	0.090	0.073	-0.050	-0.153	-0.035	-0.006	-0.001	-0.[illegible]
0.000	0.000	0.000	0.000	0.000	0.000	0.000	0.000	0.000	-0.000	-0.022	-0.029	-0.035	-0.044	0.108	0.020	0.003	0.002	0.026	0.030	0.025	0.016	-0.077	-0.017	-0.003	-0.000	-0.[illegible]
0.000	0.000	0.000	0.000	0.000	0.000	0.000	0.000	0.000	0.001	0.022	0.029	0.034	0.043	-0.107	-0.020	-0.002	-0.001	-0.026	-0.031	-0.026	-0.016	0.078	0.018	0.003	0.000	0.0[illegible]
0.000	0.000	0.000	0.000	0.000	0.000	0.000	0.000	0.000	0.003	0.066	0.086	0.103	-0.011	-0.203	-0.038	-0.005	-0.002	-0.079	-0.091	-0.074	0.050	0.154	0.035	0.006	0.001	0.0[illegible]
0.000	0.000	0.000	0.000	0.000	0.000	0.000	0.000	0.000	0.004	0.110	0.140	0.046	-0.103	-0.162	-0.032	-0.004	-0.003	-0.133	-0.150	-0.009	0.129	0.130	0.030	0.005	0.001	0.0[illegible]
0.000	0.000	0.000	0.000	0.000	0.000	0.000	0.000	0.000	0.003	0.150	0.081	-0.041	-0.073	-0.098	-0.020	-0.003	-0.001	-0.189	-0.087	0.074	0.098	0.082	0.019	0.003	0.000	0.0[illegible]
0.000	0.000	0.000	0.000	0.000	0.000	0.000	0.000	0.000	0.001	0.084	-0.001	-0.018	-0.025	-0.033	-0.007	-0.001	0.000	-0.108	0.003	0.035	0.035	0.027	0.007	0.001	0.000	0.0[illegible]

Figure A.26 Data of Vertical Velocity of Case 13 (Table 4.6, 15°) in Chapter IV

U VELOCITY (m/s) MATRIX IN AIR FLOW THROUGH FILTER

3.00	3.00	3.00	3.00	3.00	3.00	3.00	3.00	2.98	2.93	2.47	2.00	2.02	2.25	2.54	2.79	2.93	3.04	3.56	4.16	4.22	3.94	3.58	3.28	3.12	3.04	3.01	3.00	3.00	3.00	3.00	3.00	3.00	3.00	3.00	3.00
3.00	3.00	3.00	3.00	3.00	3.00	3.00	3.00	2.99	2.97	3.05	2.75	2.30	2.33	2.57	2.81	2.94	3.01	2.91	3.14	3.62	3.67	3.46	3.23	3.10	3.03	3.01	3.00	3.00	3.00	3.00	3.00	3.00	3.00	3.00	3.00
3.00	3.00	3.00	3.00	3.00	3.00	3.00	3.00	3.00	3.01	3.13	3.39	3.12	2.64	2.70	2.87	2.96	2.98	2.87	2.57	2.74	3.18	3.22	3.12	3.05	3.02	3.00	3.00	3.00	3.00	3.00	3.00	3.00	3.00	3.00	3.00
3.00	3.00	3.00	3.00	3.00	3.00	3.00	3.00	3.01	3.05	3.17	3.43	3.78	3.55	3.09	3.04	3.01	2.97	2.84	2.57	2.21	2.35	2.77	2.89	2.95	2.98	2.99	3.00	3.00	3.00	3.00	3.00	3.00	3.00	3.00	3.00
3.00	3.00	3.00	3.00	3.00	3.00	3.00	3.00	3.02	3.06	3.20	3.45	3.79	4.22	4.09	3.48	3.16	3.00	2.83	2.56	2.22	1.85	1.96	2.46	2.78	2.92	2.98	2.99	3.00	3.00	3.00	3.00	3.00	3.00	3.00	3.00
3.00	3.00	3.00	3.00	3.00	3.00	3.00	3.00	3.02	3.06	3.20	3.45	3.79	4.22	4.09	3.49	3.16	3.00	2.83	2.56	2.22	1.84	1.96	2.46	2.78	2.92	2.98	2.99	3.00	3.00	3.00	3.00	3.00	3.00	3.00	3.00
3.00	3.00	3.00	3.00	3.00	3.00	3.00	3.00	3.01	3.05	3.18	3.43	3.77	3.54	3.09	3.05	3.01	2.97	2.84	2.57	2.20	2.35	2.77	2.89	2.95	2.98	2.99	3.00	3.00	3.00	3.00	3.00	3.00	3.00	3.00	3.00
3.00	3.00	3.00	3.00	3.00	3.00	3.00	3.00	3.01	3.13	3.37	3.10	2.65	2.70	2.87	2.96	2.98	2.87	2.57	2.72	3.19	3.23	3.12	3.05	3.02	3.01	3.00	3.00	3.00	3.00	3.00	3.00	3.00	3.00	3.00	3.00
3.00	3.00	3.00	3.00	3.00	3.00	3.00	3.00	2.99	2.96	3.03	2.73	2.30	2.34	2.58	2.81	2.94	3.01	2.90	3.13	3.63	3.68	3.47	3.24	3.10	3.04	3.01	3.00	3.00	3.00	3.00	3.00	3.00	3.00	3.00	3.00
3.00	3.00	3.00	3.00	3.00	3.00	3.00	2.99	2.98	2.90	2.45	2.00	2.03	2.26	2.55	2.79	2.93	3.03	3.54	4.17	4.23	3.96	3.59	3.29	3.12	3.05	3.02	3.00	3.00	3.00	3.00	3.00	3.00	3.00	3.00	3.00

Figure A.27 Data of Horizontal Velocity of Case 13 (Table 4.6, 45°) in Chapter IV

V VELOCITY (m/s) MATRIX IN AIR FLOW THROUGH FILTER

0.000	0.000	0.000	0.000	0.000	-0.000	-0.000	-0.001	-0.005	-0.019	-0.169	-0.027	0.036	0.058	0.063	0.039	0.021	0.025	0.190	0.060	-0.037	-0.077	-0.075	-0.046	-0.022	-0.009	-0.(
0.000	0.000	0.000	0.000	0.000	-0.000	-0.001	-0.002	-0.011	-0.046	-0.296	-0.218	0.046	0.154	0.188	0.115	0.060	0.063	0.324	0.271	-0.026	-0.184	-0.205	-0.131	-0.063	-0.025	-0.(
0.000	0.000	0.000	0.000	0.000	-0.000	-0.001	-0.003	-0.013	-0.051	-0.210	-0.319	-0.152	0.169	0.294	0.179	0.087	0.076	0.223	0.344	0.167	-0.175	-0.284	-0.188	-0.091	-0.036	-0.(
0.000	0.000	0.000	0.000	0.000	0.000	-0.000	-0.002	-0.009	-0.036	-0.124	-0.193	-0.242	-0.035	0.327	0.199	0.091	0.064	0.135	0.199	0.230	0.006	-0.275	-0.190	-0.092	-0.036	-0.(
0.000	0.000	0.000	0.000	0.000	0.000	0.000	-0.000	-0.002	-0.011	-0.040	-0.065	-0.082	-0.111	0.167	0.097	0.044	0.028	0.046	0.064	0.071	0.071	-0.120	-0.084	-0.040	-0.016	-0.(
0.000	0.000	0.000	0.000	0.000	0.000	0.001	0.002	0.006	0.017	0.044	0.062	0.073	0.094	-0.157	-0.091	-0.038	-0.022	-0.044	-0.070	-0.083	-0.083	0.125	0.091	0.045	0.018	0.0(
0.000	0.000	0.000	0.000	0.000	0.000	0.001	0.004	0.013	0.043	0.128	0.190	0.227	0.022	-0.325	-0.193	-0.085	-0.057	-0.133	-0.205	-0.245	-0.014	0.280	0.196	0.096	0.038	0.0
0.000	0.000	0.000	0.000	0.000	0.000	0.001	0.004	0.016	0.060	0.215	0.308	0.137	-0.173	-0.292	-0.175	-0.082	-0.069	-0.220	-0.357	-0.181	0.173	0.288	0.193	0.094	0.038	0.0
0.000	0.000	0.000	0.000	0.000	0.000	0.001	0.004	0.014	0.058	0.293	0.205	-0.051	-0.156	-0.186	-0.113	-0.056	-0.053	-0.327	-0.285	0.020	0.185	0.209	0.134	0.065	0.026	0.0(
0.000	0.000	0.000	0.000	0.000	0.000	0.000	0.001	0.006	0.026	0.163	0.024	-0.037	-0.058	-0.063	-0.038	-0.020	-0.019	-0.195	-0.064	0.036	0.078	0.076	0.047	0.023	0.009	0.0(

Figure A.28 Data of Vertical Velocity of Case 13 (Table 4.6, 45°) in Chapter IV

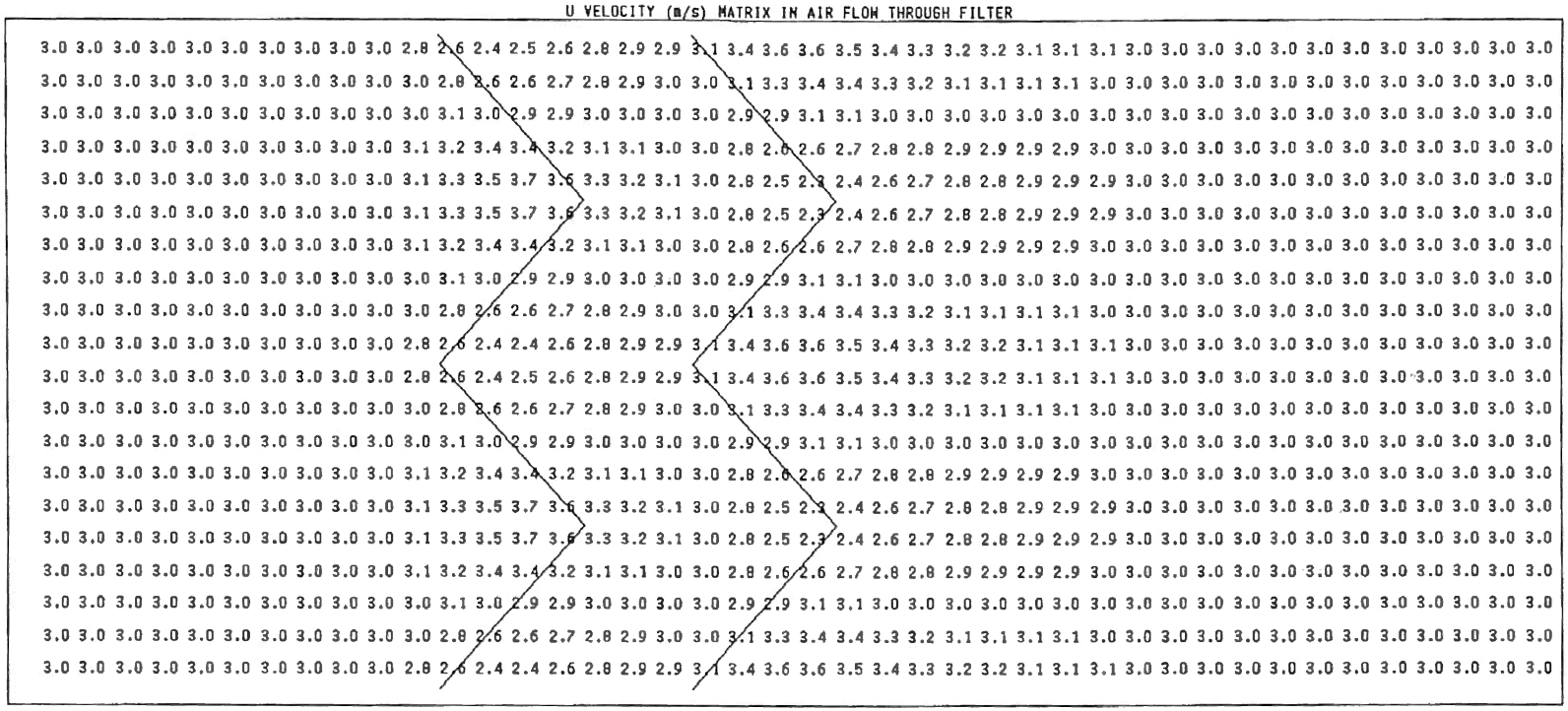

Figure A.29 Data of Horizontal Velocity of Case 14 (Table 4.2) in Chapter IV

V VELOCITY (m/s) MATRIX IN AIR FLOW THROUGH FILTER

0.00	0.00	0.00	0.00	-0.00	-0.02	-0.00	0.01	0.01	0.03	0.01	-0.01	-0.01	-0.00	-0.00	-0.00	-0.00	-0.00	-0.0(
0.00	0.00	0.00	0.00	-0.00	-0.05	-0.01	0.04	0.01	0.05	0.02	-0.03	-0.02	-0.01	-0.00	-0.00	-0.00	-0.00	-0.0(
0.00	0.00	0.00	0.00	-0.00	-0.04	-0.04	0.06	0.02	0.05	0.04	-0.04	-0.02	-0.01	-0.01	-0.00	-0.00	-0.00	-0.0(
0.00	0.00	0.00	0.00	-0.00	-0.03	-0.04	0.06	0.02	0.03	0.05	-0.04	-0.02	-0.01	-0.00	-0.00	-0.00	-0.00	-0.0(
0.00	0.00	0.00	0.00	0.00	-0.01	-0.02	0.03	0.01	0.01	0.02	-0.02	-0.01	-0.00	-0.00	-0.00	-0.00	-0.00	0.00
0.00	0.00	0.00	0.00	0.00	0.01	0.02	-0.03	-0.01	-0.01	-0.02	0.02	0.01	0.00	0.00	0.00	0.00	0.00	0.00
0.00	0.00	0.00	0.00	0.00	0.03	0.04	-0.06	-0.02	-0.03	-0.05	0.04	0.02	0.01	0.00	0.00	0.00	0.00	0.00
0.00	0.00	0.00	0.00	0.00	0.04	0.04	-0.06	-0.02	-0.05	-0.04	0.04	0.02	0.01	0.01	0.00	0.00	0.00	0.00
0.00	0.00	0.00	0.00	0.00	0.05	0.01	-0.04	-0.01	-0.05	-0.02	0.03	0.02	0.01	0.00	0.00	0.00	0.00	0.00
0.00	0.00	0.00	0.00	0.00	0.02	0.00	-0.01	-0.01	-0.03	-0.01	0.01	0.01	0.00	0.00	0.00	0.00	0.00	0.00
0.00	0.00	0.00	0.00	-0.00	-0.02	-0.00	0.01	0.01	0.03	0.01	-0.01	-0.01	-0.00	-0.00	-0.00	-0.00	0.00	0.00
0.00	0.00	0.00	0.00	-0.00	-0.05	-0.01	0.04	0.01	0.05	0.02	-0.03	-0.02	-0.01	-0.00	-0.00	-0.00	-0.00	0.00
0.00	0.00	0.00	0.00	-0.00	-0.04	-0.04	0.06	0.02	0.05	0.04	-0.04	-0.02	-0.01	-0.01	-0.00	-0.00	-0.00	0.00
0.00	0.00	0.00	0.00	-0.00	-0.03	-0.04	0.06	0.02	0.03	0.05	-0.04	-0.02	-0.01	-0.00	-0.00	-0.00	-0.00	0.00
0.00	0.00	0.00	0.00	0.00	-0.01	-0.02	0.03	0.01	0.01	0.02	-0.02	-0.01	-0.00	-0.00	-0.00	-0.00	0.00	0.00
0.00	0.00	0.00	0.00	0.00	0.01	0.02	-0.03	-0.01	-0.01	-0.02	0.02	0.01	0.00	0.00	0.00	0.00	0.00	0.00
0.00	0.00	0.00	0.00	0.00	0.03	0.04	-0.06	-0.02	-0.03	-0.05	0.04	0.02	0.01	0.00	0.00	0.00	0.00	0.00
0.00	0.00	0.00	0.00	0.00	0.04	0.04	-0.06	-0.02	-0.05	-0.04	0.04	0.02	0.01	0.01	0.00	0.00	0.00	0.00
0.00	0.00	0.00	0.00	0.00	0.05	0.01	-0.04	-0.01	-0.05	-0.02	0.03	0.02	0.01	0.00	0.00	0.00	0.00	0.00
0.00	0.00	0.00	0.00	0.00	0.02	0.00	-0.01	-0.01	-0.03	-0.01	0.01	0.01	0.00	0.00	0.00	0.00	0.00	0.00

Figure A.30 Data of Vertical Velocity of Case 14 (Table 4.2) in Chapter IV

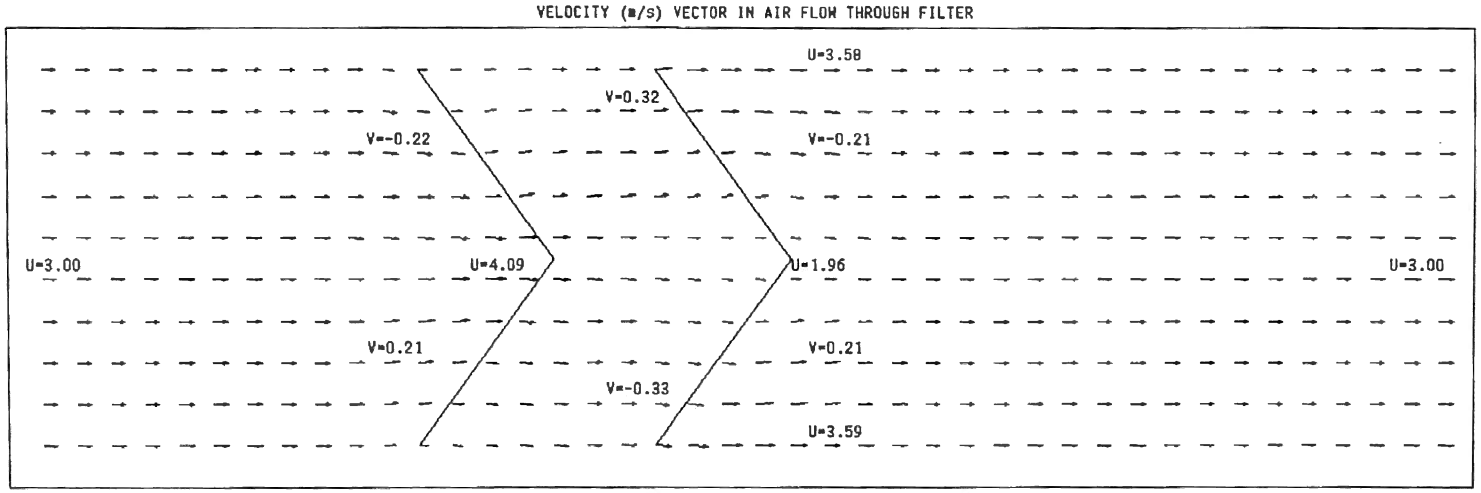

a. Scaled Velocity Vectors

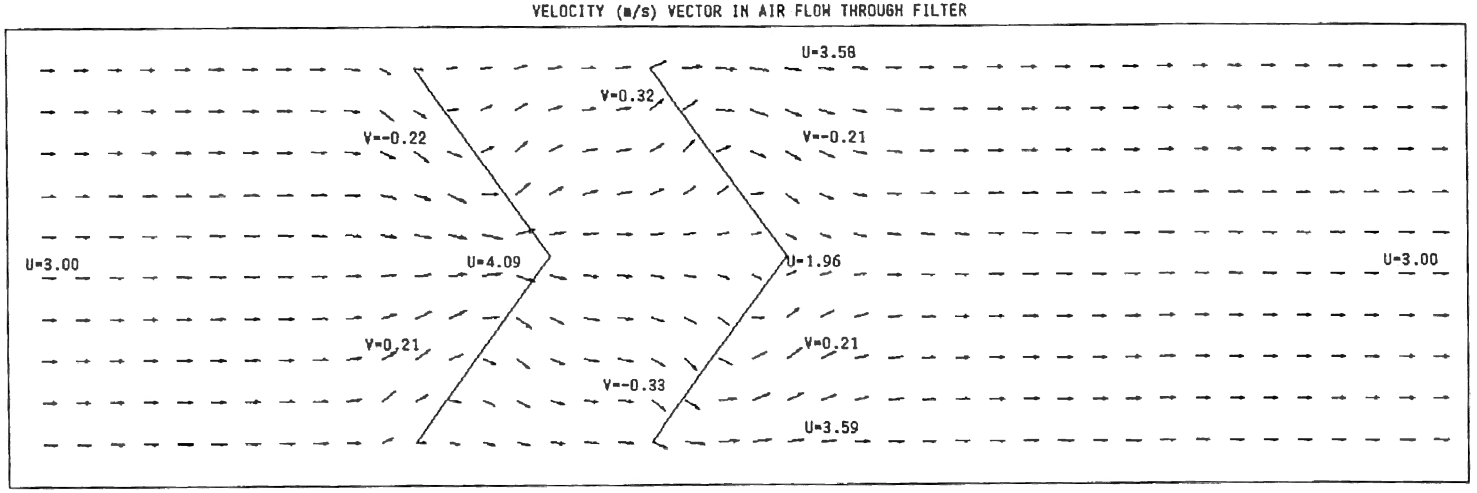

b. Amplified Flow Velocity Vectors

Figure A.32 Velocity Vector Plots for 45° Pleat Angle (Table 4.6)

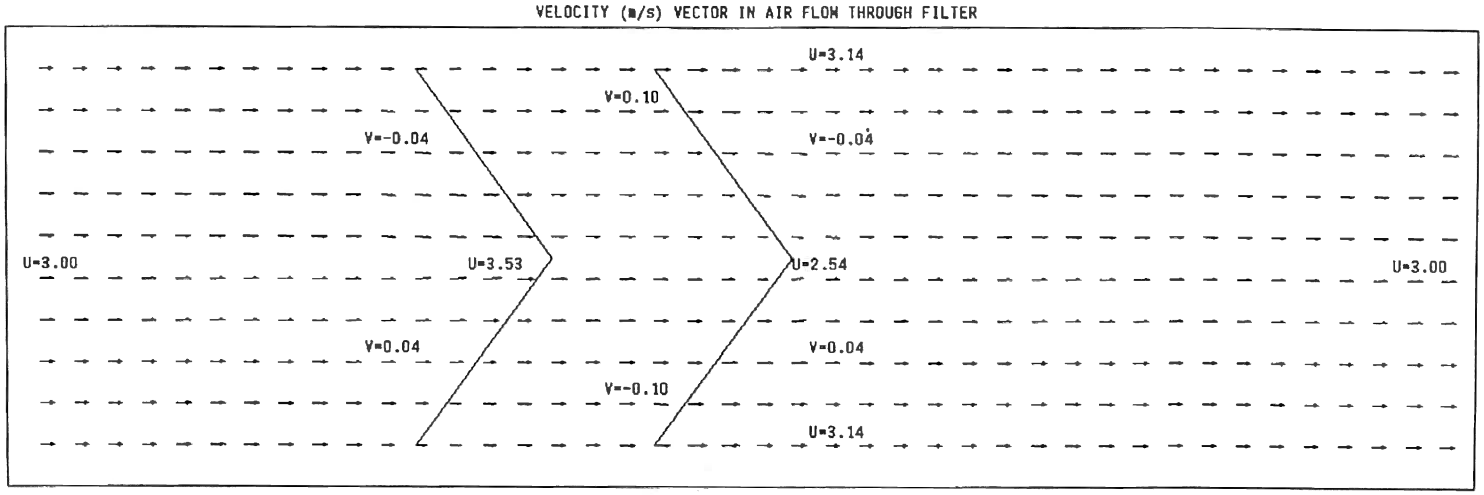

a. Scaled Velocity Vectors

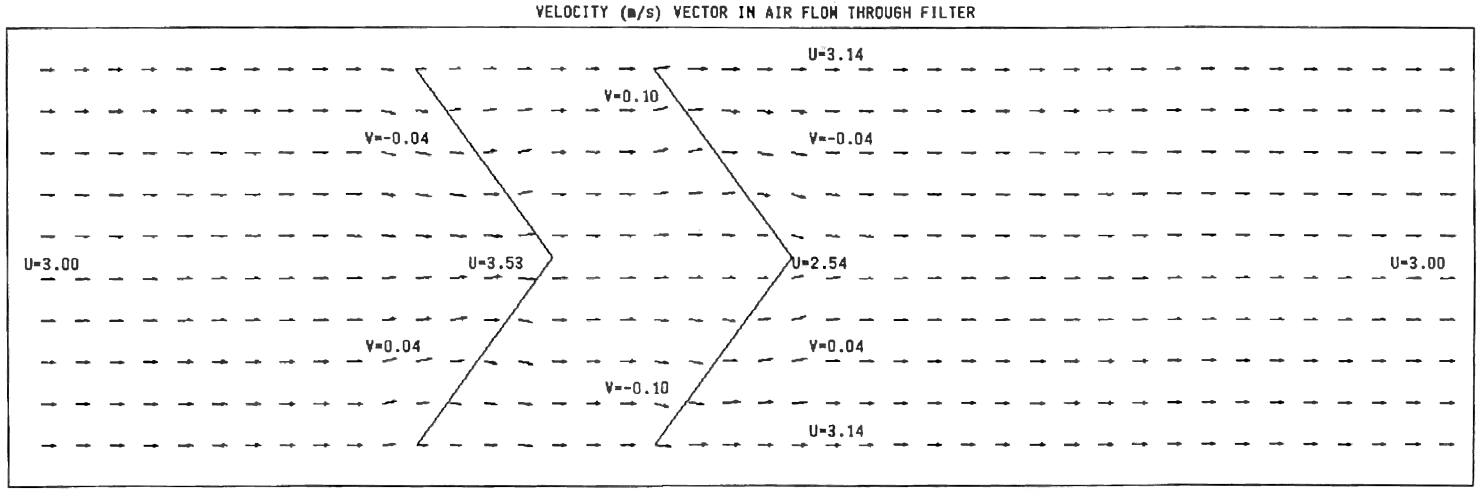

b. Amplified Flow Velocity Vectors

Figure A.31 Velocity Vector Plots for 15° Pleat Angle (Table 4.6)

APPENDIX B

VELOCITY VECTOR PLOT TECHNIQUE

The vector plot of the flow velocity is a good way to see how flow passes through the filter. The vector plot in this thesis is written in C language using GL graphics library on RISC6000. The theory of draw the arrow is to connect four points with three lines. Figure A1 shows four arrows in possible four directions. The first quadrant arrow is used here to derive the point equations.

The arrow tail point (x_1, y_1) is given in grid setup. The arrow head point (x_2, y_2) is obtained by using the calculated or measured velocity.

$$x_2 = x_1 + \frac{u}{u_{max}} \Delta x$$

$$y_2 = y_1 + \frac{v}{v_{max}} \Delta y$$

The distance between this two points is given as following equation:

$$d = \sqrt{(x_2 - x_1)^2 + (y_2 - y_1)^2}$$

The angle β showing in the figure can be calculated as:

$$\beta = \tan^{-1} \frac{|x_2 - x_1|}{|y_2 - y_1|}$$

Suppose the arrow head line length r is 40% length of the arrow length d or :

$$r = d \cdot 0.4$$

Then the point (x_0, y_0) on the lower part of the arrow is:

$$x_0 = x_2 - r \cdot \sin(\beta - \theta)$$
$$y_0 = y_2 - r \cdot \cos(\beta - \theta)$$

Here the θ is the angle of arrow head which is chosen by user.

The point of upper part of the arrow head is derived from following equation:

$$x_0 = x_2 - r \cdot \sin(\beta + \theta)$$
$$y_0 = y_2 - r \cdot \cos(\beta + \theta)$$

Similarly, the equations of arrow head in other quadrant are given as:

Quadrant (II) (x<0, y>0):

$$x_0 = x_2 + r \cdot \sin(\beta \pm \theta)$$
$$y_0 = y_2 - r \cdot \cos(\beta \pm \theta)$$

Quadrant (III) (x<0, y<0):

$$x_0 = x_2 + r \cdot \sin(\beta \pm \theta)$$
$$y_0 = y_2 + r \cdot \cos(\beta \pm \theta)$$

Quadrant (IV) (x>0, y<0):

$$x_0 = x_2 - r \cdot \sin(\beta \pm \theta)$$
$$y_0 = y_2 + r \cdot \cos(\beta \pm \theta)$$

$$x_0 = x_2 - r \cdot \sin(\beta - \theta)$$
$$y_0 = y_2 - r \cdot \cos(\beta - \theta)$$

Here the θ is the angle of arrow head which is chosen by user.

The point of upper part of the arrow head is derived from following equation:

$$x_0 = x_2 - r \cdot \sin(\beta + \theta)$$
$$y_0 = y_2 - r \cdot \cos(\beta + \theta)$$

Similarly, the equations of arrow head in other quadrant are given as:

Quadrant (II) (x<0, y>0):

$$x_0 = x_2 + r \cdot \sin(\beta \pm \theta)$$
$$y_0 = y_2 - r \cdot \cos(\beta \pm \theta)$$

Quadrant (III) (x<0, y<0):

$$x_0 = x_2 + r \cdot \sin(\beta \pm \theta)$$
$$y_0 = y_2 + r \cdot \cos(\beta \pm \theta)$$

Quadrant (IV) (x>0, y<0):

$$x_0 = x_2 - r \cdot \sin(\beta \pm \theta)$$
$$y_0 = y_2 + r \cdot \cos(\beta \pm \theta)$$

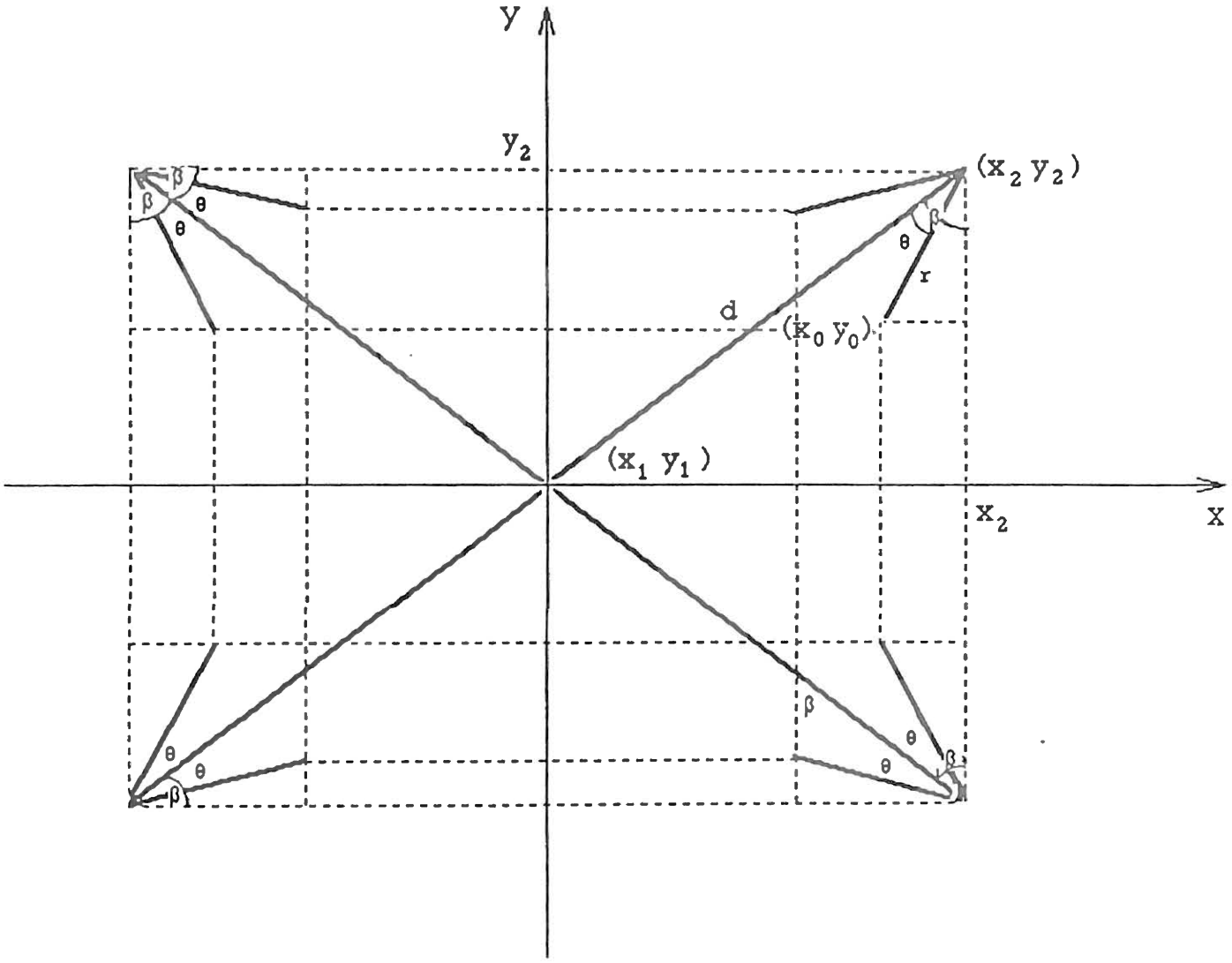

Figure B.1 Arrow Head Calculation

VITA

Qian Cai

Candidate for the Degree of

Master of Science

Thesis: A STUDY OF AIR FILTER FLOW BY COMPUTATIONAL FLUID DYNAMICS

Major Field: Mechanical Engineering

Biographical:

Personal Data: Born in Shanghai, China, September 28, 1967, the son of Qiming Cai and Zhongxiu Ye.

Education: Graduated from The First Middle School, Lanzhou, China, in June 1985; received Bachelor of Science Degree from Zhejiang University in July 1989; completed requirements for the Master of Science degree at Oklahoma State University in July, 1993.

Professional Experience: Assistant Engineer, Zhejiang University, August, 1989, to July 1991; Research Assistant, Department of Mechanical and Aerospace Engineering, Oklahoma State University, January, 1992, to May 1993.